Pair Production of Leptophilic Dark Matter at Next-to-Leading Order

by

Anders Lauvland

Thesis

for the degree of

Master of Science

Faculty of Mathematics and Natural Sciences
University of Oslo

May 2016

Abstract

We study an extension of the Standard Model which introduces a Leptophilic Majorana WIMP candidate and an $SU(2)_L$ scalar doublet. We calculate the one-loop contribution for $SM \times S\bar{M} \to \chi\chi$ by evaluating vertex corrections in this leptophilic model. We calculate the cross section for free quarks annihilating into a pair of WIMPs in the photon channel for this higher order process. This constitutes the ground work for further analyses of this process in the context of LHC pp collisions, e.g. in monojet plus missing E_T events.

Contents

Chapter 1

Introduction

The theory describing all the known elementary particles today is the Standard Model of Particle Physics (SM). It describes interactions between particles and light, and also radioactive decay and nuclear binding forces. These interactions are mediated by three different fundamental forces, namely the electromagnetic force and the weak and strong nuclear forces. The SM seems near its completion, as a particle compatible with the Standard Model Higgs boson was discovered at the ATLAS and CMS experiments at the Large Hadron Collider (LHC) at CERN in 2012 [1, 2]

Despite the scientific triumphs of the SM, it still leaves several questions unanswered. One example is how the presence of gravitational interactions fits with the SM, as a quantum theory for gravity has not yet been successfully developed. Furthermore, observations over the past 100 years of the rotational velocity of spiral galaxies and kinematic behavior of galaxy clusters imply that they contain more mass than the visible light can account for. This new matter has to be uncharged under electromagnetic interactions, and is therefore known as Dark Matter (DM).

There is no particle in the SM that can be used to explain DM. Therefore, extensions of the SM must be studied for a quantum field theory that contains a DM particle. Several such theories exist, Supersymmetry (SUSY) with R-parity is one example. Some such SUSY models predict the existence of the *neutralino*, which is a stable Majorana fermion and a good DM candidate. The neutralino belongs to a larger class of DM candidates known as Weakly Interacting Massive Particles (WIMPs). In what is referred to as the "WIMP miracle", such a particle naturally provides the observed relic density of DM.

This thesis is devoted to study one such WIMP model. We extend the SM field content with an additional stable Majorana fermion χ as the WIMP candidate and a doublet of decaying scalar fields. In the model we study, the WIMP can only interact with the SM leptons and with one beyond SM scalar particle. Appropriately, this DM candidate is referred to as Leptophilic Dark Matter. We wish to study how these DM particles can be pair produced from a collision

between SM particles. We therefore motivate and perform studies of the effective coupling $\gamma^*/Z^* \to \chi\chi$ and aim to uncover its general features, i.e. what kind of couplings we find in the effective vertex, and how the γ and Z effective couplings to χ relate to each other. We also study the ultra-violet behavior of the vertex corrections to this coupling and determine how they cancel.

We proceed to find the closed form expressions for the effective coupling. Then we perform a cross section calculation using the exact form of the effective vertex. This is in order to get a first look at the process $\bar{q}q \to \chi\chi$, which is a highly relevant process for LHC applications.

Calculation of the effective vertex for χ pair production is necessary in order to facilitate searches for DM using particle colliders. However, for the purpose of estimating cross sections for detection at LHC, the cross section for pair production of χ is insufficient, as they are only interacting weakly and thus can not be detected by the experimental apparatus. Therefore, further studies of, for instance, a final state consisting of $\chi\chi + jet$ and analysis of the missing transverse momentum are needed, and we lay the groundwork for such an analysis.

1.1 Outline

The thesis is structured as follows. In Chapter 2 we give an introduction to the field content of the SM. In order to do so we also introduce the necessary framework of group theory and symmetries in order to highlight the guiding principles for constructing the SM. We focus especially on the electroweak sector of the SM, as the WIMP in our model is interacting with electroweak gauge bosons as a higher order process. In this chapter we also introduce the Majorana fermion field and the concept of Weyl spinors, which are important ingredients for this leptophilic DM model.

In Chapter 3 we discuss some of the open questions left by the SM, before we give a thorough introduction to the motivation for DM and the WIMP scenario. We also introduce and discuss the Minimal Supersymmetric Standard Model, a proposed extension of the SM which among other things could provide an explanation for DM.

In Chapter 4 we introduce the Leptophilic DM model, and pave the way towards a calculation of a next-to-leading order amplitude. We calculate the vertex correction for χ pair production via a neutral off-shell electroweak gauge boson, γ^* or Z. We then derive a general expression in terms of form factors.

Chapter 5 introduces the Passarino-Veltmann scheme for solving loop integrals. We apply this method to find explicit expressions for the form factors. We finalize by calculating the cross section in the γ^* channel, before making our conclusions.

Chapter 2

The Standard Model of Particle Physics

In this chapter we give a description of the Standard Model (SM) of particle physics. It is well known that the SM is not the complete theory of nature. However, after the discovery of the SM Higgs boson in 2012 [1,2] made independently by the CMS- and ATLAS-collaborations at the Large Hadron Collider (LHC) the SM provides a complete picture (with the exception of neutrino physics) of the observed particles and phenomena in high energy physics.

Before delving into the SM, we state some of the most important framework needed to understand it, including group theory and symmetries. We also motivate and state properties of Majorana fermions, which are not included in the SM, but which is the topic of chapter 3 and 4. We also make a remark on the mechanism of Spontaneous Symmetry Breaking before we present some details of the SM.

2.1 Symmetries in Particle Physics

The laws of nature as we know them, are deeply connected to symmetries. Any differentiable symmetry of a physical system corresponds to a conserved quantity. The relationship between symmetries and conservations laws is described by Noether's theorem [3]. In particle physics the symmetries of a system or a model, determines the interactions in the model. Before we look at the internal symmetries of the SM we will introduce some group theory.

2.1.1 Lie Groups

Formally, a group is a set G combined with a binary operation $\circ$ that has to satisfy four axioms for all elements $g_i \in G$ we must have

- Closed under group operation: For all $g_i \circ g_j \in G$.

- Associativity of $\circ$: $(g_i \circ g_j) \circ g_k = g_i \circ (g_j \circ g_k)$.
- Identity element e: There exists an element $e \in G$ such that $e \circ g_i = g_i \circ e = g_i$
- Inverse element: For each $g_i \in G$ there is an element $g_i^{-1} \in G$ such that $g_i \circ g_i^{-1} = g_i^{-1} \circ g_i = e$, where $e \in G$ is the identity element.

We will, however, suppress the group operation symbol $\circ$, as the groups we will discuss can be represented by sets of non-singular matrices under matrix multiplication.[1]

A Lie group is, in mathematical terms, a smooth differentiable manifold. A manifold is a mathematical object where there is an open set around each point on the manifold that can be mapped onto $\mathbb{R}^N$ (or $\mathbb{C}^N$ if the manifold is complex) via a differentiable bijection (N is then referred to as the dimension of the manifold). This allows for calculus to be performed on the manifold. The elements in Lie group G can be reached by successive infinitesimal transformations belonging to the group. The infinitesimal elements of the Lie group are the elements that lie arbitrary close to the identity. They can be written in the form

$$\delta g = 1 + i\alpha^a T^a + \mathcal{O}(\alpha^2), \tag{2.1}$$

where α is an infinitesimal parameter specifying the transformation, T^a are the generators of the Lie group, and summation over a repeated index a is implied. The generators span a vector space, this vector space together with the commutation relation

$$[T^a, T^b] = if^{abc}T^c, \tag{2.2}$$

form what is called a Lie *algebra*. The coefficients f^{abc} are called the *structure constants*. For the Lie groups that are of interest in QFT a general group action can be represented locally by exponentiating the generators in the following manner

$$e^{i\alpha^a T^a}. \tag{2.3}$$

2.1.2 Representations of a Lie Algebra

We now turn to the concept of *representations* of a Lie group. For the symmetry groups describing the internal symmetries of particle physics we are mainly interested in two representations, namely the *fundamental* and *adjoint* representations. The elements of a Lie group G transforms elements in a vector space V,

[1] That is, as *subgroups* of the *General Linear Group* $GL(n, \mathbb{F})$, where $\mathbb{F}$ is either $\mathbb{R}$ or $\mathbb{C}$ and n is the dimensionality of the matrices.

we define the representation as a map from G to the set of non-singular matrices that acts on V, this is the general linear group on V denoted $GL(V)$. We demand that the map preserves the group structure of G, that is, the map is homomorphism. For any $g_i \in G$ a homomorphism ρ on G satisfies

$$\rho\left(g_i g_j\right) = \rho\left(g_i\right)\rho\left(g_j\right). \tag{2.4}$$

Thus, the map $\rho : G \to GL(V)$ is a representation of G if it is a homomorphism. If there is another representation of G given by $\rho' : G \to GL(V')$ then ρ and ρ' are said to be *equivalent* if there is an isomorphism A such that, $A\rho(g)A^{-1} = \rho'(g)$ for $g \in G$.

The symmetry group $SU(N)$ is defined from the set of all unitary complex $N \times N$ matrices V such that $\det(V) = 1$. For a general *representation* of $SU(N)$ the dimensionality of the matrices need not be $N \times N$, if the group is represented by $d \times d$ matrices it is referred to as a d-dimensional representation of $SU(N)$. An infinitesimal $SU(N)$-transformation of vectors $\mathbf{x} \in \mathbb{C}^d$ can be written as

$$\begin{gathered}\mathbf{x} \to (1 + i\alpha^a T^a)\mathbf{x}, \\ a = 1, \ldots, N^2 - 1 \text{ for } SU(N)\text{-transformations.}\end{gathered} \tag{2.5}$$

Here α^a are real infinitesimal parameters, T^a are $N^2 - 1$ linearly independent Hermitian matrices orthogonal to the identity, i.e. $\mathrm{tr}(T^a) = 0$. These matrices satisfy a commutation relation as in Eq. (2.2) and and together they form the Lie algebra for this d-dimensional representation of $SU(N)$. If the generators T^a are equivalent to a representation where there they are simultaneously block diagonal, the representation is *reducible*. Hence the sub blocks of the generators T^a in a reducible representation constitutes *irreducible* representations if they are not reducible themselves. An irreducible representation will be denoted by r and the generators by t_r^a.

Associated to an irreducible representation is the *conjugate* representation denoted $\bar{r}$, with the corresponding generators $t_{\bar{r}}^a$. If $\mathbf{x}$ transforms according to Eq. (2.5) in a d-dimensional irreducible representation where $T^a = t_r^a$, then $\mathbf{x}^*$ (let * denote complex conjugation) transforms in the conjugate representation, where the generators are $t_{\bar{r}}^a$. By taking complex conjugation the infinitesimal transformation of a vector $\mathbf{x} \in \mathbb{C}^d$ transforming in an irreducible representation r of a group G

$$\mathbf{x}^* \to \mathbf{x}^{*'} = \left(1 - i\alpha^a (t_r^a)^*\right)\mathbf{x}^*. \tag{2.6}$$

Thus we have the generators in the conjugate representation given by

$$t_{\bar{r}}^a = -(t_r^a)^*. \tag{2.7}$$

We can then combine group invariants by the product of a object transforming in r with another object transforming in $\bar{r}$.

In an irreducible representation r of a group G the structure constants f^{abc} can always be defined such that they are completely antisymmetric with respect any permutation of the indices a, b, c. Furthermore, there exists another irreducible representation called the adjoint representation, where the generators t^a_G are related to the structure constants by

$$(t^b_G)_{ac} = i f_{abc}. \tag{2.8}$$

For $SU(N)$ the matrices in this representation are $(N^2-1)\times(N^2-1)$ and they satisfy the same commutation relation as t^a_r.

The *fundamental* representation of the $SU(N)$ is the simplest irreducible representations of the group. They are the unitary matrices with determinant one which transform N that keeps the innerproduct of complex vectors invariant. In SM we are interested in the cases $N = 2$ (weak isospin) and $N = 3$ (Quantum Chromodynamics). The generators for $SU(2)$ in the fundamental representation (denoted $r = \mathbf{2}$) the proportional to the Pauli matrices, and for $SU(3)$ ($r = \mathbf{3}$)they are proportional to the Gell-Mann matrices. Furthermore, $SU(2)$ is *pseudoreal*, meaning that for $\mathbf{x}, \mathbf{y}$ transforming in $\mathbf{2}$ (or both in $\bar{\mathbf{2}}$) the combination $\mathbf{x}^T E \mathbf{y}$ is invariant with respect to $SU(2)$ transformations for an antisymmetric matrix E. For $SU(N)$ with $N \geq 3$ the irreducible representations meaning that only the combination of a vector transforming in $\mathbf{3}$ and one in $\bar{\mathbf{3}}$ can form group invariants.

2.1.3 Representations of the Lorentz group

The Lorentz group is also a Lie group. For a general Lorentz transformation Λ, demanding that $\det\Lambda = 1$ ensures that space is not inverted (*proper*, removes parity) and $\Lambda^0{}_0 \geq 1$ ensures that time flows forward (*orthochronous* removes time reversal) yields the proper orthochronous Lorentz group $L^\uparrow_+$. In the set of all proper orthochronous Lorentz transformations any infinitesimal transformation of a four-vector x^μ can be written as

$$\delta\Lambda^\mu{}_\nu = \delta^\mu_\nu - \frac{i}{2}\omega_{\rho\sigma}\,(J^{\rho\sigma})^\mu{}_\nu + \mathcal{O}(\omega^2). \tag{2.9}$$

Where $\omega_{\rho\sigma} = -\omega_{\sigma\rho}$ are infinitesimal parameters specifying the transformation (boost, rotation or both), and $(J^{\rho\sigma})^\mu{}_\nu$ are the generators of $L^\uparrow_+$. The span of the generators forms the Lie algebra for $L^\uparrow_+$, together with the commutation relation

$$[J^{\mu\nu}, J^{\rho\sigma}] = i\left(g^{\nu\rho}J^{\mu\sigma} - g^{\mu\rho}J^{\nu\sigma} - g^{\nu\sigma}J^{\mu\rho} + g^{\mu\sigma}J^{\nu\sigma}\right). \tag{2.10}$$

The generic form of $J^{\rho\sigma}$ is

$$J = \begin{pmatrix} 0 & -K_1 & -K_2 & -K_3 \\ K_1 & 0 & J_3 & -J_2 \\ K_2 & -J_3 & 0 & J_1 \\ K_3 & J_2 & -J_1 & 0 \end{pmatrix}. \tag{2.11}$$

where K_i and J_i are the generators of boosts and rotations, respectively. Then any finite boost or rotation can be written as

$$\Lambda^{\mu}{}_{\nu} = \left(e^{-\frac{i}{2}\omega_{\rho\sigma}J^{\rho\sigma}}\right)^{\mu}{}_{\nu}. \tag{2.12}$$

The four component Dirac spinor ψ is another representation of $L_+^{\uparrow}$. The generators in this representation are given in terms of the Dirac matrices γ^μ by

$$\mathcal{M}^{\mu\nu} = \frac{i}{4}\left[\gamma^\mu, \gamma^\nu\right], \tag{2.13}$$

where the Dirac matrices must satisfy a Clifford algebra $\{\gamma^\mu, \gamma^\nu\} = 2g^{\mu\nu}$. The matrices $\mathcal{M}^{\mu\nu}$ satisfy the commutation relation in Eq. (2.10). An arbitrary basis can be transformed to the chiral basis by a suitable unitary transformation of the Dirac matrices $\gamma^\mu \to W\gamma^\mu W^\dagger$. In the chiral basis they are given by

$$\gamma^\mu = \begin{pmatrix} 0 & \sigma^\mu \\ \bar{\sigma}^\mu & 0 \end{pmatrix}. \tag{2.14}$$

Where σ^i denotes the Pauli matrices and $\sigma^\mu = (1, \sigma^i)$, $\sigma^\mu = (1, -\sigma^i)$. In the Weyl basis one construct the four component Dirac spinor from two-component spinors ψ_L and ψ_R, such that a Dirac spinor can be written as

$$\psi = \begin{pmatrix} \psi_L \\ \psi_R \end{pmatrix}. \tag{2.15}$$

The left-handed component refers to ψ_L and the right-handed component refers to ψ_R. We can recover the left- and right-handed components of ψ in an arbitrary basis by

$$\psi_{L/R} = P_{L/R}\psi, \tag{2.16}$$

where $P_L = (1 - \gamma^5)/2$ and $P_R = (1 + \gamma^5)$ are projection operators and $\gamma^5 = i\gamma^0\gamma^1\gamma^2\gamma^3$. In the Weyl basis, however, the reducibility of the spinor representation of the Lorentz algebra becomes manifest as the generators of boosts and rotations $\mathcal{M}^{\mu\nu}$ are block diagonal

$$\mathcal{M}^{0i} = -\frac{i}{2}\begin{pmatrix} \sigma^i & 0 \\ 0 & -\sigma^i \end{pmatrix}, \ \mathcal{M}^{ij} = -\frac{1}{2}\epsilon^{ijk}\begin{pmatrix} \sigma^k & 0 \\ 0 & \sigma^k \end{pmatrix}. \tag{2.17}$$

Hence, that a boost or rotation of the spinor ψ can be viewed as a boost or rotation of the two component spinors $\psi_{L/R}$ separately as two inequivalent fundamental representation of the proper orthochronous Lorentz group. The spinor ψ_L transforms in a the fundamental representation of the complex 2×2 matrices with determinant one, which is the special linear group $SL(2, \mathbb{C})$, while the spinors ψ_R transform in the conjugate representation and these are two inequivalent representations. The spinors $\psi_{L/R}$ are called left- and right-handed Weyl spinors, respectively. If the spinor ψ_L is a left-handed Weyl spinor then the spinor $-i\sigma^2\psi_L^*$ is a right-handed Weyl spinor.

Weyl spinors

It is often used a specific notation for the Weyl spinors. One introduces indices $\alpha, \dot{\alpha} = 1, 2$ and writes the left-handed Weyl spinor λ_α and right-handed Weyl spinor $\bar{\chi}^{\dot{\alpha}}$ as two component objects. The raising and lowering of the indices is performed by $(i\sigma^2)_{\alpha\beta} = \varepsilon_{\alpha\beta}$, and the same for dotted indices $\dot{\alpha}$. Then a Dirac spinor is the combination of a left- and right-handed Weyl spinor, written generally as

$$\psi = \begin{pmatrix} \lambda_\alpha \\ \bar{\chi}^{\dot{\alpha}} \end{pmatrix}. \tag{2.18}$$

We have $(\lambda^\alpha)^* = \bar{\lambda}^{\dot{\alpha}}$. Contraction between two Weyl spinors is defined as $\lambda\lambda' = \lambda^\alpha \lambda'_\alpha$ and for the right-handed Weyl spinors $\bar{\chi}\bar{\chi}' = \bar{\chi}_{\dot{\alpha}}\bar{\chi}'^{\dot{\alpha}}$. The Lorents invariant $\psi'^\dagger \gamma^0 \psi$ can then be written as

$$\psi'^\dagger \gamma^0 \psi = \chi'\lambda + \bar{\lambda}'\bar{\chi}. \tag{2.19}$$

The convention of using Weyl spinors provides a convenient formalism to describe the four component Dirac field in the chiral basis, as the formalism "hides" the application of the matrix $i\sigma^2$ appearing. We note that this formalism using the block matrices occurring in γ^μ in Eq. (2.14) carry both dotted and undotted indices $\bar{\sigma}^{\mu\alpha\dot{\alpha}}, \sigma^\mu_{\dot{\alpha}\alpha}$, furthermore they are related by $\bar{\sigma}^{\mu\dot{\alpha}\alpha} = \varepsilon^{\alpha\beta}\varepsilon^{\dot{\alpha}\dot{\beta}}(\sigma^\mu_{\beta\dot{\beta}})^T$ which is equivalent to applying the identity for the Pauli matrices $\sigma^2(\sigma^i)^T\sigma^2 = -\sigma^i$.

In order to represent a physical Dirac field we need to include both a separate left-handed and right-handed Weyl spinor. It is still unclear if a single Weyl spinor alone can be used to represent a fermion in nature. However, some collective excitations in solids known as quasiparticles that behaves as Weyl fermions been discovered [4].

2.2 Majorana Equation and Charge Conjugation Matrix

We consider an equation of motion for a charged Dirac field who interacts with an electromagnetic potential A^μ

$$(i\gamma^\mu(\partial_\mu + ieQA_\mu) - m)\,\psi = 0.$$

If we take the complex conjugate of this equation, we get an equation of motion for the field ψ^*

$$(i(-\gamma^\mu)^*(\partial_\mu - ieQA_\mu) - m)\,\psi^* = 0.$$

We note that the (electromagnetic) charge has flipped sign, and there is a different representation of the Dirac matrices $-(\gamma^\mu)^* = -\gamma^0(\gamma^\mu)^T\gamma^0 = -\gamma^0(\gamma^0\gamma^2\gamma^\mu\gamma^2\gamma^0)\gamma^0$. Wich we can recognize as a unitary transformation of the Dirac matrices by defining $C = \eta\gamma^2\gamma^0$, where η is phase we can not yet determine.The charge conjugation satisfies (in any basis for the Dirac matrices)

$$C^{-1} = C^\dagger = -\eta^\dagger\gamma^0\gamma^2, \tag{2.20}$$

if we demand $|\eta|^2 = 1$. We can thus write

$$-(\gamma^\mu)^* = \gamma^0 C^{-1}\gamma^\mu C\gamma^0$$

We can then write the equation of motion as

$$\gamma^0 C^\dagger i\gamma^\mu(\partial_\mu - ieQA_\mu)C\gamma^0\psi^* - m\psi^* = 0.$$

Defining $\psi^c \equiv C\gamma^0\psi^*$ we have

$$i\gamma^\mu(\partial_\mu - ieQA_\mu)\psi^c - m\psi^c = 0$$

It transforms as an ordinary spinor under Lorentz transformations, this makes the terms $\psi^T C\psi$ and $\bar\psi C\bar\psi^T$ Lorentz invariant. If the field has a nonzero $U(1)$-charge however these terms are not gauge invariant. Thus a $U(1)$-charge neutral fermion field ψ may have a Majorana mass term

$$\mathcal{L} = \frac{1}{2}\bar\psi i\partial\!\!\!/\psi - \frac{1}{2}m\bar\psi C\bar\psi^T + \text{h.c.} \tag{2.21}$$

Here we choose the phase $\eta = \pm i$, such that $\psi^T C\psi = (\bar\psi C\bar\psi^T)^\dagger$. Upon varying the action with the Lagrangian from Eq. (2.21) with respect to $\bar\psi$ gives the Majorana equation:

$$i\partial\!\!\!/\psi = m\psi^c. \tag{2.22}$$

The Majorana mass term can be suited to describe charge neutral fermions, and thus the neutrinos could possibly have a Majorana-component in its mass term. Observation of neutrinoless double beta decay could imply this [5].

2.2.1 Charge Conjugation in the Weyl Basis and the Majorana Field

In the Weyl basis the we have the Dirac field ψ in terms of the Weyl spinors λ_α and $\bar\chi^{\dot\alpha}$ as in Eq. (2.18). The chargec onjugated field is then [6]

$$\psi^c = \begin{pmatrix}\chi_\alpha \\ \bar\lambda^{\dot\alpha}\end{pmatrix}. \tag{2.23}$$

A Majorana field must satisfy the Majorana condition $\psi^c = C\bar{\psi}^T$ and introduce the Majorana spinor in the chiral basis

$$\psi_M = \begin{pmatrix} \chi_\alpha \\ \bar{\chi}^{\dot{\alpha}} \end{pmatrix}. \tag{2.24}$$

Writing out the Lagrangian in Eq. (2.21) in terms of the left- and right-handed components of the general Dirac field ψ in Eq. (2.18) yields

$$\mathcal{L} = \frac{1}{2}\left(\chi i\sigma^\mu \partial_\mu \bar{\chi} + \bar{\lambda} i\bar{\sigma}^\mu \partial_\mu \lambda - m(\lambda\lambda + \bar{\chi}\bar{\chi})\right) + \text{h.c.}. \tag{2.25}$$

We note how the mass term is different from the Dirac mass term $m_{\text{Dirac}}(\chi\lambda + \bar{\lambda}\bar{\chi})$. Inserting for the Majorana spinor in Eq. (2.28) gives

$$.\mathcal{L}_{\text{Majorana}} = \chi i\sigma^\mu \partial_\mu \bar{\chi} - \frac{1}{2} m(\chi\chi + \bar{\chi}\bar{\chi}) \tag{2.26}$$

Where we do not add the hermition conjugate for a self-conjugate expressions, as this will give the correct overall normalization for the Majorana field. In four component notation the Lagrangian in Eq. (2.26) is equal to

$$\mathcal{L}_{\text{Majorana}} = \frac{1}{2}\left(\bar{\psi}_M i\partial\!\!\!/ \psi_M - m\bar{\psi}_M \psi_M\right) \tag{2.27}$$

2.2.2 The Quantized Majorana Field

In four component notation we describe the propagation of Majorana fermions by the Lagrangian in Eq. (2.21). For Majorana the equation of motion is the Majorana equation in Eq. (2.22), equivalently, the Dirac equation under the Majorana condition $\psi_M^c = \psi_M$.

Ettore Majorana found a basis for the Dirac matrices in where the components of these are purely imaginary [7]. In this basis the Dirac equation has only real coefficients and therefore well suited for discussing real solutions to the Dirac equation, i.e. fields satisfying $\psi = \psi^*$, which in an arbitrary basis translates to $\psi = \psi^c$ [8].

The free Majorana field (i.e. the solution to Eq. (2.22) where $\psi_M = \psi_M^c$) can be represented by the Fourier expansion [8, 9]

$$\psi_M(x) = \sum_{s=\pm 1/2} \int \frac{\mathrm{d}^3 p}{(2\pi)^3} \frac{1}{\sqrt{2E_{\mathbf{p}}}} \left[b_{\mathbf{p}}^s u^s(p) e^{-ipx} + b_{\mathbf{p}}^{s\dagger} v^s(p) e^{ipx}\right]. \tag{2.28}$$

Where $b_{\mathbf{p}}^s$ are Fourier coefficients, $E_{\mathbf{p}} = \sqrt{m_\chi^2 + \mathbf{p}^2}$, and $u^s(p)$ and $v^s(p)$ are solutions to the momentum-space Dirac equation. The Majorana condition forces

the fourier coefficients to be complex conjugate of each other. Complex conjugation for the Fourier coefficients is denoted in by a †, since these will be particle creators and annihilators upon quantizing ψ_M. We get the quantized Majorana field by imposing the commutation relations for the Fourier coefficients

$$\left\{b^r_{\mathbf{p}}, b^{s\dagger}_{\mathbf{q}}\right\} = (2\pi)^3\delta^{rs}\delta^{(3)}(\mathbf{p}-\mathbf{q}). \tag{2.29}$$

The free vacuum $|0\rangle$ can get excited to a one particle state by applying $\sqrt{2E_{\mathbf{p}}}b^\dagger_{\mathbf{p}}$ to it. We then denote

$$|\mathbf{p}, s\rangle = \sqrt{2E_{\mathbf{p}}}b^{s\dagger}_{\mathbf{p}}\,|0\rangle\,. \tag{2.30}$$

We will suppress the spin-index and denote a one-particle excitation of the free vacuum by $|\mathbf{p}\rangle_0$, and a multiparticle state by

$$\prod_{i=1}^{n}\sqrt{2E_{\mathbf{p}_i}}b^{s_i\dagger}_{\mathbf{p}_i}\,|0\rangle = |\mathbf{p}_1\rangle_0 \otimes \ldots \otimes |\mathbf{p}_n\rangle_0 \equiv |\mathbf{p}_1, \ldots, \mathbf{p}_n\rangle_0\,. \tag{2.31}$$

When multiple creation operators excite the vacuum, the order in which they act is important due to the anti commutation relation. Furtheremore any interchange of two particle creation operators in Eq. (2.31) will change the overall sign, which is consistent for a set of particles obeying Fermi-Dirac statistics. For an outgoing Majorana particle we define the contraction

$$\begin{aligned}\overbrace{\psi_M(x)|\mathbf{q}\rangle}_0 &\equiv \psi_M(x)|\mathbf{q}\rangle_0 \\ &= e^{-iqx}u(q)\,|0\rangle\,.\end{aligned} \tag{2.32}$$

And we also have

$$\begin{aligned}\overbrace{\bar{\psi}^T_M(x)|\mathbf{q}\rangle}_0 &\equiv \bar{\psi}^T_M|\mathbf{q}\rangle_0 \\ &= e^{-iqx}\bar{v}^T(q)\,|0\rangle\,.\end{aligned} \tag{2.33}$$

Contrary to Dirac fermions, where the expansion corresponding to Eq. (2.28) has distinct operators since it is not subjected to the Majorana condition.
We will use the Feynman rules for fermions as in [Ref Peskin], Feynman rules for Majorana fermions are also taken from [9].

2.3 Non Abelian Gauge Theory

All interactions in the SM relies on the principle of exploiting the gauge symmetries of the theory. We start out by considering N free Dirac fields with the same mass m. They are described by the Lagrangian

$$\mathcal{L}_0 = \bar{\psi}_a\left(\delta_{ab}i\partial\!\!\!/ - \delta_{ab}m\right)\psi_b, \tag{2.34}$$

where we we have introduced the multiplet $(\psi_a) = (\psi_1, \ldots, \psi_N)^T$. In Eq. (2.34) we have for clarity included the summation indices $a, b = 1, \ldots, n$ which we will omit from now on and refer to ψ as the multiplet of Dirac fields. Lagrangian in Eq. (2.34) is invariant under the transformation in the fundamental representation of $SU(N)$. By applying the exponential map we can write a $V \in SU(N)$ as

$$V = e^{i\theta_j t_j}, \tag{2.35}$$

where the θ_j's are real constants, and the summation index j runs from 1 to N^2-1. The $n \times n$ matrices t_j are the generators in the fundamental representation of $SU(N)$. The generators span a $n^2 - 1$ dimensional vector space which forms the Lie algebra for $SU(N)$ together with the commutation relation

$$[t_i, t_j] = i f_{ijk} t_k \tag{2.36}$$

The gauge parameters θ_j are real numbers for a *global* $SU(N)$ transformation. We get a local $SU(n)$-transformation by making θ_j functions of spacetime $\theta_j \to \theta_j(x)$. If we transform the multiplet under a local $SU(N)$ transformation in Eq. (2.34) the kinetic term will pick up an extra term

$$\mathcal{L}_0 \overset{SU(n)}{\to} \bar{\psi}\left(i\partial\!\!\!/ - m\right)\psi + V^\dagger i\partial\!\!\!/ V \tag{2.37}$$

$$= \mathcal{L}_0 + U^\dagger i\partial\!\!\!/ U \neq \mathcal{L}. \tag{2.38}$$

And the Lagrangian is clearly not invariant under local $SU(2)$ transformations. However, we can modify the differential operator by introducing the *connection* $A^i_\mu(x)$ in the *covariant derivative*

$$D_\mu = \partial_\mu - igt^i A^i_\mu \tag{2.39}$$

The connection is now $n^2 - 1$ independent gauge-fields $A^\mu_i(x)$. We now make the substitution $\partial_\mu \to D_\mu$ in Eq. (2.34), and if the new Lagrangian is to be invariant with respect to local $SU(N)$-transformations we can derive the transformation property for the gauge fields under such a transformation. If we demand that the Lagrangian is invariant under a local transformation $U \in SU(n)$ we must have

$$D_\mu \psi \overset{SU(n)}{\to} U D_\mu \psi, \tag{2.40}$$

Which will result in the desired transformation property of the $SU(n)$ gauge fields. We have

$$D_\mu \Psi = (\partial_\mu - igt^i A^i_\mu)\Psi \overset{SU(n)}{\to} (\partial_\mu - ig(t^i A^i_\mu)')U\Psi$$

$$= U\left(U^\dagger \partial_\mu U + \partial_\mu - igU^\dagger t^i A'^i_\mu U\right)\Psi.$$

And we see that Eq. (2.40) is fulfilled only if

$$U^\dagger t^i A'^i_\mu U + \frac{i}{g} U^\dagger \partial_\mu U = t^i A^i_\mu. \tag{2.41}$$

We have $U\partial_\mu U^\dagger = -(\partial_\mu U)U^\dagger$ so the general transformation property of the gauge fields can be written as

$$t^i A'^i_\mu = U\left(t^i A^i_\mu + \frac{i}{g}\partial_\mu\right)U^\dagger,$$

for any local $U \in SU(n)$. We define the *field tensor* $F^j_{\mu\nu}$ from the commutator of the covariant deriative with itself. The field tensor is given by

$$\begin{aligned}[D_\mu, D_\nu] &= igt^i\left(\partial_\mu A^i_\nu - \partial_\nu A^i_\mu\right) - ig^2 f^{ijk} t^i A^j_\nu A^k_\mu \\ &\equiv igt^i F^i_{\mu\nu}.\end{aligned}$$

where $F^i_{\mu\nu} = \partial_\mu A^i_\nu - \partial_\nu A^i_\mu - g\epsilon^{ijk} A^j_\nu A^k_\mu$ is the $SU(N)$ field tensor. Due to its definition the field strength inherits the transformation property under local $SU(N)$-transformations from D_μ, thus it is not gauge invariant since it transforms as

$$t^i F^i_{\mu\nu} \overset{SU(N)}{\to} V t^i F^i_{\mu\nu} V^\dagger. \tag{2.42}$$

We can make a gauge invariant term from tracing over the generators. The term

$$\begin{aligned}\mathrm{tr}\left[t^i F^i_{\mu\nu} t_j F^{\mu\nu}_j\right] &\overset{SU(N)}{\to} \mathrm{tr}\left[V t^i F^i_{\mu\nu} V^\dagger V t_j F^{\mu\nu}_j V^\dagger\right] \\ &= \mathrm{tr}\left[t^i t_j\right] F^{\mu\nu}_j F^i_{\mu\nu}.\end{aligned} \tag{2.43}$$

And in the fundamental representation the generators satisfy $C(N)\delta^i_j = \mathrm{tr}\left[t^i t_j\right]$, where $C(r)$ is just a number which depends on the irreducible representation r of the generators t^i_r. In the fundamental representation it is $C(N) = 1/2$. With the correct normalization factor in for the contracted field tensor we can write down the Lagrangian

$$\mathcal{L}_{\mathrm{YM}} = \bar{\Psi}\left(i\not{D} - m\right)\Psi - \frac{1}{4}F^{\mu\nu}_i F^i_{\mu\nu}. \tag{2.44}$$

It is called the Yang-Mills Lagrangian, and it is invariant under local $SU(N)$-gauge transformations. The contracted field tensor represent the kinetic energy of the gauge fields just as for QED, however, due to the $\propto g$-term in $F^{\mu\nu}_i$ it also contains other terms. We have

$$\begin{aligned}-\frac{1}{4}F^i_{\mu\nu}F^{\mu\nu}_i = &-\frac{1}{4}\left(\partial_\mu A^i_\nu - \partial_\nu A^i_\mu\right)^2 + \frac{1}{2}gf^{ijk}A^j_\nu A^k_\mu\left(\partial^\mu A^\nu_i - \partial^\nu A^\mu_i\right) \\ &- \frac{1}{4}g^2 f^{ijk} f^{ilm} A^\nu_l A^\mu_m A^j_\nu A^k_\mu.\end{aligned} \tag{2.45}$$

Where the squared term is a full contraction of all gauge- and spacetime indices. We recognize the first term as the Lagrangian of a free abelian gauge field account for propagation of the gauge fields, in addition we also see three and four point self-interactions.

Prelude to Electroweak Theory

We will first consider a theory for a single, massless, free Dirac fermion fields ψ, by inserting for the left- and right-handed components $\psi = \psi_L + \psi_R$ we can state the Lagrangian in the following form

$$\mathcal{L}_{\text{Dirac}} = \bar{\psi}_L i\partial\!\!\!/ \psi_L + \bar{\psi}_R i\partial\!\!\!/ \psi_R. \tag{2.46}$$

We will now make the $U(1)$ transformations of the left- and right-handed components

$$\psi_L \to \psi_L{}' = e^{iy_L\theta}\psi_L \tag{2.47}$$
$$\psi_R \to \psi_R{}' = e^{iy_R\theta}\psi_R \tag{2.48}$$

Where y_L, y_R are the $U(1)$-charges, the gauge parameter θ are real numbers. The Lagrangian in Eq. (2.46) is invariant under such local transformations. Note that a mass term would not be gauge invariant if $y_L \neq y_R$, as they generally are. For SM-fields we will refer to Y_L, y_R as *hypercharges* and denote the abelian symmetry group as $U(1)_Y$. The Lagrangian for an arbitrary number massless fermions can be written as

$$\mathcal{L} = \sum_{i=1}^{n} \left((\bar{\psi}_i)_L \; i\partial\!\!\!/ \; (\psi_i)_L + (\bar{\psi}_i)_R \; i\partial\!\!\!/ \; (\psi_i)_R \right), \tag{2.49}$$

The $U(1)_Y$ charges $y_{i,L}, y_{i,R}$ can, generally, all be distinct for all fields.

For further discussion relating this to the SM we will restrict the field content to be $N = 2$ fermion fields. However, similar discussion can be made for arbitrary N.

Aiming at the Electroweak interactions of the standard model we set the hypercharges for the left-handed fields equal $y_{1,L} = y_{2,L} = y_L$ and keep the hypercharges for the right-handed fields general. We also introduce the doublet

$$\mathbf{\Psi}_L = \begin{pmatrix} (\psi_1)_L \\ (\psi_2)_L \end{pmatrix}, \; \bar{\mathbf{\Psi}}_L = \left((\bar{\psi}_1)_L, (\bar{\psi}_2)_L \right) \tag{2.50}$$

We can write the Lagrangian in Eq. (2.49) as

$$\mathcal{L} = \bar{\mathbf{\Psi}}_L i\partial\!\!\!/ \mathbf{\Psi}_L + \sum_{i=1}^{2} (\bar{\psi}_i)_R \; i\partial\!\!\!/ \; (\psi_i)_R. \tag{2.51}$$

And we immediately recognize a global $SU(2)_L$ symmetry for doublet $\mathbf{\Psi}$ in addition to the global $U(1)_Y$ symmetry. Applying the gauge principle as outlined in Sec. 2.3, by making these symmetries we introduce the $SU(2)_L$ gauge fields A^a_μ

$i = 1, 2, 3$ and the $U(1)_Y$ gauge field B_μ. The covariant derivative then acts on the field $\mathbf{\Psi}_L$ and the right-handed fields as

$$D_\mu = \left(\partial_\mu - igt^a W_\mu^a - ig' y_L B_\mu\right) \mathbf{\Psi}_L \tag{2.52}$$

$$D_\mu = \left(\partial_\mu - ig' y_{i,R} B_\mu\right) (\psi_i)_R, \tag{2.53}$$

where g is the $SU(2)_L$ coupling and g' is the $U(1)_Y$ coupling. The generators for $SU(2)$ in the fundamental representation are $\sigma^i/2$ where σ^i are the Pauli matrices, i.e. $t^a = \sigma^a/2$. The commutation relation in the corresponding Lie algebra is $[t^a, t^b] = i\epsilon^{abc}t^c$ where the structure constants ϵ^{abs} are the components of the three dimensional Levi-Civita tensor. For the abelian gauge symmetry we do not have a set of generators, however, all the results from Sec. 2.3 still holds by neglecting the structure constants. We define the field tensors from the commutator of the general covariant derivative with itself as in Eq. (2.42) with the covariant derivative in Eq. (2.52)

$$W_{\mu\nu}^i = \partial_\mu W_\nu^i - \partial_\nu W_\mu^i + g\epsilon^{ijk} W_\mu^j \, W_\nu^k \tag{2.54}$$

$$B_{\mu\nu} = \partial_\mu B_\nu - \partial_\nu B_\mu. \tag{2.55}$$

Then we have arrived at the electroweak Lagrangian for the massless fermions ψ_1 and ψ_2

$$\begin{aligned} \mathcal{L}_{\mathrm{SU(2)_L \times U(1)_Y}} =& \bar{\mathbf{\Psi}}_L i\not{D} \mathbf{\Psi}_L + \sum_{i=1}^{2} (\bar{\psi}_i)_R \, i\not{D} \, (\psi_i)_R \\ & - \frac{1}{4} W_{\mu\nu}^i W_i^{\mu\nu} - \frac{1}{4} B^{\mu\nu} B_{\mu\nu}. \end{aligned} \tag{2.56}$$

2.3.1 Spontaneous Symmetry Breaking and Goldstone's Theorem

Before we indulge the Higgs mechanism in the SM we state how the process of spontaneous symmetry breaking (SSB) occurs for a multiplet $\Phi = (\phi^a)$, $a = 1, \ldots, N$. We consider the Lagrangian

$$\mathcal{L} = \partial_\mu \phi^a \partial^\mu \phi^a - V(\Phi), \tag{2.57}$$

where the *potential* $V(\Phi)$ is non-zero when the fields ϕ^a minimizes the total energy of the system. This is obtain for a potential of the form in Fig. 2.1, written for the multiplet Φ it is

$$V(\Phi) = \frac{1}{2}\mu^2 \phi^a \phi^a + \frac{\lambda}{4}(\phi^a \phi^a)^2. \tag{2.58}$$

For $\mu^2 < 0$ and $\lambda > 0$ the minimum of the potential will be non-zero. The fields occupying the ground state will be the constant value Φ_0 which minimizes V,

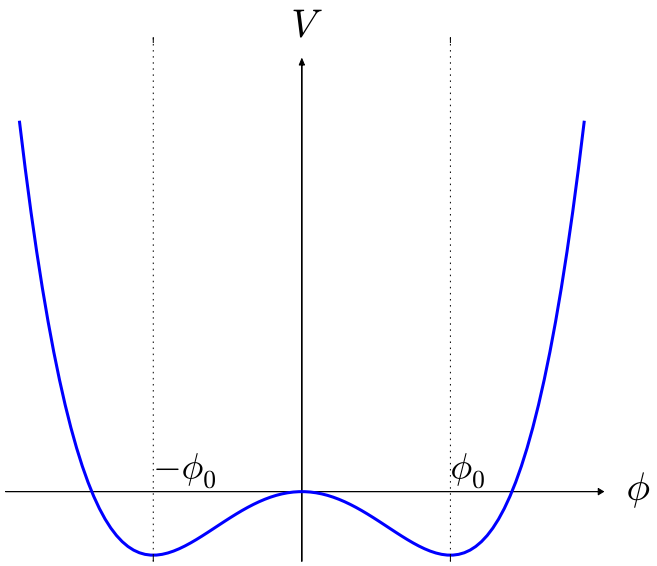

Figure 2.1: The Higgs potential of a single real scalar field ϕ, $V(\phi) = \frac{1}{2}\mu^2\phi^2 + \frac{\lambda}{4}\phi^4$. The field values at the two lower extrema of the potential are $\pm\phi_0$.

this the referred to as the vacuum expectation value (VEV). We assume that the vacuum expectation value is $\langle\Phi\rangle_v = \Phi_0$ with the (generally) non-vanishing components ϕ_0^a. We assume from now on that the potential is general, but with the desired property of Fig. 2.1. Expanding the potential around its minimum gives

$$V(\Phi) = V(\Phi_0) + \frac{1}{2}(\phi^a - \phi_0^a)(\phi^b - \phi_0^b)\frac{\partial^2 V}{\partial\phi^a\partial\phi^b}\bigg|_{\Phi=\Phi_0} + \cdots . \tag{2.59}$$

The matrix $\frac{\partial^2 V}{\partial\phi^a\partial\phi^b}\Big|_{\Phi=\Phi_0} = m_{ab}^2$ can be diagonalized by an orthogonal matrix W, and the fields $\tilde{\phi}^a = W^{ab}(\phi - \phi_0)^b$ attains a mass equal to one of the eigenvalues of m_{ab}^2. Since the mass matrix is the Hessian of V with respect to the fields, the masses must be non-negative since the Hessian V is positive (semi-)definite at a minimum of V. We will now see that there is a one-to-one correspondence between the vanishing eigenvalues of m_{ab}^2 and the spontaneously broken symmetries in the ground state.

We assume that the Lagrangian in Eq. (2.57) is invariant under symmetry transformations belonging to a Lie group G. An infinitesimal transformation of the components of Φ can be written as

$$\phi^a \to \phi^a + \epsilon^i f^i(\Phi)^a, \tag{2.60}$$

where ϵ_i are infinitesimal parameters, and the summation over i runs over n independent symmetry transformations. For instance, if the fields where complex an infinitesimal $SU(N)$ in an irreducible representation r then the transformation is specified by $f^i(\Phi)^a = i(t_r^i)^{ab}\phi^b$, with $i = 1, \ldots N^2 - 1$, i.e., runs over the number of generators which is the independent $SU(N)$ symmetry transformation that can be performed of ψ^a. However, we will consider the transformation in Eq. (2.60) to be completely general. Since the Lagrangian in Eq. (2.60) is invariant with respect to the constant transformation in Eq. (2.60) by assumption, then the potential must be invariant

$$V(\phi^a) = V\left(\phi^a + \epsilon^i f^i(\Phi)^a\right) \tag{2.61}$$

$$= V(\phi^a) + \epsilon^i f^i(\Phi)^a \frac{\partial V}{\partial \phi^a}. \tag{2.62}$$

Thus, we have, since ϵ^i are arbitrary

$$f^i(\Phi)^a \frac{\partial V}{\partial \phi^a} = 0, \tag{2.63}$$

taking the derivative with respect to the fields and evaluating at the minimum Φ_0

$$f^i(\Phi_0)^a \frac{\partial^2 V}{\partial \phi^a \phi^b}\bigg|_{\Phi=\Phi_0} = 0. \tag{2.64}$$

Where we recognize the matrix m_{ab}^2 defined from Eq. (2.59). We see that for some i two possibilities emerge:

a) The transformation $f^i\left(\Phi_0\right)^a = 0$ leaves the vacuum, and is still a symmetry for small fluctuations about the VEV.

b) The transformation breaks the symmetry $f^i(\Phi_0)^a \neq 0$, but has mass-eigenvalue equal to zero.

This implies that there is a one-to-one correspondence between the number of massless fields, and the number of broken symmetries. These massless fields are referred to as Goldstone bosons and this result is known as *Goldstones theorem*. Even if we proved it here using real scalar fields the theorem generalizes to complex fields as well, as an N complex fields can be written as $2N$ real fields.

The Higgs mechanism is similar in the SM, however here the symmetry is not global but local. This implies that the field which aqcuire VEV interacts with gauge fields. We shall see in the following section that SSB give mass terms to gauge fields by fixing the gauge.

2.4 Feynman Calculus and Higher Order Corrections

Richard Feynman provided a physical picture for performing perturbation theory in particle physics diagramatically through Feynman diagrams. However going to higher order in perturbation theory makes seeming infinites appear when calculating amplitudes.We will take Quantum electrodynamics (QED) to illustrate how higher order corrections can be treated. The QED Lagrangian for a single fermions field ψ (whose excitations are positrons and electrons) is

$$\mathcal{L} = \bar{\psi}\left(i(\partial\!\!\!/ + ieA\!\!\!/) - m_e\right)\psi - \frac{1}{4}F_{\mu\nu}F^{\mu\nu}. \tag{2.65}$$

It is a $U(1)$ (abelian) gauge theory, $F_{\mu\nu}$ is the field tensor and m_e is the electron charge. When calculating higher order contributions for QED would demand calculation of diagrams in Fig. 2.2. The different diagrams in Fig. 2.2 have

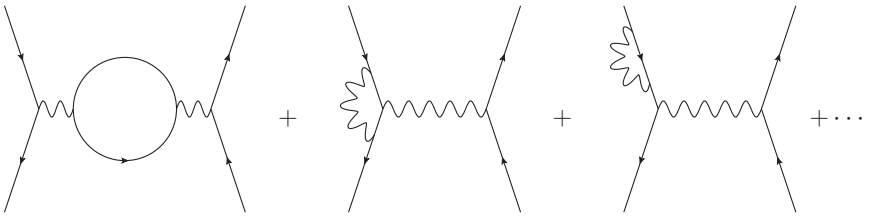

Figure 2.2: Feynman diagrams contributiong to fermion scattering in QED for higher order. All contribution must be added together for the final amplitude. In addition there are finite diagrams that contribute to the same order which we have neglected to draw. Figure made using JaxoDraw [10].

different physical interpretations, and they end up as quantum corrections to the ingredients in the QED Lagrangian. The first diagram where an electron loop appears in the photon propagator account for renormalization of the electron charge. The second diagram is the vertex correction, which accounts for the anamolous magnetic moment of the electron ,$(g-2)_e$ and its infinites cancels with the external leg contribution in the last diagram.

We can clearly see that the diagrams in Fig. 2.2 are divergent. For instance, for the first diagram the momentum integral has the form with the use of QED Feynman rules from [11]

$$I^{\mu\nu}(q; m_e) \propto \int \frac{\mathrm{d}^4k}{(2\pi)^4}\mathrm{tr}\left[\gamma^\mu \frac{1}{(k\!\!\!/ - q\!\!\!/) - m_e}\gamma^\nu \frac{1}{k\!\!\!/ - m_e}\right] \tag{2.66}$$

where q is the momentum carried in the propagator k is the loop momentum, and m_e is the mass of the electron. When the loop variable dominates, the integral

it will go like (ignoring the spacetime structure)

$$I^{\mu\nu} \sim \int_0^\infty |k|^3 \mathrm{d}|k| \ \frac{1}{|k|^2} \to \infty. \tag{2.67}$$

Such divergences for large momenta are referred to as Ultra Violet (UV) divergences. One method for taking care of the UV-divergences is to introduce a cut-off energy Λ for the upper limit. However, this procedure does not breaks gauge invariance [11], as $q_\mu I^{\mu\nu} \neq 0$ for a physical photon with $q^2 = 0$. Another method which preserves gauge invariance is Pauli-Villars procedure, where propagators for several massive fermions are introduced [12]

$$I^{\mu\nu}(q; m_e) \to I^{\mu\nu}(q; m_e) - \sum_i C_i(M_i) I_{\mu\nu}(q; M_i^2),$$

which cuts of smoothly for a large masses M_i^2 and $C_i(M_i^2)$ ensures that the integral converge. Another option, is to use dimensional regularization where the integral is performed in d-spacetime dimensions. We can performing a Wick rotation in the time component of k by the substitution $ik_E^0 = k^0$ and $k_E^i = k^i$, this shifts to Euclidian coordinates from Minkowski as $-k_E^2 = -(k^0)^2 - \mathbf{k}^2$. By Wick rotating we can evaluate the integral using four dimensional spherical coordinates (justifying the asymptotic behavior of the integrand in Eq. (2.67)). Further details on dimensional regularization can be found in appendix B.

The fields (ψ, A_μ) and constants (e, m_e) that are present in the QED Lagrangian are *bare* quantities. They can be rescaled to the to the physical, *renormalized*, quantities (subscripted r) by

$$\begin{aligned} \psi = Z_2^{1/2}\psi_r, \quad A^\mu \ &= Z_3^{1/2} A_r^\mu \\ eZ_2^1 Z_3^{1/2} &= e_r Z_1 \end{aligned} \tag{2.68}$$

The $Z_{2,3}$ are the residues at the poles of the fermion- and photon propagators, respectively when calculating the higher order corrections to them, Z_1 is defined as the scaling for the for the electron charge. Furthermore, the scale factors can be written as $Z_1 = 1+\delta_1$, $Z_2 = 1+\delta_2$ and $Z_3 = 1+\delta_3$. Inserting the renormalized fields in the Lagrangian it can be written as

$$\mathcal{L} = \mathcal{L}_{\text{renormalized}} + \mathcal{L}_{\text{counterterms}}, \tag{2.69}$$

where $\mathcal{L}_{\text{renormalized}}$ is the same Lagrangian as in Eq. (2.65) but with all renormalized quantities. In $\mathcal{L}_{\text{counterterms}}$ all the terms that are proprotional to δ_i occur. The counter terms appear as additional Feynman rules, that needs to be included for every order in perturbation theory, furthermore, they represent the (unobservable) difference between the renormalized quantities and the bare quantities. By setting the renormalization scale we demand, to a given order in perturbation

theory that the amplitude we are calculating corresponds to a measured value at a specific energy. The δs are then determined (to the specific order in perturbation theory) in order to yield a finite amplitude. The physical parameters $m_{e,r}$ and e_r will then correspond to the measured value at the specific energy, and they can be calculated at a different energy to a given order in perturbation theory however their values will change — this is referred to as *running*.

This procedure can be made at each order in perturbation theory in QED, thus QED is *renormalizable*. That is, divergences appear at every order in perturbation theory, however, only a finite number of amplitudes appear to diverge and only a finite number of counterterms are needed (none are needed at tree-level).

It is enough to refer to the mass dimension of the coupling constant in a given theory in order to see if it is renormalizable or not. If the coupling constant is dimensionless or has a positive mass dimension the theory is renormalizable, however, if the coupling constant has a negative mass dimension, all amplitudes diverge at a certain order in perturbation theory. For non-renormalizable theory an infinite number of counterterms are needed to renormalize it, hence renormalization is not possible, and the theory will predict infinite amplitudes.

2.5 Contents of the Standard Model

We will now state the most important features of the Standard Model (SM) of particle physics. It is a theory following from the past $\sim$100 years of development of particle physics. It covers all known interactions between the known fermions, gauge bosons and the Higgs boson. There are two types of fermions as indicated in Fig. 2.3. The leptons and quarks. Quarks are assumed to be the fundamental particles in *hadrons*, up until recently (Aug. 2015) they where only known to form mesons (bound states of two quarks with a short lifetime) and baryons (bound states of three quarks, most are short lived but the proton is stable or has a lifetime comparable to the age of the universe) before observations consistent with a five quark state – the pentaquark – was observed at the LHCb experiment at CERN [13]. In Fig. 2.3 all the particle content of the SM is displayed. The three columns to the left are the known fermions, and the other particles are gauge bosons and one scalar boson. In addition to the 12 fermions in the SM there are also 12 *anti* fermions not displayed in the figure. The anti fermions carry opposite charge but have the same mass and spin properties of the fermions. Reading the fermion columns in Fig. 2.3 left to right we see that they are arranged hierarchically in increasing mass; each column is referred to as a *generation* of fermions according to the mass hierarchy.

There are six distinct types of quark in the SM, often referred to as six *flavors*. It is usual to look at the consider the two types of quarks what we will call the *up*-type quarks, and the *down*-type quarks. The up-type quarks are the *up*- (u), *charm*- (c) and *top* (t) quark, and the down type quarks are the *down*- (d),

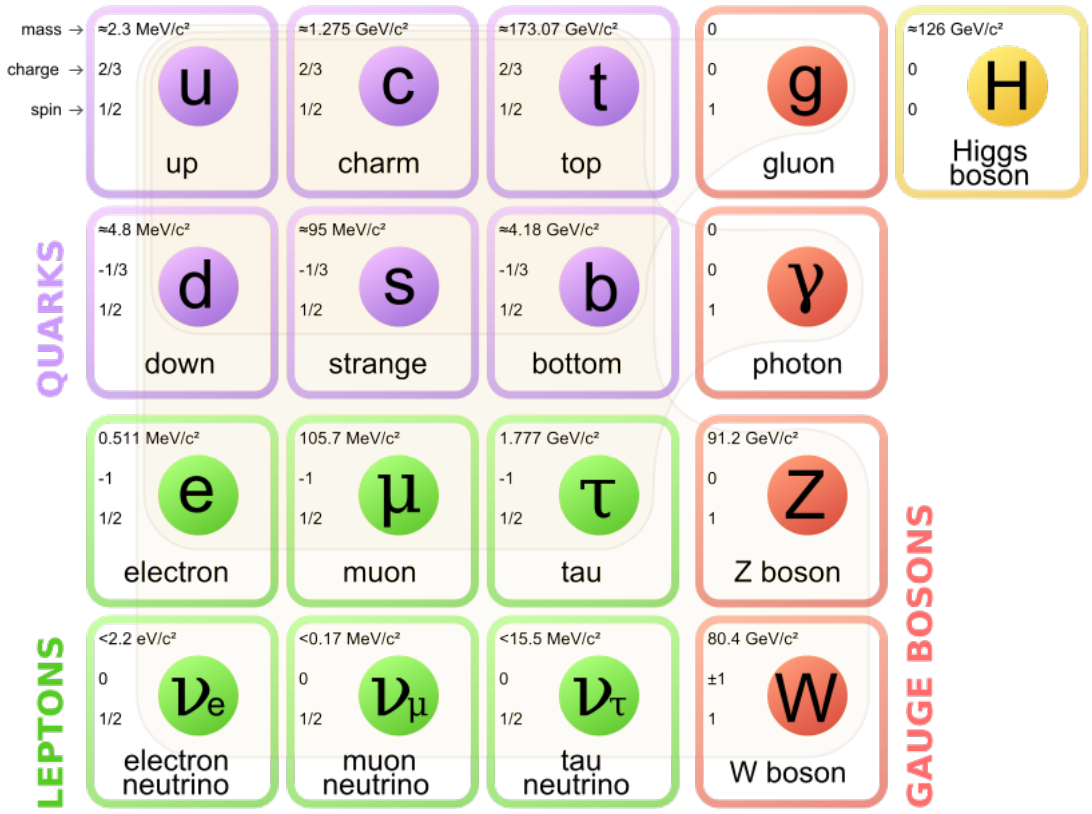

Figure 2.3: The entire particle content of the Standard Model of particle physics. Each tile in the figure refers to an elementary particle, with the mass, charge (in units of $|e|$) and spin is indicated in the upper right corner. The 12 elementary fermions of the model are fitted in the three columns to the left. The upper six (purple) are the quarks – the building blocks for the baryons. The lower six (green) are the known leptons. The force carriers, or gauge bosons, are listed in the complete column to the right (red), and the last piece of the puzzle is the scalar Higgs boson (yellow). From [14]

strange- (s) and *botton* (b) quark. The electromagnetic charges of the quarks are in units of the proton charge $+2/3$ and $-1/3$ for the up- and down- type quarks respectively. Each quark carry an associated flavor quantum number conserved independently in strong and neutral electroweak processes. For example, the top quark has a *topness* quantum number of $+1$ and the bottom quark has *bottomness* of[2] -1, and the charm quark has *charm* of $+1$ (and zero topness, or bottomness), while the strange quark has *strangeness* of -1. The corresponding anti-particles have the same flavor quantum number with opposite sign.

We find six different types of leptons in the SM. The electromagnetically charged leptons are the *electrons* (e),*muons* (μ) and *tau* (τ) -particles. They all

[2]It is conventional that the down type quarks has a negative flavour quantum number.

carry an electromagnetic charge in a single unit of the electron charge. Associated with each charged lepton are the neutrinos, they are charge neutral and were initially postulated by Wolfgang Pauli in 1930, however, Enrico Fermi coined the term *neutrino* [15]. The leptons (both charged and neutrinos) also come with an associated lepton number $L_i = +1$ $i = e, \mu, \tau$, and their respective anti particles carry the same quantum number with opposing sign.

We proceed to look at the different sectors of the SM. The *strong* and *electroweak* sectors are pure gauge theories. In the strong sector interactions among the quarks are found, and the gauge theory is referred to as *Quantum Chromodynamics* (QCD). The electroweak sector is a gauge theory for *massless* fermions and gauge bosons. The mass terms appear in the *Higgs* sector, by fermion and gauge couplings to the scalar Higgs doublet.

The Strong Sector The quarks also have three internal degrees of freedom, known as *color*. That is a quark field is multiplet $q = (q_1, q_2, q_3)^T$. Through this color symmetry the quark multiplets exhibit an $SU(3)$-symmetry, and the Yang-Mills Lagrangian in Eq. (2.44) with $N = 3$ for six distinct multiplets constitutes QCD. However, due to the strength of QCD the quarks rapidly form color singlets as hadrons, hence color charge is never directly observed. We can write the QCD Lagrangian as

$$\mathcal{L}_{\text{QCD}} = \sum_q \bar{q}\gamma^\mu \left(i\partial_\mu - ig_s \frac{\lambda^a}{2} G^a_\mu - m_q \right) q - \frac{1}{4} G^a_{\mu\nu} G^{\mu\nu}_a, \tag{2.70}$$

where the sum is over all quarks $q = u, d, c, s, t, b$, m_q is the mass of quark q, g_s is the strong coupling constant, G^a_μ $a = 1, \ldots, 8$ are gauge fields, λ^a are the Gell-Mann matrices and $\lambda^a/2$ forms the generators of QCD, $G^{\mu\nu}_a$ are the field tensors accounting for the propagation and self interactions of the gauge bosons. Due to the self-interactions of the gauge bosons of QCD (called gluons) the QCD charge exhibits an anti-screening effect, which effectively results in a stronger force at low energies. QCD is at low energies (below $\sim$200 MeV) not well understood, as this is in the so-called unperturbative regime of the theory which makes calculations practically unsolvable.

The Electroweak Sector The electroweak sector is also a gauge theory for fermions, however the left- and right-handed components of the fermion fields are treated differently and the fermions are massless. The fermions (except the neutrinos) will get Dirac mass terms from interactions to the Higgs doublet. In Sec. 2.3 we laid the groundwork for the electroweak interactions for two massless Dirac fermions. We define the $SU(2)_L$ doublets for quarks as

$$Q^i = \begin{pmatrix} u^i \\ d^i \end{pmatrix}_L = \left\{ \begin{pmatrix} u \\ d \end{pmatrix}_L, \begin{pmatrix} c \\ s \end{pmatrix}_L, \begin{pmatrix} t \\ b \end{pmatrix}_L \right\}, \tag{2.71}$$

and note that the color degree of freedom is suppressed, i.e. u^i and d^i are multiplets with three right-handed fermion fields. The $SU(2)_L$ doublets for the leptons are defined as

$$L^i = \begin{pmatrix} \nu^i \\ \ell^i \end{pmatrix}_L = \left\{ \begin{pmatrix} \nu_e \\ e \end{pmatrix}_L, \begin{pmatrix} \nu_\mu \\ \mu \end{pmatrix}_L, \begin{pmatrix} \nu_\tau \\ \tau \end{pmatrix}_L \right\} \tag{2.72}$$

, The for the right-handed fields we define $u^i_R = (u_R, c_R, t_R), (d^i_R) = (d_R, s_R, b_R)$,. and for the leptons we define $\ell^i_R = (e_R, \mu_R, \tau_R)$. We will not make a definition of the right-handed neutrinos as they ave zero hypercharge in the SM. We remark that the hypercharges are independent of the generation index i, however, different for the leptons and quarks. We can now simply state the Electroweak Lagrangian making substituting the quark- and lepton doublets for $\mathbf{\Psi}_L$ in Eq. (2.56) and the lepton quark singlets for ψ_i in Eq. (2.56). We then get the Lagrangian

$$\begin{aligned} \mathcal{L}_{\text{EW}} = &\bar{Q}^i \; i\not{D} \; Q^i + \bar{u}^i_R \; i\not{D} \; u^i_R + \bar{d}^i_R \; i\not{D} \; d^i_R \\ &+ \bar{L}^i \; i\not{D} \; L^i + \bar{\ell}^i_R \; i\not{D} \; \ell^i_R \\ &- \frac{1}{4} W^j_{\mu\nu} W^{\mu\nu}_j - \frac{1}{4} B^{\mu\nu} B_{\mu\nu}, \end{aligned} \tag{2.73}$$

By including the gluon self-interctions and propagation ter $-\frac{1}{4} G^a_{\mu\nu} G^{\mu\nu}_a$ we have the locally $SU(3)_C \times SU(2)_L \times U(1)_Y$-symmetric where the general covariant derivative is

$$D_\mu = \partial_\mu - i g_s Q_C \frac{\lambda^a}{2} G^a_\mu - i g Q_I \sigma^j W^j_\mu - i g' \frac{Y}{2} B_\mu \tag{2.74}$$

where the Q_C, Q_I and Y have values in the SM according to table 1.1. We note that we have extracted an additional factor of $1/2$ for what we now will refer to as hypercharge Y. In table 1.1. we have also included the hypercharge for a complex

Field	Q_C	Q_I	Y
Q^i	1	1	1/3
u^i_R	1	0	4/3
d^i_R	1	0	-2/3
L^i	0	1	-1
ℓ^i_R	0	0	-2
Φ	0	1	1

Table 2.1: The values for the charges in the covariant derivative for fields in the SM.

scalar doublet Φ. This is the Higgs doublet, and through its gauge couplings in the covariant derivative the massive $W^\pm$- and $Z-$ bosons will emerge.

Higgs sector The Higgs part of the SM can be written as the Lagrangian

$$\mathcal{L}_{\text{Higgs}} = |D_\mu \Phi|^2 - V(\Phi), \tag{2.75}$$

where Φ is

$$\Phi = \begin{pmatrix} \phi^{(+)} \\ \phi^{(0)} \end{pmatrix}, \tag{2.76}$$

where $\phi^{(+)}$ and $\phi^{(0)}$ are complex scalar fields. The covariant derivative acts on Φ according to Eq. (2.74) with the charges non-zero charges Q_I and Y are specified in table 1.1 The potential have the assumed form

$$V(\Phi) = \mu^2 |\Phi|^2 + \frac{\lambda}{4} |\Phi|^4. \tag{2.77}$$

The potential makes the Higgs doublet to take a non-vanishing VEV, which will break the $SU(2)_\times U(1)_Y$ symmetry, and leave one massive scalar field (the physical Higgs field), and three Goldstone bosons, one for each broken symmetry. However, the Goldstone bosons will not appear if we consider a *unitary gauge*, which we define below. First, we can write the Higgs doublet in terms of a local $SU(2)_L \times U(1)_Y$ as

$$\Phi = U(x) \begin{pmatrix} 0 \\ \frac{1}{\sqrt{2}} H(x) \end{pmatrix}. \tag{2.78}$$

Where H is a real scalar field. The transformation $U(x)$ has the form

$$U(x) = e^{i\theta^i(x)\frac{\sigma^i}{2}} e^{i\beta(x)}. \tag{2.79}$$

Due to the form of the potential V. In unitary gauge we fix the gauge parameters $\theta^1(x) = \theta^2(x) = 0$ and $\theta^3(x) = \beta(x)$, this leaves the lower component of Φ invariant. We expand H about the VEV

$$H(x) = h(x) + v, \tag{2.80}$$

where v is the VEV and $h(x)$ is a real scalar field with vanishing VEV. In unitary gauge we find

$$|D_\mu \Phi|^2 = \frac{1}{2}(\partial_\mu h)^2 + \left(\frac{g^2}{8} v^2 |W_\mu^1 - i W_\mu^2|^2 + \frac{v^2}{8} (g W_\mu^3 - g' B_\mu)^2 \right) \left(1 + \frac{h}{v} \right)^2. \tag{2.81}$$

Inserting Eq. (2.80) for H we get mass terms for superpositions of the $SU(2)_L$ and $U(1)_Y$ gauge bosons. We define the massive $W^\pm$ boson as

$$W_\mu^\pm = \left(\frac{1}{\sqrt{2}} W_\mu^1 \mp i W_\mu^2 \right), \tag{2.82}$$

and the massive Z-boson as

$$Z_\mu = \frac{1}{\sqrt{g^2+g'^2}}\left(gW_\mu^3 - g'B_\mu\right). \tag{2.83}$$

They have the masses

$$m_W = \frac{g^2}{2}v^2, \;\; m_Z = \sqrt{g^2+g^2}\frac{v^2}{2} \tag{2.84}$$

Defining the mixing angles

$$\sin\theta_W = \frac{g'}{\sqrt{g^2+g'^2}}, \quad \cos\theta_W = \frac{g}{\sqrt{g^2+g'^2}}, \tag{2.85}$$

clarifies that the definition of the Z-boson is a rotation in the (W_μ^3, B_μ) - plane. There is another superposition orthogonal to the superposition in Eq. (2.83) and this is the photon A_μ which does not get a mass from the SSB. The mixing in of (W^3, B) can be written as

$$\begin{pmatrix} Z_\mu \\ A_\mu \end{pmatrix} = \begin{pmatrix} \cos\theta_W & -\sin\theta_W \\ \sin\theta_W & \cos\theta_W \end{pmatrix} \begin{pmatrix} A_\mu^3 \\ B_\mu \end{pmatrix}.$$

This concludes the mass generation of the $W^\pm$- and Z- boson. Due to the choice of unitary gauge, the Goldstone bosons in the scalar Higgs doublet are not apparent as separate degrees of freedom. However, their degrees of freedom appears as the massive gauge bosons, as massive vector fields also have longitudinal polarizations in addition to the two degrees of freedom in the transverse polarizations.

We can now rewrite the covariant derivative from Eq. (2.74) in terms of the photon A and $W^\pm$-, Z-bosons

$$\begin{aligned} D_\mu =& \partial_\mu - g_s\frac{\lambda^a}{2}G_\mu^a - iQ_I\frac{g}{\sqrt{2}}\left(W_\mu^+\sigma^+ + W_\mu^-\sigma^-\right) \\ & - i\frac{g}{\cos\theta_W}Z_\mu\left(Q_I\frac{\sigma^3}{2} - \sin^2\theta_W\mathcal{Q}\right) \\ & - ig\sin\theta_W\mathcal{Q}A^\mu, \end{aligned} \tag{2.86}$$

where $\sigma^\pm = \frac{1}{2}(\sigma^1 \pm i\sigma^2)$, and we have introduced the charge matrix

$$\mathcal{Q} = Q_I\frac{\sigma^3}{2} + \frac{Y}{2}, \tag{2.87}$$

and we see that the fields get the corresponding as the particles in Fig. 2.3 charges according to the weak isospin Q_I and the hypercharge Y from table 1.1. in units of $e = g\sin\theta_W$ where e is the electron charge.

We can form $SU(3)_C \times SU(2)_L \times U(1)$ invariant couplings between fermions and the Higgs doublet

$$\mathcal{L}_{\text{Hff}} = - y_d^{ij} \bar{Q}^i \Phi \; d_R^j - y_u^{ij} \bar{Q}^i \hat{\Phi} \; u_R^j + \text{h.c.} \tag{2.88}$$

$$- y_\ell^{ij} \bar{L}^i \Phi \; \ell_R^j + \text{h.c.}, \tag{2.89}$$

where $\hat{\Phi} = i\sigma^2 \Phi^*$ is introduced to give mass to the in a manner that is both $U(1)_Y$ and $SU(2)_L$ gauge invariant. After SSB when the Higgs doublet acquires VEV we have in unitary gauge.

$$\begin{aligned} \mathcal{L}_{\text{Hf}} = & - y_d^{ij} v \bar{d}_L^i \; d_R^j - - y_u^{ij} v \bar{u}_L^i \; u_R^j + \text{h.c.} \\ & - y_\ell^{ij} v \bar{\ell}_L^i \; \ell_R^j + \text{h.c.} \\ & + (\text{Yukava interactions with the physical Higgs boson}), \end{aligned} \tag{2.90}$$

where the Yukawa couplings $y_{d/u/\ell}^{ij}$ are diagonal for the physical fields. However, they are not required to be diagonal by the *weak eigenstates* in Eq. (2.71), what then appears are the Dirac mass terms for the charged leptons and the quarks. The mixing of the mass eigenstates to the weak basis for the quarks is quantified by the Cabbibo-Kobayasi-Maskava (CKM) matrix [16, 17] and we shall not go into the details, however, we mention that the CKM matrix contains one complex phase which parametrizes the CP violation in the SM [18]. Furthermore, it also makes it possible for quark interactions across generations. There could be a similar matrix for the leptons, however due to the non-interacting right-handed neutrinos such a matrix disappears from the SM.

Neutrinos in the SM Right-handed neutrinos does not interact with anything in the SM. However, it has been proven experimentally that neutrinos can oscillate across generations [19] suggesting that lepton number is not conserved overall. Neutrinos have been found to have a small mass ($\mathcal{O}(1 \text{ eV})$), but the nature of the mass term is not known (whether it is Dirac or Majorana). Neutrino oscillations suggests that the $\nu_{e,\mu,\tau}$ which take part in weak neutral- and charged currents are not the mass eigenstates. The neutrino mixing is parametrized by the Pontecorvo-Maki-Nakagawa-Sakata [20, 21] (PMNS) matrix, which rotates the mass basis neutrinos $\nu_{i=1,2,3}$ into the lepton number carrying neutrinos $\nu_{e,\mu,\tau}$.

Chapter 3

Extending the Standard Model

Though tremendously successful, the SM still leaves a lot of questions unanswered. Why do seemingly large higher-order contributions to the Higgs mass cancel? How do particles at the subatomic level interact gravitationally? What is the link between the vacuum energy in QFT and the vacuum energy of cosmology? In addition to the matter-particles in the SM there are also conclusive cosmological evidence for a state of matter not found in experiments or theoretical predictions of the SM – another type of matter, not consisting of leptons or quarks, that we know nothing about – Dark Matter (DM).

In this chapter we address some of these unanswered questions, and we shall keep our focus on DM and its history. We will also discuss some possible candidates in pre-existing extensions of the SM, with a focus on Supersymmetric extensions – a class of theories capable of providing adequate answers to some of the problems the SM faces.

3.1 What are we missing?

Hierarchy problem In order to give the measured mass of the Higgs boson of $125.98 \pm 0.42(\text{stat.}) \pm 0.28(\text{sys.})$ GeV [22], divergent higher-order contributions need to cancel. When calculating higher order contributions to its mass, the Higgs self interaction and Yukawa couplings to the fermions, using a cut-off scheme to regularize the divergent loop integrals, the Higgs mass gets a correction of the form

$$\delta m_h^2 = -\frac{|g_f|^2}{8\pi^2}\Lambda^2 + \frac{g_s}{16\pi^2}\Lambda^2 + \cdots , \tag{3.1}$$

where Λ is the cutoff energy of the loop integral, g_f is the Yukawa coupling to the fermions and g_s is the coupling for the Higgs self interaction, the dots indicate finite and less "severe" UV-divergences. The cutoff is typically $\Lambda \sim 10^{19}$ GeV (Planck mass). Hence there must occur a cancellation in Eq. (3.1) between terms

of of order $(10^{19}\ \text{Gev})^2$. The SM does not provide an answer to how, or why, this cancellation occurs.

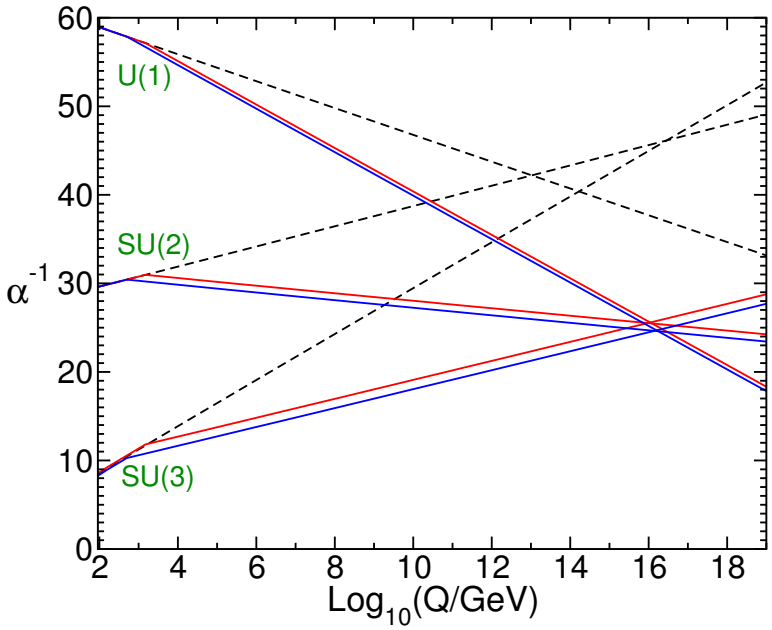

Figure 3.1: Running SM coupling constants (dashed lines) and the Minimal Supersymmetric Standard Model prediction of the running of the coupling constants (red and blue). $\alpha_s(m_z)$ is varied between 0.117 and 0.121. The β-functions for the relevant couplings are calculated to two-loop precision. From [23].

Unification The SM has 19 free parameters which can be seen in Table 2.1. These have to be fixed to fit data from experiments. There are also open questions such as the number fermion generations, as there is no mechanism explaining why there should be only three generations of quarks and leptons. We have no explanation to why the apparent gauge structure of the SM is precisely $SU(3)_C \times SU(2)_L \times U(1)_Y$.

Quantum corrections beyond leading order results in the *running* of the gauge couplings g_s, g, and g (equivalently; $\alpha_s = g_s^2/4\pi$, $\sin\theta_W = g/\sqrt{g^2+g'^2}$ and $\alpha_{\text{EM}} = e^2/4\pi^2$ with $e = g\sin\theta_W$). The running refers to them being energy dependent quantities, and not constants. Good measurements have been made of how these couplings run. For the QCD coupling constant the measurement goes up to energies of 1.4 TeV [24,25]. The electroweak couplings are used for precision tests of the SM, and measurements of the numerical value of α_{EM} are known to to astonishing accuracy experimentally [26,27], agreeing with theoretical predictions up to 10 loop order [28] taking into account both weak and QCD corrections. However, a *Grand Unified Theory* attempt to consider $SU(3)_C \times SU(2)_L \times U(1)_Y$

as the result of spontaneous symmetry breaking of a larger gauge group, would reduce the number of free gauge parameters to one single coupling parameter α_G at some breaking scale M_G. A premise for such unification is that the running gauge coupling constants of the SM intersect at one breaking scale M_G. The SM prediction for the running of the inverse coupling constants g_s^2, g^2 and g'^2 are indicated by the dashed lines in Fig. 3.1. With the current content of the SM, the coupling constants appear to not all intersect at the same energy. However, the three points of intersection are close (though spanning ~ 2 orders of magnitude in energy), which entertains the idea of unification. The colored lines in Fig. 3.1 show the running with additional field content and couplings introduced through an extension of the SM in the Minimal Supersymmetric Standard Model (MSSM). We will return to the MSSM in in Sec. 3.3.

Parameter	
Gauge couplings for $SU(3)_C$, $SU(2)_L$ and $U(1)_Y$ interactions	3
Fermion masses	9
Quark mixing (CKM-matrix)	4
VEV and four-point coupling for the Higgs	2
QCD θ-parameter	1
In total	19

Table 3.1: The free parameters of the SM, not including neutrinos.

Gravity The three fundamental interactions in particle physics are the weak and strong interactions and the electromagnetic interaction. However, this is not the exhaustive list of the known interactions in physics. The missing piece is the gravitational interaction. Including gravitational interactions would imply unifying QFT with Einstein's General Relativity (GR). This would require developing a quantized theory for gravity. However, we can address the Newtonian gravitational potential for two massive objects with masses M, m separated by a distance r

$$V_N(r) = -G_N \frac{Mm}{r}, \tag{3.2}$$

where $G_N = 6.674 \times 10^{-11}\ \frac{\mathrm{Nm}^2}{\mathrm{kg}^2}$ is the gravitational constant. Comparing Eq. 3.2 with the Coulomb potential between two charges of opposite sign in units of e, $V(r) = -\alpha_{\mathrm{EM}}/r$, we recognize G_N as the coupling constant for a quantized theory of gravity. However, in natural units the mass dimension of G_N is -2. This makes gravity fundamentally non-renormalizable, and it produces infinite answers beyond leading order. In a cutoff regularization scheme this might indicate the appearance of new physics at the *Planck mass* $\sqrt{1/G_N} = M_{\mathrm{Planck}} \sim \mathcal{O}(10^{19}\ \mathrm{GeV})$.

It is not necessary to account for gravitational interactions in the SM, as the gravitational attraction is ~ 29 orders of magnitude weaker than the weak interactions below the electroweak scale.

Dark Matter There is now compelling evidence that the content of the Universe is not dominated by the baryonic states of matter described by the SM. More recent observations of the formation of the structures in the universe today can not be explained without an invisible matter component now known as Dark Matter (DM). In order to account for the structures we see in th universe today, this invisible non-baryonic matter is mostly cold, meaning non-relativistic, at the time when these structures started to form. There are no viable DM candidates among the field content of the SM. We will turn to a more thorough discussion of DM in Sec 3.2.

Dark Energy Supernova explosions of type 1a (SNe 1a) have been used as standard candles to measure distances to galaxies. Studies of distances to distant galaxies using SNe 1a [29, 30] have proven that the universe is expanding at an accelerating rate. This is is incorporated in the *cosmological constant* Λ in Einsteins field equations. The cosmological constant is interpreted as the energy density of empty space, referred to as Dark Energy (DE). The measured value of the cosmological constant is very small, $\Lambda \sim (10^{-3}\text{ eV})^4$. In a QFT we can make a rough estimate of the contribution to the vacuum energy by taking into account all diagrams with no external legs and setting the cutoff at the Planck mass $M_{\text{Planck}} \sim 10^{19}$ GeV. This gives a discrepancy of $\Lambda/(M^4_{\text{Planck}}) \sim 10^{-124}$, which is referred to as the *Cosmological Constant Problem*.

3.2 Dark Matter and the Matter-Energy Components of the Universe

The history of evidence for DM spans nearly all of the past century in observational cosmology. However, the idea that the DM must be a significant fraction of the matter-density component of the universe gained momentum in the 1980s as more galaxy clusters and galaxies were studied. We will in this section go through some of the cosmological evidence for DM, leading up to what properties we might expect from DM in particle physics.

Early hints of dark matter In 1933 Fritz Zwicky [31] calculated the required mass to fit with the observations of the motion of the luminous matter (the matter inferred from the observed galaxies and gas which emits electromagnetic radiation, i.e. *visible* matter) in the galaxy cluster "Coma Cluster". Zwicky arrived to the conclusion that the cluster must be more massive than the observed

luminous matter content. He called this excess of matter "dunkle materie", which translates to "dark matter". In 1970 Vera Rubin studied the rotation curves

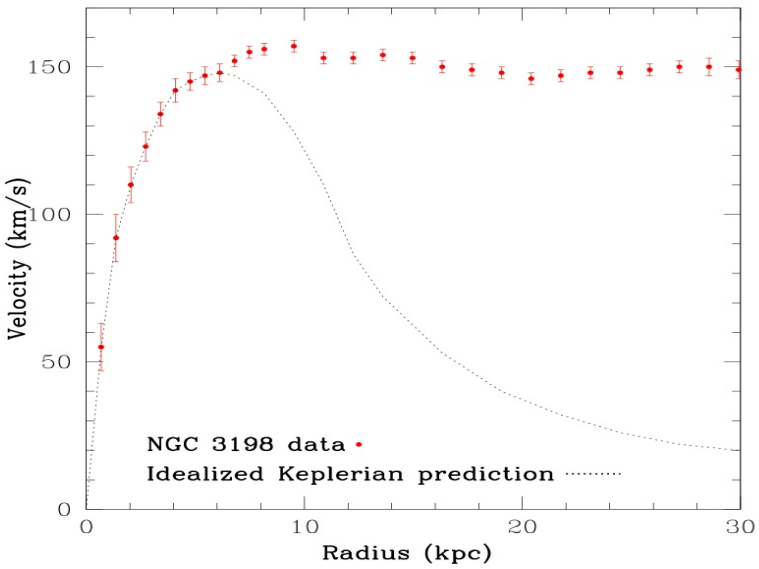

Figure 3.2: Observed rotational velocities (red points) in the spiral galaxy NGC 3198 [32] compared with idealized Keplerian motion (dashed line). Figure from [33].

of several rotating spiral galaxies [34]. Newtonian dynamics predicts that the rotational velocity of objects moving a large radial distances r from the center of the galaxy follows ideal Keplerian motion, such that the velocity goes as $\propto r^{-1/2}$. However, by studying the Doppler shifts for several galaxies, no such fall-off for objects distant from the galactic center was observed, which could be explained if the galaxies are more massive than observations imply.

These were the first two indications of the existence of DM. However, these observations alone are not considered evidence, as a modified theory of gravity could also account for these discrepancies.

Gravitational Lensing The studies put forward by Zwicky and Rubin raises two suspicions; either our descripition of gravity is wrong and needs modification, or they indicate the presence of DM. Further studies of gravitational lensing from galactic clusters provide evidence for deflection of light which can not be explained by the observed amount of luminous matter [36]. Observations of the "Bullet Cluster" in Fig.3.3 provide more conclusive evidence for DM, and of the fact that it must be collisionless, i.e. that DM exhibits no significant self-interactions. In the picture to the left in Fig.3.3 there are two galaxy clusters that have merged. The contours in this picture show the gravitational lensing effect,

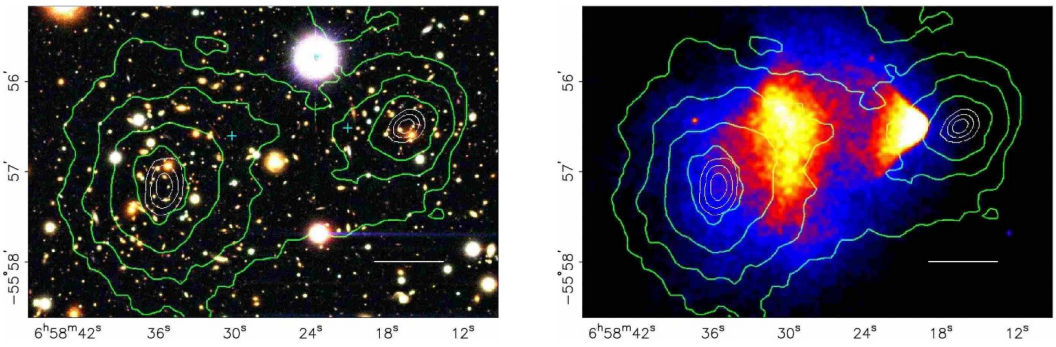

Figure 3.3: Both figures show two galaxy clusters that have collided. The contours in each plot indicate where the gravitational lensing effect is strongest, i.e. where the significant matter components of the galaxy clusters are located. To the right we see the clusters in the optical spectrum. The objects emitting light in this spectrum are galaxies. To the left we see the same image in the X-ray spectrum, and the same contours. The gas in the galaxy clusters have interacted, resulting in hotter gas closer to the collision point, and a larger concentration of gas further from the other matter component. The figure is from [35].

indicating that most of the matter exhibiting gravitational attraction is centered around the galaxy components in the clusters. However, there is not enough luminous matter observed in the galaxy clusters to account for this gravitational lensing effect. In the picture to the right we see the same image in the X-ray spectrum. We see that the gas component of the galaxy clusters have interacted forming a collision front with higher temperature gas indicated by the yellow color. We also see the same contours as in the picture to the left, indicating that most of the matter components on the galaxy clusters have interacted far less in the cluster collision. We observe that the gas in galaxy clusters make up a significantly higher mass fraction of the cluster than the galaxies and objects emitting light in the visible spectrum. Thus, the Bullet Cluster provides direct evidence of DM without significant self-interactions present on the scale of galaxy clusters.

Cosmic Microwave Background In the primordial plasma immediately after the Big Bang, the universe was too hot and dense for electrically neutral hydrogen to form, photons scattered on electromagnetically charged particles at a high rate and as a result the universe was opaque. After the universe had expanded and cooled, neutral hydrogen was able to form (referred to as "recombination"). The photon radiation was still present, but the photons did not interact with matter at the same rate as prior to recombination. Immediately after the photons decoupled from matter in recombination the radiation is well described as that of infrared

black body radiation from a gas at a high temperature. Due to the expansion of the universe, this radiation has been redshifted to the microwave-spectrum and is now observable as the Cosmic Microwave Background (CMB) radiation, which has a current temperature of $\sim 2.725 \pm 0.0057$ K. First discovered by Penzias and Wilson in 1965 [37], the CMB has a nearly uniform temperature. However, small density perturbations in the early universe have resulted in small anisotropies in the temperature of the CMB. These anisotropies have been studied recently by the Planck [38] satellite, and also WMAP [39] before that, in order to describe the densities of the different matter-energy components in the universe today. The density for a given matter component ρ is given in terms of a density parameter Ω as

$$\Omega = \frac{\rho}{\rho_0}, \tag{3.3}$$

where $\rho_0 = \frac{3H^2}{8\pi G_N}$, where H is the Hubble parameter, ρ_0 is the critical density for a flat universe. Combined analyses of the CMB, and of early structure formation known as Baryonic Acoustic Oscillation (BAO) and SNe 1a, results in a non-zero DE-component Ω_Λ versus the total matter content Ω_m as we can see from Fig. 3.4. We state the latest (2015) estimates from the Planck collaboration for the cosmological parameters in the universe today at 68%-confidence from [38]:

$$\begin{array}{ccl} \text{(Baryonic matter)} & \Omega_\mathrm{b}h^2 & = 0.02230 \pm 0.0014 \\ \text{(DM)} & \Omega_\mathrm{DM}h^2 & = 0.1188 \pm 0.0010 \\ \text{(DE)} & \Omega_\Lambda & = 0.6911 \pm 0.062 \\ \text{(Hubble's parameter)} & H_0 & = 67.74 \pm 0.46 \ \frac{\mathrm{km}}{\mathrm{s\ Mpc}} \\ \text{(Universe lifetime)} & t_0 & = 13.799 \pm 0.021 \ \mathrm{Gyr}, \end{array} \tag{3.4}$$

$$h = \frac{H_0}{100\ \mathrm{km^2 s^{-1} Mpc^{-1}}}.$$

The sum of the densities are close to unity, implying that the universe is close to flat, i.e. the "spatial curvature density" $\Omega_k = 1 - \sum_{i=\mathrm{b,DM},\Lambda} \Omega_i = 0.0008^{+0.0039}_{-0.004}$ is small. From the values in Eq. (3.4) we can conclude that we have a close to flat universe dominated by DE ($\sim 69\%$), and the total matter content is $\sim 31\%$, where $\sim 5\%$ is baryonic matter and $\sim 26\%$ is DM.

3.2.1 Hot DM vs. Cold DM

Hot dark matter (HDM) are invisible particles (i.e. not emitting any light) that moved at ultrarelativistic velocities at the time of recombination. If the DM after recombination was dominantly hot, it would predict a structure formation of the universe known as the "top-down" scenario. In this scenario large "pancakes" of matter form after recombination. The pancakes increase in size until they fragment and form the large scale structures of filaments and voids, and eventually

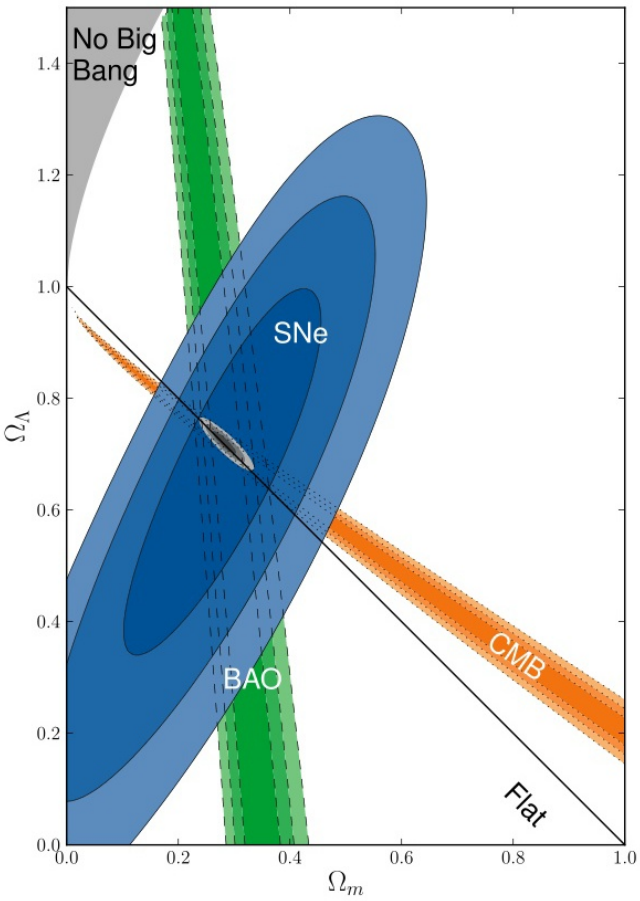

Figure 3.4: Limits on the DE and total matter densities $\Omega_\Lambda, \Omega_\mathrm{m}$ in the universe. The limits are from Baryonic Acoustic Oscillations-, Superovae 1a- and Cosmic Background radiation observations. The black line indicates the matter/DE profile for a flat universe. From [40].

then the super clusters, galaxy clusters and the galaxies we observe today. In short, in the top-down scenario the largest structures form prior to the smaller — clusters and galaxies. Candidates for HDM are light (mass in the eV range) ultrarelativistic particles, e.g. neutrinos.

Cold dark matter (CDM) refers to DM particles moving at low velocities at the time of recombination. This kind of DM would predict a different scenario for the formation of structures in the universe, referred as the "bottom-up" scenario. Here dwarf galaxies form first after recombination and merge into larger galaxies, eventually forming the large-scale structures in the universe.

In the top-down scenario HDM prevents early clustering of smaller galaxies. In contrast, the bottom-up scenario predicts galaxies old enough to be compared

with the lifetime of the universe, which is what we observe. Further observations of the large-scale structures of the universe [41, 42]and numerical N-body simulations [43] are also consistent with the bottom-up scenario. Hence, the observed universe is consistent with DM being dominated by CDM. This excludes the neutrinos as potential DM candidates. The simplest way to account for the cosmological observations of the universe today is formulated in the ΛCDM-model, which describes a universe dominated by DE and CDM. The ΛCDM-model is referred to as the Standard Model of Cosmology.

3.2.2 Candidates for CDM in Particle Physics

There are many candidates for CDM provided from extensions of SM in particle physics. Maybe the most popular are the Weakly Interacting Massive Particles (WIMPs). This is a class of DM candidates which only interacts with SM fields by a weak scale interaction, in addition to gravity, and they have a mass $\mathcal{O}(100\text{ GeV}) - \mathcal{O}(1\text{ TeV})$. Possible popular WIMP candidates can be found in for instance theories of universal extra dimensions as the lightest Kaluza-Klein particle [44], as the lightest supersymmetric particle in supersymmetric theories or as an inert Higgs boson. Another popular candidate which is not a WIMP is the *axion* [45]. Despite not being massive (it acquires a small mass $\mathcal{O}(10^{-5}\text{eV})$), it is a candidate for CDM.

The spin statistics of a WIMP particle is model dependent. There is no consensus of whether it should be a boson (vector or scalar) or a fermion. The existence of a WIMP particle χ (and its antiparticle $\bar{\chi}$, if it exists) leads naturally to a DM relic density (observed DM density today) if the WIMPs can annihilate via a weak scale interaction into SM particles f and f'.

When the temperature of the universe is much greater than the mass of the WIMPs, i.e. $T >> m_\chi$, both $ff' \to \chi\bar{\chi}$ and $\chi\bar{\chi} \to ff'$ can occur as a thermal process. As the time moves forward, the temperature decreases, and when $T < m_\chi$ only DM annihilation to SM particles can occur as the opposite reaction is Boltzmann suppressed since the SM particles must have velocities from the tail of the Boltzmann distribution. The comoving[1] number density of the WIMPs n_χ can be described by the Boltzmann equation

$$\frac{\mathrm{d}n_\chi}{\mathrm{d}\chi} = -3Hn_\chi - \langle\sigma_{\text{ann.}}v\rangle\left(n_\chi^2 - (n_\chi^{\text{eq.}})^2\right), \tag{3.5}$$

where $H = \dot{a}/a$ (a being the scale factor of the universe in the Friedmann-Robertson-Walker metric [46]) is Hubble's constant at the time denoting the expansion rate, $n_\chi^{\text{eq.}}$ is the comoving number density for the WIMPs at thermal equilibrium, and $\langle\sigma_{\text{ann.}}v\rangle$ is the thermally averaged total annihilation cross section for the annihilation process $\chi\bar{\chi} \to ff'$ times the relative velocity of the

[1] A comoving volume expands with the expansion rate H of the universe.

WIMPs. If the WIMPs stay at thermal equilibrium Eq. 3.5 makes the comoving number density drop exponentially. If this were to continue the DM relic density would vanish. However, approximately when the annihilation rate $n_\chi \langle \sigma_{\text{ann.}} v \rangle$ becomes lower than the expansion rate H the probability of WIMPs meeting in a collision becomes small, and the comoving number density remains constant from this point. This is referred to as *freeze out*. The number density at freeze out corresponds to the relic density observed today $\Omega_{\text{DM}} h^2 \sim 0.1$. For a small $\langle \sigma_{\text{ann.}} v \rangle$, freeze out occurs at a high temperature, resulting in a lower value of the relic density as is seen in Fig. 3.5. For WIMPs annihilating via weak scale

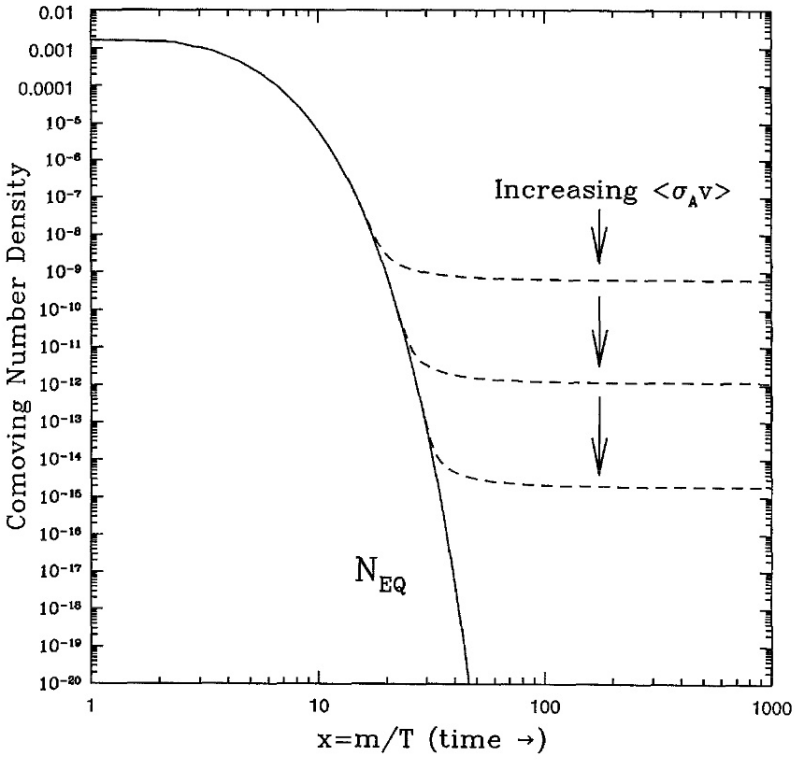

Figure 3.5: Comoving WIMP-number density as a function of $x = m/T$ where, T is temperature and m is the mass of the WIMPs. Increasing the thermally averaged total cross section times velocity $\langle \sigma_{\text{ann.}} v \rangle = \langle \sigma_{\text{A}} v \rangle$ decreases the relic density of the WIMPs as indicated by the dashed curves. The solid curve shows the exponential fall-off in the number density if the WIMPs stay in thermal equilibrium. From [47].

interactions the freeze out occurs at a temperature $T_{\text{crit.}} \approx m_\chi/20$. Here the WIMPs are non-relativistic, i.e. cold. Calculating the resulting DM relic density,

assuming CDM [48] gives

$$\Omega_{\mathrm{DM}}h^2 = \frac{n_{\chi,\mathrm{today}}m_\chi}{\rho_{0,\mathrm{today}}} \approx \frac{3\times10^{-27}\ \mathrm{cm^3s^{-1}}}{\langle\sigma_{\mathrm{ann.}}v\rangle}. \tag{3.6}$$

Between freeze out and today the WIMPs loose the ability to inelastically collide (known as kinetic decoupling) and they do not track the temperature of the SM particles in the universe, so that cold non-interacting DM is what remains — which, incidentally, are the features of DM consistent with observations. Furthermore, for weak scale WIMPs annihilating via the weak interaction we have, roughly

$$\langle\sigma_{\mathrm{ann.}}v\rangle \sim \frac{\alpha^2_{\mathrm{weak}}}{m^2_{\mathrm{weak}}} \sim \frac{(10^{-2})^2}{(100\ \mathrm{GeV})^2} \sim 10^{-25}\ \mathrm{cm^3s^{-1}}, \tag{3.7}$$

thus leaving a DM relic density corresponding remarkably well with the measured relic density $\Omega_{\mathrm{DM}}h^2 \approx 0.1$. This is referred to as the *WIMP miracle*.

Features of WIMPs as DM

We can now summarize a some properties for the WIMPs as DM candidates.

- The WIMPs must be electrically neutral and only interact weakly and gravitationally, as they can not be directly observed as luminous matter.
- They must be stable particles. Since the relic density is set in in the early ages of the universe, the WIMPs must be stable in order to keep the relic density through the eons, or at least metastable with a lifetime comparable to the age of the universe.
- The mass of WIMPs is assumed to be comparable to the weak scale to get the observed relic density, thus the mass is in the range $\mathcal{O}$(100 GeV) -$\mathcal{O}$(1 TeV).

3.2.3 Detection Methods Dark Matter

Several experiments try to measure DM in order to describe the properties of the particles. Experiments for measuring DM can be divided in three categories: *Direct-* and *indirect detection*, and *production*.

Direct detection experiments try to observe DM particles interacting with SM particles. High-sensitivity experiments aim to measure events where WIMPs scatter of massive nuclei in large volumes. The WIMP scattering cross section off nuclei can be calculated model dependently. However, the WIMPs are assumed to constitute the galactic DM halo, and its mass- and velocity distribution in

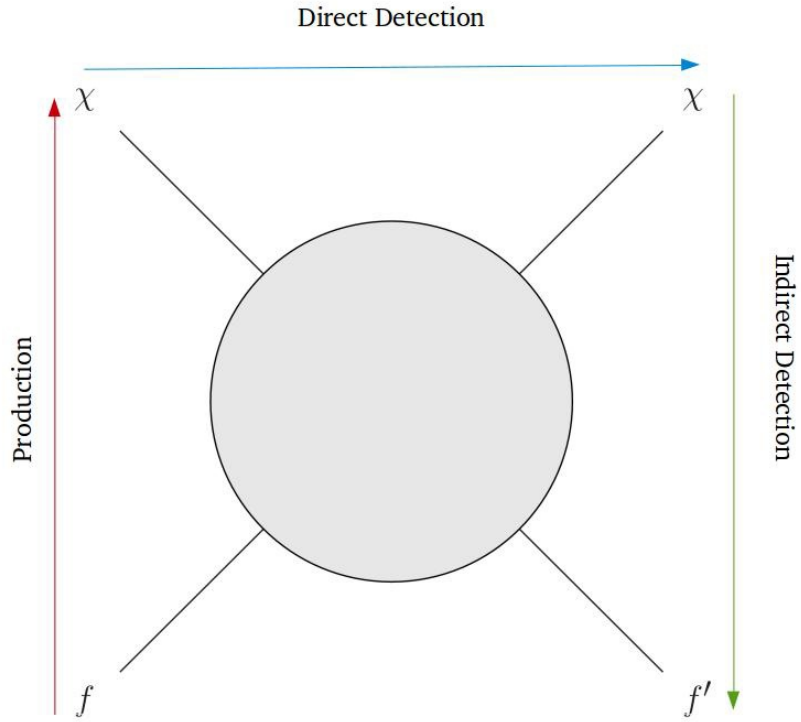

Figure 3.6: Diagram illustrating the different experimental approaches for discovering DM by considereing time-flow in three different directions. With time moving from bottom to top it illustrates SM particles ff' annihilating to a pair of DM $\chi\chi$. Reading it left to right illustrates a generic direct detection, and from top to bottom we have DM annihilation to SM particles.

the Milky Way have large uncertainties. The known velocity parameters in the galactic rest frame are the velocities of the sun with respect to nearby stars (proper velocity) and the sun's rotational velocity around the center of the Milky Way, as well as the annular modulation from Earth's orbit around the sun. Taking into account that observed velocities of bodies in the reference frame of the Milky Way are of $\mathcal{O}(10^{-3}c)$ the deposited recoil energies for DM particles in the mass range $10\text{GeV} - -1\text{TeV}$ would be in the range $1 - 100$ KeV [49]. The differential scattering rate N for a WIMP scattering of a nucleus with mass M giving it a recoil energy E_r is generally [50]

$$\frac{\mathrm{d}N}{\mathrm{d}E_r} = \frac{\sigma\rho}{2\mu^2 m_\chi}|F(q)|^2 \int_{v_{\min}}^{v_{\text{esc}}} \frac{f(v)}{v}\mathrm{d}^3 v, \tag{3.8}$$

where σ is the cross section for the scattering, m_χ is the WIMP mass, $F(q)$ is the nuclear form factor, μ is the reduced mass $\mu = m_\chi M/(m_\chi + M)$ and $f(v)$ is the WIMP's velocity distribution. The integral is to be taken from the minimum

WIMP velocity in order to recoil of the nucleus, to the escape velocity v_{esc} where the WIMPs escape the galactic DM halo.

Detecting DM by studying annular modulation on top of a constant background are being performed by e.g. DAMA/LIBRA [51]. Experiments such as XENON [52] and LUX [53] does not consider annular modulation but trying to measure WIMP scattering of nuclei through high-sensitivity measurements and suppressing the background. In Fig. 3.7 we see the limits from several high sensitivity experiments. We see that the discovery regions from DAMA/LIBRA and CDMS are in the excluded area from the most recent XENON and LUX results, thus these discovery regions are not compatible with these exclusion limits.

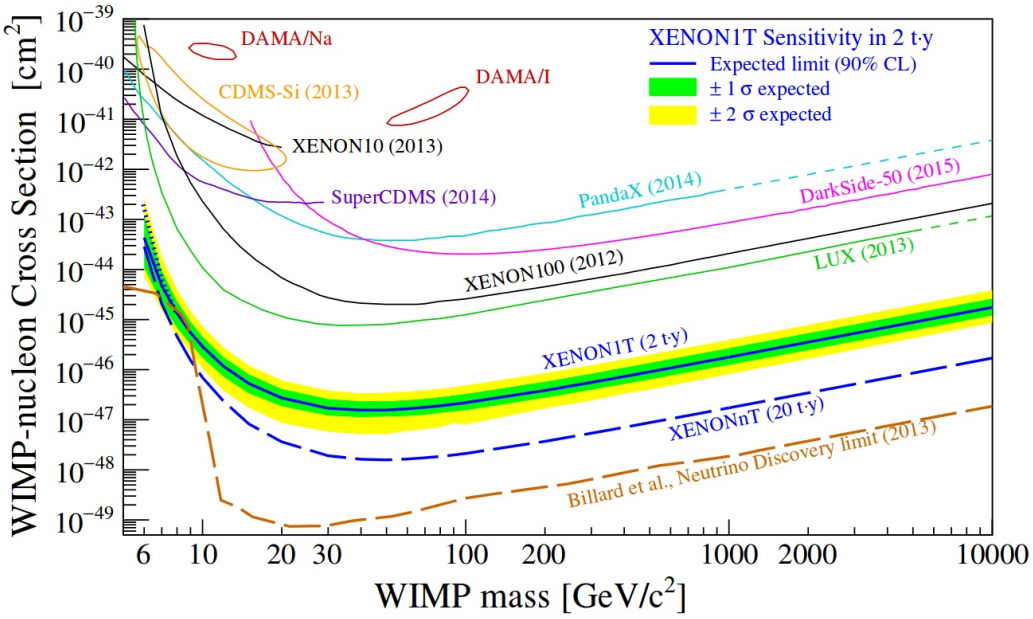

Figure 3.7: Limits on WIMP-nucleus cross section, several direct detection experiments are displayed. The strongest limits are from the LUX collaboration (light green). The estimated limits from upcoming XENON1T-experiment displayed for 2-20 yrs of exposure time. From [54].

Indirect detection Reading the diagram in Fig. 3.6 with time going downwards is the generic process behind indirect detection, where experiments are set up measure products from DM annihilation (or possibly decay) in cosmic rays. It is paramount that the SM particles are stable in order to detection experiments on Earth or in orbit. Excess from background is studied, and photons and neutrinos are favoured as they point to the source while other particles such as positrons, antiprotons and anti-deuterons can diffuse in the galactic magnetic field. The process $\chi\chi \to \gamma\gamma$ or γZ would result in a sharp peak at the DM invariant mass if the photons are detected. As the photons would point to the

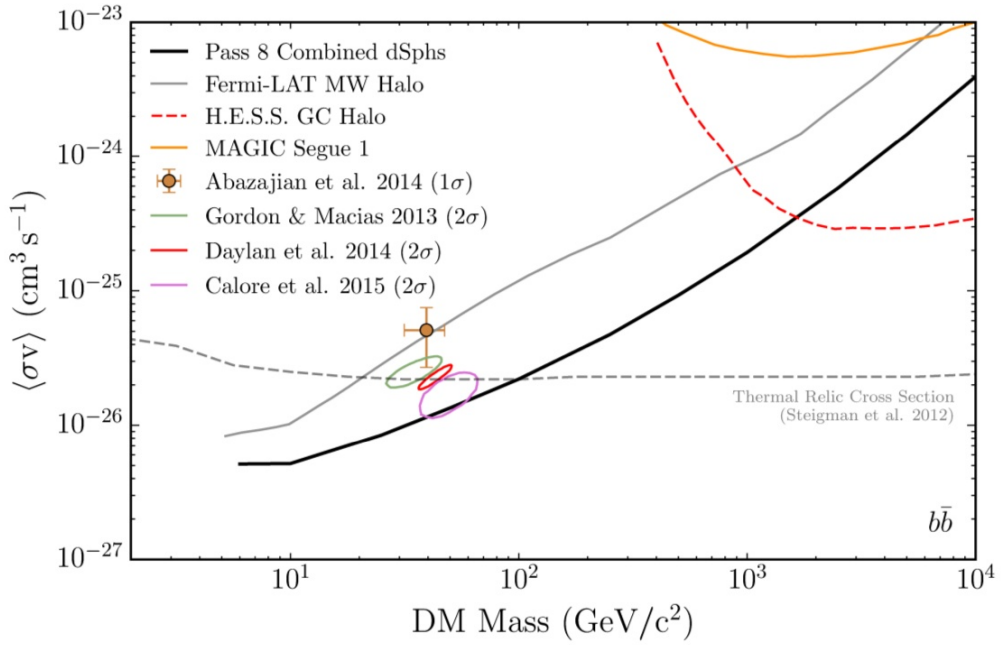

Figure 3.8: Constraints on DM annihilation cross section from six years of data from Fermi-LAT for gamma rays in $\chi\chi \to b\bar{b}$ process. Other experiments are also visualized. The grey and black line show the limits from Milky Way halo search and Milky Way dwarf spheroidal galaxy search, respectively. From [55].

source one might observe radiation from regions in the galaxy with assumed large DM densities, in order to potentially reduce background. We can calculate the expected flux of photons at earth, this would depend on the DM distribution in the galaxy. Measuring the photon spectrum can then be used to set bounds on the dark matter annihilation cross section by assuming a WIMP scenario with the canonical expression for the (low energy) temperature averaged cross section

$$\langle \sigma_{\text{ann.}} v \rangle \simeq 3 \times 10^{-26} \text{ cm}^3\text{s}^{-1}. \tag{3.9}$$

The PAMELA [56] experiment is observing the high energy electrons in cosmic rays, and Fermi-LAT [57] studying gamma rays are two examples of experiments looking to indirectly detect DM. In Fig. 3.8 shows limits put on the DM annihilation cross section from Fermi-LAT.

Direct Detection Reading with time flowing from the bottom to top yields the generic process for production of DM. This is done, for instance in particle accelerators, where SM particles are accelerated to near light-speed velocities an collide in a detector. At the LHC the proton-proton collisions at a center of mass energies of 14 TeV are performed.

The protons themselves are not fundamental particles but they consist of quarks and gluons collectively referred to as *partons*. The partons in the proton carry fractional amount x of the protons total momentum. The fraction x is unknown, however, the its probability distribution function is obtained by deep inelasic scattering of electrons off protons. Since it is the partons in the proton are the interacting particles in a collision total momentum along the collision axis is unknown. Hence, momentum and energy conservation is constricted to apply only in a direction transverse to the collision axis, this is referred to a transverse momentum or transverse energy.

The ATLAS and CMS detectors are sensitive to particles that couple electromagnetic and strong coupling particles, thus if a WIMP particle is produced it can not be detected directly by the experiment. However, if the WIMP is produced together with a muons or jets with large amounts of transverse momentum it can be detected as missing transverse momentum. For instance if one of the initial state quarks radiate a high energetic (hard) gluon, the gluon will quickly hadronize to form a jet. The jet will recoil of the WIMP, and an event with missing transverse energy will be detected if the transverse momentum of the jet is passes a given cut. In Fig. 3.10 there recent results from a jet search from ATLAS, with the cut at 250GeV.

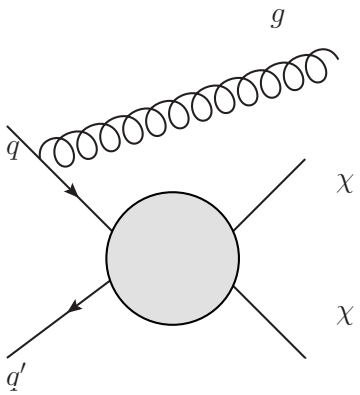

Figure 3.9: Diagram for initial state radiation of high energetic gluon from the incident quarks. The quarks eventually annihilates and a WIMP pair is produced which escapes the detector.

3.3 A Brief Introduction to Supersymmetry

Supersymmetry (SUSY) appeared from an attempt to unify the exterior symmetries of Special Relativity with the interior symmetries of particle physics. As we have seen, the symmetry group of SM relies on the internal spaces that the

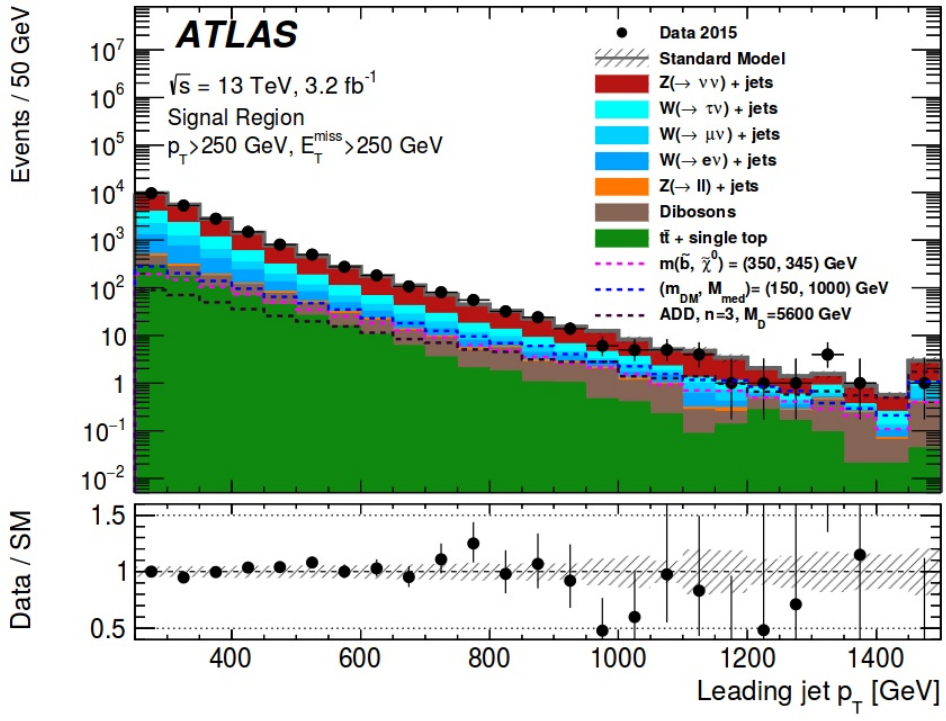

Figure 3.10: Monojet analysis performed by the ATLAS experiment at LHC. It shows the distribution of the jet with the leading p_T which passes the cut $p_T > 250$ GeV, and missing energy of E_T >250 GeV. In blue dashed the missing energy is the distribution for a model with a Dirac WIMP with mass $m_\chi = 150$ GeV whose interactions to SM quarks are mediated by a massive new vector boson with mass $m_{\text{med}} = 1000$ GeV. From [58].

SM quantum fields can be arranged in, the well known gauge symmetry group $SU(3)_C \times SU(2)_Y \times U(1)_Y$.

It was shown in [59] that an attempt to extend the Poincarè group to also include the internal gauge symmetries of particle physics can not be done. In [60] the concept of a graded Lie algebra was introduced in order to successfully unite the external symmetries of spacetime with the internal symmetries of particle physics. In short, in order to extend the spacetime symmetries described by the Poincarè group one extends the Lie algebra with new operators (called the Majorana central charges, or spinor charges) and *anti*-commutation relations among themselves. The *graded Lie algebra*, or *superalgebra* is realized by introducing the Majorana spinor charges Q_a, $a = 1, \ldots, 4$. The Majorana spinor charges can be considered as the components of spinor

$$Q_a = \begin{pmatrix} Q_\alpha \\ \bar{Q}^{\dot{\alpha}} \end{pmatrix}_a . \tag{3.10}$$

which satisfies the relations

$$\{Q_\alpha, Q_\beta\} = \left\{\bar{Q}^{\dot{\alpha}}, \bar{Q}^{\dot{\beta}}\right\} = 0 \tag{3.11}$$

$$[Q_\alpha, P_\mu] = [\bar{Q}_{\dot{\alpha}}, P_\mu] = 0 \tag{3.12}$$

$$\left\{Q_\alpha, \bar{Q}_{\dot{\alpha}}\right\} = 2\sigma^\mu_{\alpha\dot{\alpha}} P_\mu \tag{3.13}$$

$$[Q_\alpha, J^{\mu\nu}] = \frac{i}{4}\left(\bar{\sigma}^\mu\sigma^\nu - \sigma^\nu\bar{\sigma}^\mu\right)_\alpha{}^\beta Q_\beta, \tag{3.14}$$

$$\tag{3.15}$$

where $\sigma^\mu = (1, \sigma)$ and $\bar{\sigma}^\mu = (1, \sigma)$, $P_\mu = i\partial_\mu$ is the momentum operator (generator of translations) and $M^{\mu\nu}$ are the generators of boosts and rotations. The relations in Eqs. (3.11)-(3.14), along with the commutation relations for the Poincarè algebra form the Super-Poincaré algebra, which is a graded Lie algebra.

We define a SUSY transformation as

$$\delta_\eta = \eta^\alpha Q_\alpha + \bar{\eta}_{\dot{\alpha}}\bar{Q}^{\dot{\alpha}}, \tag{3.16}$$

where η and $\bar{\eta}$ are Grassmann variables ordered in left- and right-handed Weyl spinors, considered infinitesimal. By studying the irreducible representations of the Super-Poincarè algebra one encounters superfields. Analogous to Weyl-spinors being irreducible representations of the $L_+^\uparrow$-algebra, the vector superfields and left-, right- handed superfields are the irreducible representations of the Super-Poincarè algebra relevant for forming the Minimal Supersymmetric Standard Model (MSSM). One left-handed superfield (right-handed) contain the physical degrees of freedom of left-handed Weyl fermion (right-handed Weyl fermion) as well as a one complex scalar field. And the physical degrees of freedom in one vector superfield are those of one real four-vector field, and the left- and right-handed versions of a Weyl fermion – forming a Majorana fermion.

In a supersymmetric theory there will, in general, be one scalar field associated with every left- or right-handed Weyl fermion, and for every four-vector field there will be associated one Majorana fermion.

3.3.1 The MSSM

One can form Lagrangians that are invarant under SUSY-transformations, such theories are referred to as *supersymmetric*. The MSSM is the supersymmetric theory which contains the SM, by introducing a minimal amount of new fields. It exhibits a symmetry between fermions and bosons, in that every SM-field gets a supersymmetric "partner": for each left-handed SM-fermion there is one associated scalar field and for every SM gauge boson there is one Majorana fermion field. We refer to these supersymmetric "partners" as *sparticles*, furthermore, the scalar sparticles are referred to as *sfermions* and Majorana sparticles are referred to as *gauginos*.

The sparticles have all the same properties as their SM partner besides spin properties. For example the sfermion partner of a charged left-handed lepton – a *slepton* $\tilde{\ell}_L i$ – has (in unbroken SUSY) the same mass, the same weak isospin and weak hypercharge as the corresponding lepton ℓ_{Li}, i.e. the sfermions have the same couplings to the Higgs scalars, and the gauge bosons as the corresponding SM fermions.

The Higgs Sector of the MSSM

It is not possible to define the MSSM with one scalar Higgs doublet in a manner that is supersymmetric, thus there are two scalar Higgs $SU(2)_L$ doublets H_u and H_d in the MSSM

$$H_u = \begin{pmatrix} h_u^{(+)}(x) \\ h_u^{(0)}(x) \end{pmatrix}, H_d = \begin{pmatrix} h_d^{(0)}(x) \\ h_d^{(-)}(x) \end{pmatrix}, \tag{3.17}$$

The neutral complex scalar fields $h^0_{u/d}$ acquires VEV, and the charged complex scalar fields $h_u^{(+)}$. Upon attaining its VEVs the scalar in H_d gives mass-terms for the down-type SM quarks and the charged SM leptons and the corresponding sparticles, the H_u-doublet gives mass to the up-type quarks (neutrinos are considered massless in the MSSM with sterile right-handed neutrinos). The physical Higgs bosons also have supersymmetric partners which are called *Higgsinos*, and there are both neutral and charged Higgsinos. Prior to electroweak symmetry breaking, which in the MSSM is referred to as Radiative Electroweak Symmetry-breaking (REWSB) there are in total eight degrees of freedom in the two (complex) Higgs doublets. Among the degrees of freedom in H_u three are Goldstone bosons which gives longitudinal polarizations to the $W^{\pm}$- and Z-gauge fields of the SM and one degree of freedom is a real scalar field. Thus there are in total five degrees of freedom after REWSB, remained in two neutral scalars h, H one complex scalar $H^{\pm}$ and one CP-odd scalar A. In fact, taking into account loop corrections to the mass of the lightest scalar Higgs h, it has an upper bound

$$m_h \lesssim 135 \text{ GeV}. \tag{3.18}$$

Had the SM Higgs discovered at the LHC had a mass higher than this it would have excluded the MSSM. The mass of the SM Higgs is found to be ~ 126 GeV, thus not excluding the MSSM.

3.3.2 Breaking of SUSY in the MSSM

For extending the SM supersymmetry predicts the apperance of sparticles as in the MSSM, however, it also predicts that the sparticles have masses equal to the corresponding SM-particles. This is not observed in any collider experiment.

A solution is that there is be a mechanism responsible for boosting the value of the sparticle masses so that they have been inaccessible in past experiments. Spontanous symmetry breaking of SUSY have been proven to be not effecitve for boosting the sparticle masses, as a there is an upper bound for the difference in sparticle-particle masses for such a mechanism [61]. At tree level it is shown in [61] that in a spontaneously broken SUSY theory the sum

$$\sum_s (-1)^{2s}(2s+1)m_s = 0, \tag{3.19}$$

where s is the spin of particle with mass m_s, this states that the bosons can not have significantly higher masses than the fermions of a SUSY-theory. The way supersymmetry is broken, is to assume that the breaking happens at a high energy scale (10^{16} or 10^{18} GeV) by an unknown mechanism as new physics enters. *Soft terms* (couplings with positive mass dimension) are added to the theory to effectively boosts the masses of the sparticles and the Higgs bosons in the MSSM. Furthermore, they provide the MSSM with 104 new parameters. The total number of free parameters in the MSSM is then 124, as unbroken MSSM introduces only one new parameter and the SM has 19 free parameters. Among the soft terms are those for the $SU(2)_L$ and $U(1)_Y$ gauginos, respectively, $\tilde{W}^a$ and $\tilde{B}$ (in two-component Weyl notation)

$$-\frac{1}{2}M_1\tilde{B}\tilde{B} - \frac{1}{2}\tilde{W}^a\tilde{W}^a. \tag{3.20}$$

where M_i are potentially complex-valued.

R-parity

When constructing a theory like the MSSM interactions which violates baryon- and lepton number conservation are not forbidden by gauge- or SUSY invariance. In the MSSM one such term leads to proton decay by $p \to e^+\pi^0$. There is a strong upper limit on the proton lifetime which renders the coupling permitting baryon number and lepton number violation indeed very small, but there is no mechanism which explicitly suppresses such couplings. However, in the MSSM there is a symmetry called R-parity. This is a multiplicative quantum number for a particle with spin s, baryon number B and lepton number L given by

$$R = (-1)^{2s+3B+L}. \tag{3.21}$$

R-parity forbids couplings that break lepton- or baryon number conservation, as every sparticle gets $R = 1$ and every SM particle gets $R = 1$. If this quantum number is conserved, lepton- and baryon number violating operators are forbidden. Furthermore, since R-parity is multiplicative than SUSY sparticles can only be produced in pair in an collision between two SM particles. Also, R-parity ensures that there exists a lightest SUSY particle (LSP) which is stable, and that every other sparticle decays to the LSP.

3.3.3 Why SUSY?

A supersymmetric theory provides a solution to the hierarchy problem. As the new scalar field contents introduced as sfermions contributes to higher one-loop order correction to the Higgs mass. When calculating the correction to the Higgs mass, the correction looks precisely like in Eq. (3.1), only the number of scalars coupling to the Higgs is exactly two times the number if fermions, as the scalars. Furthermore, from demaning that the theory is supersymmetric, the couplings must also satisfy $|\lambda_f|^2 = \lambda_s$. Hence, cancellation of quadratic UV-divergences for the Higgs mass correction is exact in a supersymmetric theory. However, due to soft breaking of SUSY the soft terms m_s boosting the masses of the sparticles must not be higher than $\mathcal{O}(1\text{ TeV})$ in order not to reintroduce the hierarchy problem for the next leading term in the UV-cut off Λ

$$\delta m_h = -m_s \frac{\lambda_s}{16\pi^2} \ln \frac{\Lambda}{m_s} + \cdots . \tag{3.22}$$

The extra field content of the MSSM also allows for unification of the coupling constants as can be seen by the colored lines in Fig.3.1. Also, SUSY provides a way to incorporate gravity in QFT, in a class of theories known as *superstring-theory*. Also, since the LSP of MSSM is assumed stable due to R-parity it (if charge neutral) also provides a candidate for DM. One such DM particle is known as the lightest neutralino.

3.3.4 Supersymmetric Dark Matter

The MSSM contains Majorana fermion fields for each gauge boson field of the SM, which are possible candidates for DM together with the neutral Hggsinos $\tilde{H}_u^0$ and $\tilde{H}_d^0$. The gauginos associated with the gluons – the *gluinos*– are not considered DM candidates as they only interact strongly. We are then left with the $SU(2)_L$ gauginos– the *winos* – $\tilde{W}^a$ and the $U(1)_Y$ gauge bosons – the *bino* – $\tilde{B}$ in addition to the Higgsinos. After electroweak symmetry breaking the $W^\pm = \frac{1}{\sqrt{2}}(W^1 \mp W^2)$ emerge as massive, charged, similarly we get the charged winos $\tilde{W}^\pm$ which leaves the $\tilde{W}^3$ in addition to the bino and Higgsinos as the only Majorana fermions in the SM. The $\tilde{B}, \tilde{W}^3, \tilde{H}_u^0$ and $\tilde{H}_d^0$ will mix to form the *neutralinos* and (the charged gauginos and Higgsinos mix to form the *charginos*) after electroweak symmetry breaking. Defining the gauge eigenstate $\tilde{\psi}^0 = (\tilde{B}, \tilde{W}^3, \tilde{H}_u^0, \tilde{H}_d^0)^T$ the MSSM Lagrangian interactions among the components of $\tilde{\psi}^0$ can be written as

$$\mathcal{L}_{\tilde{\chi}_j^0 - \text{mass}} = -\frac{1}{2} \tilde{\psi}^{0T} M \tilde{\psi}^0 + \text{c.c.}, \tag{3.23}$$

by defining the mass matrix

$$M = \begin{pmatrix} M_1 & 0 & \frac{1}{\sqrt{2}}g'v_d & -\frac{1}{\sqrt{2}}g'v_u \\ 0 & M_2 & -\frac{1}{\sqrt{2}}gv_d & \frac{1}{\sqrt{2}}gv_u \\ \frac{1}{\sqrt{2}}g'v_d & -\frac{1}{\sqrt{2}}gv_u & 0 & -\mu \\ -\frac{1}{\sqrt{2}}g'v_d & \frac{1}{\sqrt{2}}gv_u & -\mu & 0 \end{pmatrix}, \tag{3.24}$$

where M_1 and M_2 are the soft terms for the gauginos, g and g' are,respectively, the $SU(2)_L$ and the $U(1)_Y$ couplings, $v_{u/d}$ are the VEVS for $h^{(0)}_{u/d}$ and μ is the supersymmetric analogue to the mass term of the Higgs in SM, it is the only new parameter introduced in an unbroken MSSM. The matrix M can be diagonalized by a matrix N, and the mass eigenstates are the *neutralinos* $\tilde{\chi}_i = N_{ij}\psi^0_j$. In many scenarios the LSP is the lightest neutralino[2] $\tilde{\chi}_0 = N_{01}\tilde{B}+N_{02}\tilde{W}^3+N_{03}\tilde{H}^0_u+N_{04}\tilde{H}^0_d$.

[2]It is conventional to let the index j with from the lightest to the most massive neutralino.

Chapter 4

Leptophilic Dark Matter Model

We will consider a model for extending SM with a DM candidate. This model is possible in supersymmetric theories, with the lightest neutralino as the DM particle candidate. We are interested in the cross section for pair production of DM particles, and for this we have to go beyond leading order in pertubation theory. First we introduce the SM to DM coupling and next we will lay the groundwork for the next-to-leading order calculation.

4.1 Leptophilic Dark Matter

We will consider the interaction written in two-component notation as

$$\Delta\mathcal{L} = g_{\rm NP}\,\chi(\nu_L\eta^{(0)} - \ell_L\eta^{(+)}) + \text{h.c.}, \tag{4.1}$$

where χ is a left-handed Weyl-spinor and represents the Majorana DM fermion, $\eta^{(0)}, \eta^{(+)}$ are heavy scalar particles. The neutral scalar η^0 is not charged under $U(1)_{\rm EM}$, $\eta^{(+)}$ has charge $U(1)_{\rm EM}$-charge $+1$ in units of $|e|$. The left-handed fermion fields ℓ_L and ν_L are SM lepton fields, respectively a standard model lepton (electron, muon or tau) and its associated neutrino. The scalar particles $\eta^{(0)}, \eta^{(+)}$ (or χ) also carry lepton number $L_\ell = 1$ to ensure lepton number conservation, . The coupling constant for this new physics will be denoted $g_{\rm NP}$, and is assumed to be small. We will work with the interaction in Eq. (4.1) using four component notation. We introduce the Majorana spinor ψ_M from the left- and right-handed versions of χ_α, i.e. in the chiral representation we have

$$\psi_M = \begin{pmatrix} \chi_\alpha \\ \bar{\chi}^{\dot{\alpha}} \end{pmatrix}. \tag{4.2}$$

We employ the notation $\eta^\dagger = \eta^{(+)}$ and $\eta_0^\dagger = \eta^{(0)}$ (letting hermitian conjugation $\dagger$ denote complex conjugation for the scalar fields). Both scalar particles η and η_0 take on all the same quantum numbers as the relevant lepton, except spin. They

transform under the SM gauge group are in representation $(0, \mathbf{2}, 1)$ of SM, i.e. as an $SU(2)_L$ doublet with hypercharge $Y = 1$

$$\mathcal{H} = \begin{pmatrix} \eta^\dagger \\ \eta_0^\dagger \end{pmatrix}. \tag{4.3}$$

Then we can write the interaction as

$$\Delta\mathcal{L} = g_{\rm NP}\,\bar{\psi}_M L_\ell^T i\sigma^2 \mathcal{H} + \text{h.c.} \tag{4.4}$$

$$= g_{\rm NP}\bar{\psi}_M(P_L\nu_\ell\eta_0^\dagger - P_L\ell\eta^\dagger) + \text{h.c.}, \tag{4.5}$$

where $L_\ell = (P_L\nu_\ell, P_L\ell)^T$ is the left-handed lepton doublet. The Gauge interactions and propagation of the scalars η and η^0 is described by

$$\mathcal{L}_\eta = |D_\mu\mathcal{H}|^2 - \mathcal{H}^\dagger M_\eta \mathcal{H}, \tag{4.6}$$

where M_η is assumed to be the diagonal 2×2-matrix with $M_\eta = \text{diag}(M, M_0)$. In general $M \neq M_0$, but we will assume $M = M_0$ to preserve $SU(2)_L$ gauge invariance. In Eq. (4.6) we find the scalar couplings

$$|D_\mu\mathcal{H}|^2 \supset \mathcal{H}^\dagger \left(i\frac{g}{\cos\theta_W} Z_\mu \left[\frac{\sigma^3}{2} - \mathcal{Q}\sin^2\theta_W\right] + i\mathcal{Q}g\sin\theta_W A_\mu \right) \partial^\mu \mathcal{H} + \text{h.c.}, \tag{4.7}$$

where Z_μ and A_μ are the Z-boson field and the photon field, respectively. The charge matrix for an $SU(2)_L$-doublet is $\mathcal{Q} = (Y + \sigma^3)/2$, g is the $SU(2)_L$ gauge coupling, and $\sin\theta_W$ is the weak mixing angle. The explicit interactions from between the new scalar particles η and η_0 and the SM bosons Z and A are fund from Eq. (4.7)

$$\begin{aligned} \mathcal{L}_{\rm int}^{\rm NP} =& g\frac{2\sin^2\theta_W - 1}{2\cos\theta_W} Z_\mu \eta^\dagger\, i\partial^\mu\eta - g\sin\theta_W A_\mu \eta^\dagger\, i\partial^\mu\eta + \text{h.c.} \\ & - \frac{g}{2\cos\theta_W} Z_\mu \eta_0^\dagger\, i\partial^\mu\eta_0 + \text{h.c.}. \end{aligned} \tag{4.8}$$

The interactions for the ℓ and ν_ℓ with the Z and A can be found by the covariant derivative in Eq. (2.74) on the left- and right-handed lepton fields,

$$\mathcal{L}_{\rm int}^{\rm SM} = \frac{g}{2\cos\theta_W}\bar{\nu}\not{Z} P_L\nu + \frac{g}{2\cos\theta_W}\bar{\ell}\not{Z}\left(2\sin^2\theta_W - P_L\right)\ell - g\sin\theta_W\bar{\ell}\not{A}\ell, \tag{4.9}$$

where ℓ and ν are four-component fermion fields representing the a SM charged lepton and its associated neutrino, respectively. Note that only the left-handed neutrino appear in the interaction.

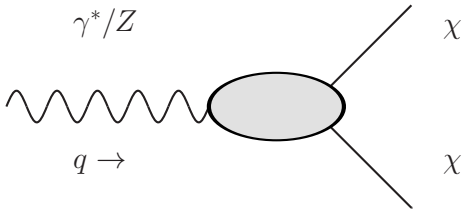

Figure 4.1: Diagram for an s-channel production of DM particles $\chi\chi$. The intermediary state γ^*/Z carries a time-like invariant center of mass energy $q^2 = s$. The grey vertex is used to indicate that this is not a tree level interaction.

Majorana Pair Production Beyond Leading Order

We will now consider the interactions in Eqs. (4.5), (4.8) and (4.9). They imply that a DM pair can not be produced at leading order. However, going beyond leading order a DM pair can be produced. They can be pair produced in an s-channel particle collision between SM particles via an electroweak neutral vector mediator Z/γ^*, as schematically illustrated in Fig. 4.1. The complete theory is then described by the Lagrangian

$$\mathcal{L} = \mathcal{L}^{\text{SM}} + \mathcal{L}_\chi + \mathcal{L}_\eta + \Delta\mathcal{L} \tag{4.10}$$
$$= \mathcal{L}_0 + \mathcal{L}_{\text{int}}. \tag{4.11}$$

Where $\mathcal{L}_{\text{int}} = \Delta\mathcal{L} + \mathcal{L}^{\text{NP}}_{\text{int}} + \mathcal{L}^{\text{SM}}_{\text{int}}$. This is the interaction Lagrangian we will use to derive the diagrams that contributes to $\chi\chi$-production beyond leading order.

We can find the diagrams contributing to $\gamma^*/Z \to \chi\chi$ from the general expression for the S-matrix element in the canonical formalism [11]

$$S_{fi} = \langle f | \, i \rangle = \left[\lim_{T\to(1+i\varepsilon)\infty} \langle 0 | \mathcal{T} \left[\mathcal{O}(\Phi) e^{-i\int_{-T}^{T} \mathrm{d}t \; H_I(t)} \right] |0\rangle \right]_{\substack{\text{Connected,} \\ \text{amputated}}}, \tag{4.12}$$

where Φ is all the field content in the interaction picture, $\mathcal{O}(\Phi)$ is some function of the field content which specifies the overlap of initial and final states and $\mathcal{T}$ is the time ordering operator. The interaction is specified by the interaction Hamiltonian $H_I = -\int \mathrm{d}^3x \mathcal{L}_{\text{int}}$. It is understood that only connected and amputated diagrams are kept.

The contribution to the non-trivial matrix element iT is then all Wick-contractions of an expression of the form

$$\begin{aligned} -i_0 \langle \mathbf{p}_1, \mathbf{p}_2 | (\bar{f} P_R \psi_M \phi_f)_x \; (\bar{\psi}_M P_L f \phi_f^\dagger)_y \times \\ \times \left(g \bar{f} B_\mu \gamma^\mu (a_f + v_f \gamma^5) \; f + \left[g k_f B^\mu \phi_f^\dagger i \partial_\mu \phi_f + \text{h.c.} \right] \right)_z |B\rangle \,, \end{aligned} \tag{4.13}$$

integrated over all the spacetime variables x, y and z. Here B_μ represents the Z-boson or photon, and $|B\rangle$ is an intermediate state with a Z or photon field.

The fermions are $f = \ell, \nu_\ell$ and the scalars are $\phi_\ell = \eta, \phi_{\nu_\ell} = \eta_0$. The coupling factors k_f, a_f and v_f are given in table 3.1. If the intermediate boson B is a

B	A	Z
k_ℓ	$-\sin\theta_W$	$\frac{2\sin^2\theta_W - 1}{2\cos\theta_W}$
k_{ν_ℓ}	0	$\frac{1}{2\cos\theta_W}$
(v_ℓ, a_ℓ)	$(-\sin\theta_W, 0)$	$\left(\frac{2\sin^2\theta_W - 1/2}{2\cos\theta_W}, \frac{1/2}{2\cos\theta_W}\right)$
$(v_{\nu_\ell}, a_{\nu_\ell})$	0	$\left(\frac{1}{4\cos\theta_W}, \frac{-1}{4\cos\theta_W}\right)$

Table 4.1: The coupling factors for the scalar and fermion coupling to the Z-boson or the photon. The coupling factors are such that they can be inserted directly into the general vertex factor in Eq. (4.13).

photon we apply the couplings in the middle column of table 3.1 in Eq. (4.13), all contractions leading to a connected diagram results in the sum of the four diagrams in Fig. 4.2. The only loop particles in this diagram are charged SM leptons ℓ and the charged scalar particles η. We see that we get a crossing of the DM particle external legs. This is because Majorana operators ψ_M and $\bar{\psi}_M$ can contract with the same external state, one permutation of these Majorana operators yields the extra factor of (-1).

If the intermediate boson B is a Z-boson, then we sum Eq. (4.13) over $f = \ell, \nu_\ell$ and apply the coupling factors of table 3.1 in the column to the right. This will give in total eight diagrams. One set of four diagrams have SM charged leptons ℓ and charged scalar η in the loop, and another set of four diagrams have the SM neutrino ν_ℓ and the scalar η_0 in the loop. Both sets of four diagrams appear as in Fig. 4.2.

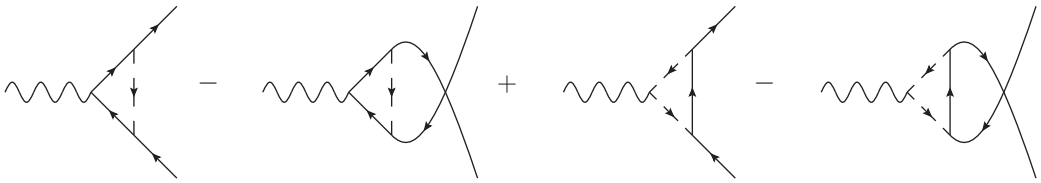

Figure 4.2: Four diagrams contributing to Dark Matter pair production from a photon or Z-boson, the final state is two Majorana DM particles. The particles are scalar particles s and SM-fermions f. If the incoming boson is a Z we sum over $f = \ell, \nu_\ell$ giving in total a sum of 8 diagrams.

4.2 Evaluation of the Diagrams

We will use some standard techniques to find a closed form expression for the diagrams in Fig. 4.2. The techniques for solving the loop integrals are elaborated in appendix C, and can be found in most books on QFT e.g. [11]

We will split the diagrams in Fig. 4.2 in two classes. The two diagrams on the left we will refer to as the fermion diagrams, and the two diagrams to the right are referred to as the scalar diagrams. For the fermion diagrams, the loop integral contains two fermion propagators and one scalar propagator. For the scalar diagrams contains two scalar propagators and one fermion propagator. However, given a positive power of the loop momentum in the scalar coupling to the gauge boson, both the scalar and fermion diagrams will contain momentum integrals which, for high loop momenta, will go as

$$\int \frac{\mathrm{d}^4 k}{(2\pi)^4} \, \frac{1}{k^4} \sim \ln(\Lambda_{\text{Cutoff}}). \tag{4.14}$$

That is, superficially, we find a logarithmic divergence in the limit $\Lambda_{\text{Cutoff}} \to \infty$ for all the diagrams in Fig. 4.2. However, this divergence should cancel between the fermion and scalar diagrams, as we note that the direction of the charge flow in the loops are opposite between these two types of diagrams. This process does not exist at tree level, therefore there is no counterterm for this vertex. Adding all diagrams contributing to each order in perturbation theory will yield a finite amplitude.

We will not employ the *cutoff*-regularization for regularizing these loop-diagrams. We will instead apply the dimensional regularization. Here we perform the integral in arbitrary dimenion d, and evaluate the integrals as functions of $\epsilon = 4 - 2d$, and eventually take the limit $\epsilon \to 0$. The symbols M, m_χ, m_f are used for the scalar mass, DM mass and SM lepton mass (neutrino or charged lepton).

We have the hierarcy $M > m_\chi >> m_f$ at all times, however we do not make use of the small lepton mass at this stage.

4.2.1 Fermion Diagrams

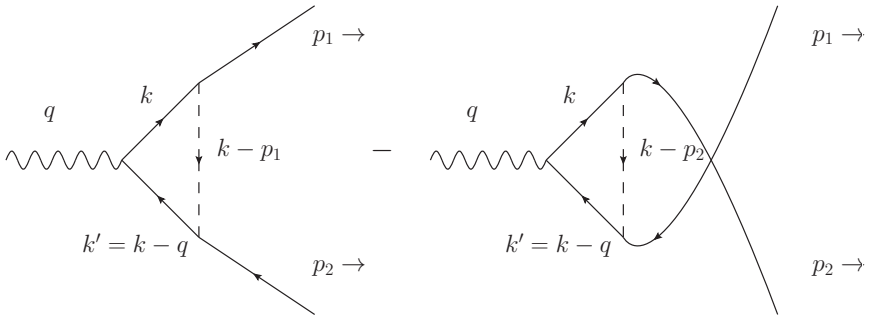

Figure 4.3: The two first diagrams in Fig. 4.2, with the momentum variables assigned. The loop momentum variable is k. In the loop it is a SM lepton and a heavy scalar η_0 or η participating. The external, physical particles of the diagram are the Majorana DM particles with momentum p_1 and p_2. The arrows following the momentum assignment dictates that they are both outgoing particles. The vertex coupling is $i\gamma^\mu V$ for the vector-fermion coupling.

The diagram to the left in Fig. 4.3 is has the amplitude

$$\begin{aligned} &-g g_{\text{NP}}^2 \int \frac{\mathrm{d}^d k}{(2\pi)^d} \frac{\bar{u}(p_1) P_L (\not{k} + m_f)\gamma^\mu (v_f + a_f\gamma^5)(\not{k}' + m_f) P_R v(p_2)}{[(k-p_1)^2 - M^2 + i\varepsilon]\left(k^2 - m_f^2 + i\varepsilon\right)\left(k'^2 - m_f^2 + i\varepsilon\right)} \\ &= -g g_{\text{NP}}^2 \int \frac{\mathrm{d}^d k}{(2\pi)^d} \frac{\bar{u}(p_1)\left[(v_f - a_f)\not{k}\gamma^\mu \not{k}' + (v_f + a_f) m_f \gamma^\mu\right] P_R v(p_2)}{[(k-p_1)^2 - M^2 + i\varepsilon]\left(k^2 - m_f^2 + i\varepsilon\right)\left(k'^2 - m_f^2 + i\varepsilon\right)} - \end{aligned} \tag{4.15}$$

We define the matrix $\Gamma_0^\mu(p_1, p_2)$ such that Eq. (4.15) has the form

$$\bar{u}(p_1)\ ig\Gamma_0^\mu(p_1, p_2) P_R\ v(p_2).. \tag{4.16}$$

We can do the same for the diagram on the right in Fig. 4.3 where the external contractions are permuted. This will then have the amplitude

$$\bar{u}(p_2)\ ig\Gamma_0^\mu(p_2, p_1) P_R\ v(p_1), \tag{4.17}$$

where $i\Gamma^\mu(p_2, p_1)$ is the same matrix as in Eq. (4.16), only with permuted external momenta. We will make the subtraction of the diagrams as indicated in Fig. 4.3, but first we make a general prescription for this. We note that since the amplitude

in Eq. (4.17) is just a complex number, i.e. it is equal to its transpose

$$\begin{aligned}\bar{u}(p_2)\ ig\Gamma_0^\mu(p_2,p_1)P_R\ v(p_1) &= v(p_1)^T\ P_R\ ig\Gamma_0^\mu(p_2,p_1)^T\bar{u}(p_2)^T. \\ &= \bar{u}(p_1)\ igC\Gamma_0^\mu(p_2,p_1)^T P_L C^{-1}\ v(p_2),\end{aligned} \tag{4.18}$$

here C denotes the charge conjugation matrix. In the matrix $\Gamma_0^\mu(p_2,p_1)^T$, each term contains an odd number of Dirac matrices, thus commuting the P_L through gives a P_L. We then get the prescribed subtraction for the two diagrams in Fig. 4.3 given by

$$\begin{aligned}&\bar{u}(p_1)\ ig\Gamma_0^\mu(p_1,p_2)P_R\ v(p_2) - \bar{u}(p_2)\ ig\Gamma_0^\mu(p_2,p_1)P_R\ v(p_1) \\ &\quad =\bar{u}(p_1)\ ig\left[\Gamma_0^\mu(p_1,p_2)P_R + C\Gamma_0^\mu(p_2,p_1)^T P_L C^{-1}\right]\ v(p_2). \\ &\quad \equiv u(p_1)\ ig\Gamma^\mu(q)\ v(p_2)\end{aligned} \tag{4.19}$$

4.2.2 Scalar Diagrams

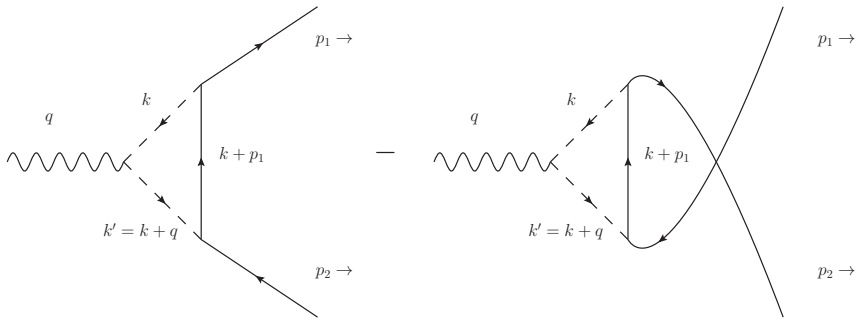

Figure 4.4: The scalar diagrams, with the momentum variables assigned. The loop momentum variable is k. It is a SM lepton and a heavy scalar η_0 or η participating in the loop. The external, physical particles of the diagram are the Majorana DM particles with momentum p_1 and p_2. The arrows following the momentum assignment indicate that they are both outgoing particles. The vertex coupling is $igk_f(k+k')^\mu$ for the vector-scalar coupling.

The first diagram in Fig. 4.4 has the amplitude

$$\bar{u}(p_1)\ ig\Lambda_0^\mu(p_1,p_2)P_R\ v(p_2), \tag{4.20}$$

where we have defined the matrix $i\Lambda_0^\mu$ as

$$\begin{aligned}ig\Lambda_0(p_1,p_2) = -k_f g_{\rm NP}^2 \int \frac{\mathrm{d}^d k}{(2\pi)^d}\times \\ \frac{(2k+q)^\mu\,(\not{k}+\not{p}_1)P_R}{\left[k^2-M^2+i\varepsilon\right]\left[(k+q)^2-M^2+i\varepsilon\right]\left[(k+p_1)^2-m_f^2+i\varepsilon\right]}\end{aligned} \tag{4.21}$$

The Feynman rules for a scalar coupling to gauge boson, and Majorana fermions final states are found in [9] to the diagram to the left in Fig. 4.4. We follow the same prescription for the subtraction of the two diagrams in Fig. 4.4 as in Eq. (4.19) and define the sum of the two diagrams in Fig. 4.4

$$\bar{u}(p_1)\ i\Lambda^{\mu}(q)P_R\ v(p_2) \equiv \bar{u}(p_1)\left[i\Lambda_0^{\mu}(p_1,p_2)P_R + C\left[i\Lambda_0^{\mu}(p_2,p_1)\right]^T P_L C^{-1}\right]\ v(p_2) \tag{4.22}$$

4.2.3 General Considerations

We can use a specific technique to see how the divergences cancel between the diagrams. The details are left to appendix B and C. The specific technique is to introduce Feynman parameters to symmetrize the integrand in a shifted loop variable. For the γ^*-channel the divergent contributions $\Gamma^{\mu}_{A,\mathrm{Div}}$ and $\Lambda^{\mu}_{A,\mathrm{Div}}$ (from the fermion diagrams and scalar diagrams, respectively) can be written in terms of $\epsilon = 4 - 2d$ as

$$ig\Gamma^{\mu}_{A,\mathrm{Div}} = \frac{ig^2_{\mathrm{NP}} g \sin\theta_W}{16\pi^2}(\epsilon - 1)\int_0^1 \mathrm{d}x\mathrm{d}y\mathrm{d}z\delta(x+y+z-1)\left(\delta_\epsilon + \ln\frac{4\pi}{\Delta} + \mathcal{O}(\epsilon)\right)\gamma^{\mu}\gamma^5 \tag{4.23}$$

$$ig\Lambda^{\mu}_{A,\mathrm{Div}} = \frac{ig^2_{\mathrm{NP}} g \sin\theta_W}{16\pi^2}\int_0^1 \mathrm{d}x\mathrm{d}y\mathrm{d}z\delta(x+y+z-1)\left(\delta_\epsilon + \ln\frac{4\pi}{\tilde{\Delta}} + \mathcal{O}(\epsilon)\right)\gamma^{\mu}\gamma^5, \tag{4.24}$$

here $\delta_\epsilon = \frac{1}{\epsilon} + \gamma_E$, and γ_E is the Euler-Mascheroni constant. Δ and $\tilde{\Delta}$ are functions of the Feynman parameters and all momentum invariants present: the charged scalar mass M^2, the DM mass m_χ^2, the SM charged lepton mass m_ℓ^2 and the invariant center of mass energy carried by the photon propagator q^2.We see that when adding the two diagrams the UV-divergences parametrized by ϵ vanish and leaves in the $\epsilon \to 0$ limit

$$\begin{aligned} &ig\Gamma^{\mu}_{A,\mathrm{Div}} + ig\Lambda^{\mu}_{A,\mathrm{Div}} \\ &= -\frac{ig^2_{\mathrm{NP}} g \sin\theta_W}{16\pi^2}\int_0^1 \mathrm{d}x\mathrm{d}y\mathrm{d}z\ \delta(x+y+z-1)\left(1 + \ln\frac{\Delta}{\tilde{\Delta}}\right)\gamma^{\mu}\gamma^5. \end{aligned} \tag{4.25}$$

For the Z-channel the cancellation occurs between the four charged lepton diagrams in the same manner as above, only with an overall factor of $\frac{\sin^2 -1/2}{\cos\theta_W}$ instead of the $\sin\theta_W$ appearing in Eqs. (4.23) and (4.24). We also get cancellation of divergences when the loop particles are SM neutrino and the neutral scalar η_0. The same divergent terms as in Eqs. (4.23) and (4.24) arise, but with an overall factor of $\frac{1}{2\cos\theta_W}$ in place for the $\sin\theta_W$.

We have learned from this that the sum of the UV-divergent amplitudes corresponding to the diagrams in Fig. 4.2 cancel in both the Z- and γ^*-channel. The cancellation is between the amplitudes corresponding to the fermion diagrams and the scalar diagrams in both channels.

4.2.4 Generic Form of the Vertex

We now state the general form of the vertex for both the Z- and γ^*-channel in terms of two form factors, and an overall constant $k_{Z/A}$

$$i\Xi^{\mu}_{Z/A}(q) = \frac{ig_{\mathrm{NP}}k_{Z/A}}{16\pi^2}\left(F_{Z/A,1}(q)\gamma^{\mu}\gamma^5 + F_{Z/A,2}(q)\gamma^5\frac{q^{\mu}}{m_{\chi}}\right). \tag{4.26}$$

It is a sum of pseudo-scalar ($q^{\mu}\gamma^5$) and pseudo-vector ($\gamma^{\mu}\gamma^5$) term. Details regarding the calculation and definitions of the form factors can be found in Appendix C. The form of the vertex factor in Eq. (4.26) tells us that pure vector (γ^{μ}) and scalar couplings (q^{μ}) vanish. The reason for this is that these terms are anti-symmetric with respect to the interchange of the Feynman parameters $x \leftrightarrow y$. This will serve as a useful guideline when we apply a different method for solving loop integrals. When we neglect the SM fermion masses $m_f,\ f = \ell, \nu_{\ell}$ the form factors for the Z- and γ^*- coupling are equal up to the coupling factor $k_{z/A}$.For the γ^*- and Z-coupling, respectively, we have $k_p = \sin\theta_W$ and $k_Z = \sin\theta_W \tan\theta_W$.

One could argue that the coupling $i\Xi_{Z/A}$ has to contain a nonzero pseudo-vector contribution and not a vector contribution. A vector coupling for $\gamma^* \to \chi\chi$ would be equivalent to the DM particles acquiring an electromagnetic charge at one-loop level, as the DM particles are assumed to be Majorana this can not happen.

Chapter 5

Loop Integrals by Tensor Reduction

In this chapter we introduce an alternative scheme to solve the vertex function for the $\gamma^* \to \chi\chi$. Since the scheme is general it, generalizes to the loop diagrams in Z-channel amplitudes. The method relies on the covariant description of a given loop integral, and reduces a complicated momentum integral to sums of several, simpler, momentum integrals. We complete the section by stating the γ^* to $\chi\chi$ vertex in terms of simpler integrals.

5.1 Loop Integrals in Tensor Reduction Scheme

We will apply a method known as tensor reduction, or the Passarino-Veltmann method [62]. The method is useful for solving integrals of the form

$$\frac{i}{16\pi^2} T_N^{\mu_1\mu_2\cdots\mu_P}\left(\{q_i, m_i\}_{i=0}^{N-1}\right) = \mu^{4-d}\int \frac{\mathrm{d}^d k}{(2\pi)^d}\ \frac{k^{\mu_1}k^{\mu_2}\ldots k^{\mu_P}}{\Pi_{i=0}^{N-1}[(k+q_i)^2 - m_i^2 + i\varepsilon]} \quad (5.1)$$

by reducing them to sums of scalar integrals of the form

$$\frac{i}{16\pi^2} T_M\left(\{q_i, m_i\}_{i=0}^{M-1}\right) = \mu^{4-d}\int \frac{\mathrm{d}^d k}{(2\pi)^d}\ \frac{1}{\Pi_{i=0}^{N-1}[(k+q_i)^2 - m_i^2 + i\varepsilon]}. \quad (5.2)$$

In Eqs. (5.1) and (5.2) k is the loop momentum variable, and q_i are sums of incoming momenta. The convention for incoming momentum in a loop diagram is illustrated in Fig. 5.1. There is an extracted factor of $i/16\pi^2$ which always appears in one-loop calculations The $i\varepsilon$ in Eqs. (5.1) and (5.2) is the Feynman prescription for the pole shift of the propagator when the propagator momentum is on-shell. We have also included a mass dimension μ to the power of $4-d$

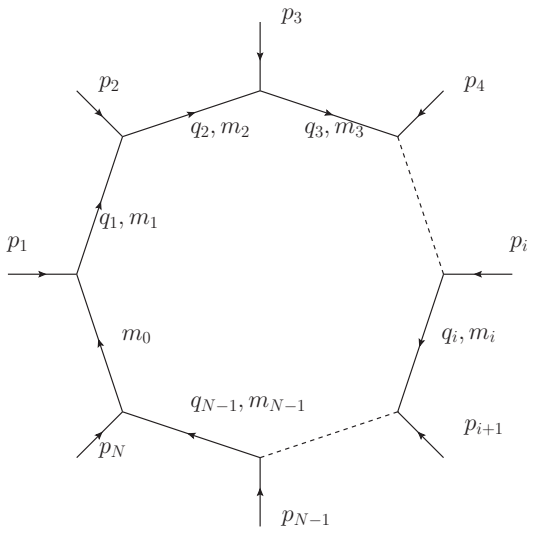

Figure 5.1: Schematic diagram for visualizing the momentum flow in an arbitrary one loop diagram. The arrows denote momentum direction. The propagators and external lines denotes those of a general particle, not necessarily fermion. Momentum is conserved at each vertex, making the propagator momentum $q_n = \sum_{i=1}^{n} p_i$ and $\sum_{i=1}^{N} p_i = 0$. The mass associated with a propagator with momentum q_i is denoted m_i. The dashed lines indicates skipping over several propagators and external momenta.

to ensure consistency of the mass dimension of the integral.[1] We shall show in Sec. 5.1.1 show by an example how this tensor reduction is done.

We refer to the tensor integral of Eq. (5.1) as the N-point rank P tensor integral, and the integral in Eq. (5.2) as the M-point scalar integral. Generally $M \leq N$. We define the propagator denominators D_i by

$$D_i = (k + q_i)^2 - m_i^2 + i\varepsilon, \ i = 0, 1, 2, \ldots, N-1. \tag{5.3}$$

Formally, we have a momentum q_0 in D_0 which can be disregarded due to a suitable linear substitution of the loop-momentum. To accommodate for this we set $D_0 = k^2 - m_0^2 + i\varepsilon$. The integral is invariant under all permutation of the Lorentz indices, as well as any interchange of the denominator factors D_i, $i = 1, 2, , \ldots N-1$ (or equivalently, any permutation of $\{(q_i, m_i)\}_{i=1}^{N-1}$).

We will here adopt the convention in [63] and refer to the N-point integrals in Eq.(5.1) by the Nth capital roman letter in the alphabet. As well as a different

[1] One might also assume that this "dimensional inconsistency" can be absorbed in the coupling constant. However we will take this approach, as the coupling constant is neglected in the general scheme

convention for the arguments. For the scalar integrals we then define

$$A_0(m_0^2) \equiv T_1(m_0) \tag{5.4}$$
$$B_0\left(q_1^2, m_0^2, m_1^2\right) \equiv T_2\left(m_0, (q_1, m_1)\right) \tag{5.5}$$
$$C_0\left(q_1^2, q_{21}^2, q_2^2, m_0^2, m_1^2, m_2^2\right) \equiv T_3\left(m_0, (q_1, m_1), (q_2, m_2)\right) \tag{5.6}$$

Where $q_{ij} = q_i - q_j$. The rank-one tensor integrals are denoted

$$B^\mu(q_1^2, m_0^2, m_1^2) \equiv T_2^\mu\left(m_0, (q_1, m_1)\right), \tag{5.7}$$
$$C^\mu\left(q_1^2, q_{21}^2, q_2^2, m_0^2, m_1^2, m_2^2\right) \equiv T_2^\mu\left(m_0, (q_1, m_1), (q_2, m_2)\right), \tag{5.8}$$

And the rank-two tensor integrals

$$B^{\mu\nu}(q_1^2, m_0^2, m_1^2) \equiv T_2^{\mu\nu}\left(m_0, (q_1, m_1)\right) \tag{5.9}$$
$$C^{\mu\nu}\left(q_1^2, q_{21}^2, q_2^2, m_0^2, m_1^2, m_2^2\right) \equiv T_3^{\mu\nu}\left(m_0, (q_1, m_1), (q_2, m_2)\right) \tag{5.10}$$

The list continues up to arbitrary rank P. However, we will not need any more scalar or tensor integral for the scope of this thesis. The rank-one tensor integrals in Eq. (5.7) and (5.8) can, to Lorents covariance, be written in terms of the momenta q_i as

$$B^\mu(q_1^2, m_0^2, m_1^2) = q_1^\mu B_1 \tag{5.11}$$
$$C^\mu\left(q_1^2, q_{21}^2, q_2^2, m_0^2, m_1^2, m_2^2\right) = \sum_{i=1}^{2} q_i^\mu C_i \tag{5.12}$$

And the Rank-two tensor integrals in Eqs. (5.9) and (5.10) can be decomposed as

$$B^{\mu\nu}(q_1^2, m_0^2, m_1^2) = g^{\mu\nu} B_{00} + q_1^\mu q_1^\nu B_{11} \tag{5.13}$$
$$C^{\mu\nu}\left(q_1^2, q_{21}^2, q_2^2, m_0^2, m_1^2, m_2^2\right) = g^{\mu\nu} C_{00} + \sum_{i,j=1}^{2} q_i^\mu q_j^\nu C_{ij} \tag{5.14}$$

The coefficients B_1, C_i, B_{ii}, C_{ij} are referred to as Passarino Veltmann coefficients. We note that the momenta q_i^μ are assumed to be independent. Note that four linearly independent four-vectors are needed to span four dimensional spacetime. This implies if $N \geq 5$ (i.e. four or more linearly independent external momenta are present) at most four linearly independent Lorentz four-vectors are needed in the expansion of the tensor integral, such that, terms containing $g_{\mu\nu}$ should then be omitted.

5.1.1 Rank-One Two-Point Tensor Integral

We will illustrate the method by performing Passarino Veltmann method on the two-point scalar integral $C^{\mu}\left(q_1^2, q_{21}^2, q_2^2, m_0^2, m_1^2, m_2^2\right) \equiv C_{\mu}$. We consider the expansion in momenta q_i^{μ} in Eq. (5.12), and take the Lorentz invariant inner product $q_i^{\mu} C_{\mu},\ i = 1, 2$

$$q_i^{\mu} C_{\mu} = \sum_{i=1}^{2} q_j \cdot q_i C_i \equiv R_j. \tag{5.15}$$

This is equivalent to the system of equations

$$\begin{pmatrix} q_1^2 & q_1 \cdot q_2 \\ q_1 \cdot q_2 & q_2^2 \end{pmatrix} \begin{pmatrix} C_1 \\ C_2 \end{pmatrix} = \begin{pmatrix} R_1 \\ R_2 \end{pmatrix}. \tag{5.16}$$

The matrix on the left hand side is referred to as the Gram matrix. The system can now easily be solved to find C_1 and C_2 in terms of R_1 and R_2 for a non-singular Gram matrix.

The expressions for R_j can be reduced to scalar integrals by using the following relation:

$$\begin{aligned} q_i \cdot k &= \frac{1}{2}\left(\left[(k+q_i)^2 - m_i^2 + i\varepsilon\right] - \left[k^2 - m_0^2 + i\varepsilon\right] + m_i^2 - q_i^2 - m_0^2\right) \\ &= D_i - D_0 + m_i^2 - q_i^2 - m_0^2. \end{aligned}$$

This gives the following expressions for $R_{1,2}$:

$$\begin{aligned} R_1 &= \frac{(2\pi\mu)^{4-d}}{i\pi^2} \int \mathrm{d}^d k \left\{ \frac{1}{D_0 D_2} - \frac{1}{D_1 D_2} + \frac{m_1^2 - q_1^2 - m_0^2}{D_0 D_1 D_2} \right\} \\ &= B_0\left(q_2^2, m_0^2, m_2^2\right) - B_0\left(q_{21}^2, m_1^2, m_2^2\right)) \\ &\quad + \left[m_1^2 - q_1^2 - m_0^2\right] C_0(q_1^2, q_{21}^2, q_2^2, m_0^2, m_1^2, m_2^2), \end{aligned} \tag{5.17}$$

and

$$\begin{aligned} R_2 &= \frac{(2\pi\mu)^{4-d}}{i\pi^2} \int \mathrm{d}^d k \left\{ \frac{1}{D_0 D_1} - \frac{1}{D_1 D_2} + \frac{m_2^2 - q_2^2 - m_0^2}{D_0 D_1 D_2} \right\} \\ &= B_0\left(q_1^2, m_0^2, m_2^2\right) - B_0\left(q_{21}^2, m_1^2, m_2^2\right) \\ &\quad + \left[m_2^2 - q_2^2 - m_0^2\right] C_0(q_1^2, q_{21}^2, q_2^2, m_0^2, m_1^2, m_2^2). \end{aligned} \tag{5.18}$$

Solving the system of equations will lead to expressions for C_1 and C_2 in terms of R_1 and R_2

$$\begin{pmatrix} C_1 \\ C_2 \end{pmatrix} = \frac{1}{(q_1)^2 (q_2)^2 - (q_1 \cdot q_2)^2} \begin{pmatrix} q_2^2 R_1 - q_1 \cdot q_2 R_2 \\ q_1 \cdot q_2 R_1 - q_2^2 R_2 \end{pmatrix}. \tag{5.19}$$

Where we can insert the expressions for R_1 and R_2 in Eqs. (5.17) and (5.18). This cives C_1 and C_2 in terms of scalar integrals B_0 and C_0.

Lastly we insert C_1 and C_2 in the expansion $C_\mu = \sum_{i=1,2} q_i C_i$. This will give the full decomposition of C_μ in scalar integrals

$$\begin{aligned} C^\mu = \frac{1}{2\left((q_1\cdot q_2)^2 - q_1^2 q_2^2\right)} \Big\{ & \left(q_1^\mu\ q_1\cdot q_2 - q_2^\mu\ q_1^2\right) B_0(q_1^2, m_0^2, m_1^2) \\ & + \left(q_2^\mu\ q_1\cdot q_2 - q_1^\mu\ q_2^2\right) B_0(q_2^2, m_0^2, m_2^2) \\ & \left[q_2^\mu\ (q_1^2 - q_1\cdot q_2) + q_1^\mu\ ((q_2^2 - q_1\cdot q_2))\right] B_0\left(q_{21}^2, m_1, m_2^2\right)\Big) \end{aligned}$$

$$\begin{aligned} & + \Big[\ q_1^\mu \left(q_2^2\left[q_1^2 + m_0 - m_1^2\right] - q_1\cdot q_2\left[q_2^2 + m_0 - m_2^2\right]\right) + \\ & + q_2^\mu\ \left(q_1\cdot q_2\left[m_1^2 - m_0^2\right] - q_1^2\left[q_1\cdot q_2 - q_2^2 - m_0^2 + m_2^2\right]\right)\Big] C_0\left(q_1^2, q_{21}^2, q_2^2, m_0^2, m_1^2, m_2^2\right)\Big\}. \end{aligned}$$

5.1.2 UV-Divergent scalar integrals

We can investigate the superficial divergence of a tensor integral like in Eq. (5.1). When looking at the leading order terms in k of the integrand of Eq. (5.1) we find

$$T_N^{\mu_1,\ldots\mu_P} \sim \int \mathrm{d}^d k \frac{k^P}{k^{2N}} \sim \int \mathrm{d}|k| \frac{|k|^{d-1}|k|^P}{|k|^{2N}}. \tag{5.20}$$

Which is UV-divergent if the power of k in the denominator is less than one. That is, the integral in Eq. (5.1) is UV-divergent if

$$P + d - 2N \geq 0.$$

Where P is the maximal number of momenta in the numerator, N is the number of numerator factors D_i's and d is the spacetime dimension.

We regularize the UV-divergence by dimensional regularization. Among the scalar integrals in Eqs. (5.4) and (5.5) the scalar one-point integral $A_0(m_0^2)$ and the scalar two-point integral $B_0(q_1^2, m_0^2, m_1^2)$ are UV-divergent. In dimensional regularization the divergence in B_0 and A_0 scales as $1/(d-4)$ where d is the dimension of spacetime. A exhaustive list of divergent scalar integrals can be found in [63].

5.2 Tensor Reduction Using Numerical Tools

The Passarino-Veltmann procedure of reducing tensor integrals to several scalar integrals quickly becomes cumbersome and tedious to perform. However, there are numerical tools to aid the reduction. We apply FeynCalc 9.0.1 [64,65], for the tensor reduction of the loop integrals.

We apply the tensor reduction scheme for the fermion diagrams and the scalar diagrams separately, and then add the contributions. Motivated by the general form of the $\gamma^* \to \chi\chi$ in Eq. (4.1) we now the desired form of the vertex. After the amplitudes for all four diagrams in Fig. 4.2 are added together we obtain an expression of the form

$$i\Xi_A^\mu = -\frac{ig_{\rm NP}^2 \sin\theta_W}{16\pi^2}\left[F_{A,1}\gamma^\mu\gamma^5 + F_{A,2}\gamma^5\frac{q^\mu}{m_\chi}\right]$$

Where the form factors $F_{A,1}$ and $F_{A,2}$ are given in terms of scalar integral $B_0(\dots)$ and $C_0(\dots)$ as

$$\begin{aligned}
F_{A,1} = \frac{1}{2(4m_\chi^2 - q^2)}\big\{ & 4(m_\chi^2 - q^2)\left[B_0(m_\chi^2, m_\ell^2, M^2) - B_0(q^2, m_\ell^2, m_\ell^2)\right] \\
& + (q^2 - 2\Delta M_+^2)\left[B_0(q^2, M^2, M^2) - B_0(q^2, m_\ell^2, m_\ell^2)\right] \\
& + 2\left[\Delta M_-^4 + m_\ell^2(q^2 - 4m_\chi^2)\right] C_0(m_\chi^2, m_\chi^2, q^2, M^2, m_\ell^2, M^2) \\
& + 2\left[\Delta M_+^4 + q^2\Delta M_+^2 + (q^2 - 4m_\chi^2)M^2\right] C_0(m_\chi^2, m_\chi^2, q^2, m_\ell^2, M^2, m_\ell^2)\ \big\} - 1,
\end{aligned} \tag{5.21}$$

and

$$\begin{aligned}
F_{A,2} = \frac{m_\chi^2}{q^2}\frac{1}{4m_\chi^2 - q^2}\big\{ & 4(m_\chi^2 - q^2)[B_0(q^2, m_\ell^2, m_\ell^2) - B_0(m_\chi^2, m_\chi^2, M^2)] \\
& - (q^2 - 2\Delta M_+^2)[B_0(q^2, M^2, M^2) - B_0(q^2, m_\ell^2, m_\ell^2)] \\
& -2\left[\Delta M_-^4 + m_\ell^2(q^2 - 4m_\chi^2)\right] C_0(m_\chi^2, m_\chi^2, q^2, M^2, m_\ell^2, M^2) \\
& -2\left[\Delta M_+^4 + q^2\Delta M_+^2 + (M^2 - q^2)(q^2 - 4m_\chi^2)\right] C_0(m_\chi^2, m_\chi^2, q^2, m_\ell^2, M^2, m_\ell^2)\ \big\} \\
& + 2\frac{m_\chi^2}{q^2},
\end{aligned} \tag{5.22}$$

Where $\Delta M_\pm^2 = M^2 \pm m_\chi^2 - m_\ell^2$. We see that from the expressions of the form factors in Eqs. (5.21) and (5.22) that the UV-divergences cancel, as they appear only in the scalar two-point integrals $B_0(\cdots)$. The form factors only depend on the difference between two UV-divergent scalar two-point integral.

5.2.1 The Scalar Integrals in the Effective Vertex

In the form factors there are two types of scalar integrals. The three-point scalar integrals and two-point scalar integrals. We state the general solutions to the two- and three-point scalar integrals below.

Two point scalar integral

The general expression or the two-point scalar integral is

$$\frac{i}{16\pi^2}B_0(p^2,m_0^2,m_1^2)=\mu^{4-d}\int\frac{\mathrm{d}^dk}{(2\pi)^d}\,\frac{1}{[k^2-m_0^2]\,[(k+p)^2-m_1^2]}. \tag{5.23}$$

The general solution for the two-point scalar integral is made in AppendixD.2.1 and can also be found in e.g. [66,67]. The general solution is for arbitrary masses m_1, m_2 and arbitrary p^2

$$B_0(p^2,m_0^2,m_1^2)=\delta_\epsilon+\ln\frac{\mu^2}{m_0^2-i\varepsilon}+2-\sum_{i=1}^{2}(1-x_i)\ln\left(\frac{x_i-1}{x_i}\right). \tag{5.24}$$

where $x_{1,2}$ are given as

$$x_{1,2}=\frac{1}{2p^2}\left(p^2-m_0^2+m_1^2\pm\sqrt{(p^2-m_1^2+m_0^2)^2-4p^2(m_0^2-i\varepsilon)}\right), \tag{5.25}$$

and

$$\delta_\epsilon=\frac{2}{\epsilon}-\gamma_E+\ln 4\pi \tag{5.26}$$

regularizes the UV-divergence in dimensional regularization with $d=4-2\epsilon$. We note that it is important to distinguish ϵ (UV-regulator) from ε, as $v\epsilon$ is the infinitesimal imaginary part in the propagator.

The scalar two-point integral is divergent, however, we see in Eqs. (5.21) and (5.22) that the form factors are dependent on the difference of the divergent integrals. Thus, these divergences cancel as we can see from the general solution of $B_0(p^2,m_0^2,m_1^2)$.

The logarithm is evaluated by taking its principal value. The principal value of the logarithm is

$$\ln z=\ln|z|+i\mathrm{Arg}z \tag{5.27}$$

where $z=|z|e^{i\mathrm{Arg}z}$ and Argz is the principal value of the argument that is $-\pi\leq\mathrm{Arg}z\leq\pi$. The logarithm then has a branch cut along the negative real axis in the complex plane, and its imaginary part takes on the values $\pm i\pi$ here. In order to determine the correct sign of $i\pi$ the infinitesimal imaginary part $i\epsilon$. As an example; if m_0 in Eq. (5.24) is negative we get

$$\ln\frac{\mu^2}{m_0^2-i\varepsilon}=\ln\frac{\mu^2}{-m_0^2}+i\pi, \tag{5.28}$$

as ε is positive and infinitesimal. The product rule for logarithms for complex z and w is given by [68]

$$\ln(zw) = \ln z + \ln w + \eta(z, w), \tag{5.29}$$

where η compensates for crossings of the branch cut and is given by

$$\eta(z, w) = 2\pi i \left[\theta(-\mathrm{Im}z)\theta(-\mathrm{Im}w)\theta(\mathrm{Im}zw) - \theta(\mathrm{Im}z)\theta(\mathrm{Im}w)\theta(-\mathrm{Im}zw)\right], \tag{5.30}$$

where η is the Heaviside function.

For the two-point scalar integral in the form factors of Eqs. (5.21) and (5.22) we get

$$\begin{aligned} &B_0(m_\chi^2, m_\ell^2, M^2) - B_0(q^2, m_\ell^2, m_\ell^2) \\ &= \ln\left(\frac{-q^2 - i\varepsilon}{M^2 - m_\chi^2 - iM\Gamma}\right) + \mu \ln\left(1 - \frac{1}{\mu}\right), \end{aligned} \tag{5.31}$$

and

$$\begin{aligned} B_0(q^2, M^2, M^2) - B_0(q^2, m_\ell^2, m_\ell^2) = &- \ln\left(\frac{M^2 - iM\Gamma}{-q^2 - i\varepsilon}\right) \\ &+ \frac{1}{2}(1 - \xi_M)\ln\left(\frac{\xi_M - 1}{\xi_M + 1}\right) \\ &- \frac{1}{2}(1 + \xi_M)\ln\left(\frac{\xi_M + 1}{\xi_M - 1}\right) \end{aligned} \tag{5.32}$$

where the width is calculated at tree-level to be $\Gamma = (g_{NP}^2/16\pi)M\left(1 - m_\chi^2/M^2\right)^2$

Three-point scalar integral

The general expression for the three point scalar integral is

$$\begin{aligned} &\frac{i}{16\pi^2} C_0(p_1^2, p_{21}^2, p_2^2, m_0^2, m_1^2, m_2^2) \\ &= \int \frac{\mathrm{d}^d k}{(2\pi)^d} \frac{1}{(k^2 - m_0^2 + i\varepsilon)\left([k + p_1]^2 - m_1^2 + i\varepsilon\right)\left([k + p_2]^2 - m_2^2 + i\varepsilon\right)}. \end{aligned} \tag{5.33}$$

We perform a shift in the momentum $k \to k - p_2$, and introduce Feynman parameters

$$\begin{aligned}
&\frac{i}{16\pi^2} C_0(p_1^2, p_{21}^2, p_2^2, m_0^2, m_1^2, m_2^2) \\
&= \int \frac{\mathrm{d}^d k}{(2\pi)^d} \frac{1}{\left([k^2 - p_2]^2 - m_0^2\right) \left([k - p_{21}]^2 - m_1^2\right) (k^2 - m_2^2)} \\
&= \int \frac{\mathrm{d}^d \ell}{(2\pi)^d} \int_0^1 \mathrm{d}x \int_0^1 \mathrm{d}y \int_0^1 \mathrm{d}z \; \delta(x + y + z - 1) \frac{2}{\left[\ell^2 - (\Delta - i\varepsilon)\right]^3} \\
&\overset{d \to 4}{=} \frac{-i}{16\pi^2} \int_0^1 \mathrm{d}x \int_0^1 \mathrm{d}y \int_0^1 \mathrm{d}z \; \delta(x + y + z - 1) \frac{1}{\Delta - i\varepsilon}.
\end{aligned}$$

Where we integrate in a shifted momentum variable $\ell = k - yp_2 - zp_{21}$ and define $\Delta = -xyp_2^2 - xzp_{21}^2 - yzp_1^2 + xm_2^2 + ym_0^2 + zm_1^2$. We solve the momentum integral using Eq. (B.9). Integrating over z and substituting $x \to 1 - x$ gives the following form of the three point scalar integral

$$\begin{aligned}
&C_0(p_1^2, p_{21}^2, p_2^2, m_0^2, m_1^2, m_2^2) = \\
&- \int_0^1 \mathrm{d}x \int_0^x \mathrm{d}y \, \{ \, x^2 p_{21}^2 + y^2 p_1^2 + xy \left(p_2^2 - p_1^2 - p_{21}^2\right) + x(m_1^2 - m_2^2 - p_{21}^2) \\
&\qquad\qquad + y(m_0^2 - m_1^2 + p_{21}^2 - p_2^2) + m_2^2 - i\varepsilon \, \}^{-1} .
\end{aligned}$$

The solution of the three-point integral on this form is given in [63], there is also detailed calculation in [68]. The general solution has the following form:

$$\begin{aligned}
&C_0(p_1^2, p_{21}^2, p_2^2, m_0^2, m_1^2, m_2^2) \\
&= \frac{1}{\alpha} \sum_{i=0}^{2} \left[\sum_{\sigma = \pm} \mathrm{Li}_2 \left(\frac{z_{0i} - 1}{y_{0\sigma}} \right) - \mathrm{Li}_2 \left(\frac{z_{0i}}{y_{0\sigma}} \right) + \right. \\
&\quad \eta \left(1 - x_{i\sigma}, \frac{1}{y_{i\sigma}} \right) \ln \frac{z_{0i} - 1}{y_{i\sigma}} - \eta \left(-x_{i\sigma}, \frac{1}{y_{i\sigma}} \right) \ln \frac{z_{0i}}{y_{i\sigma}} \\
&\quad - \left[\eta \left(-x_{i+}, -x_{i-} \right) - \eta \left(y_{i+}, y_{i-} \right) - \right. \\
&\quad \left. \left. -2\pi i \; \theta \left(-p_{ij}^2 \right) \; \theta \left(-\mathrm{Im} \left(y_{i+} y_{i-} \right) \right) \right] \ln \frac{1 - z_{i0}}{-z_{i0}}, \right]
\end{aligned} \tag{5.34}$$

where $\alpha = \kappa(p_1^2, p_{21}^2, p_2^2)$ and κ is the function

$$\kappa(x, y, z) = \sqrt{x^2 + y^2 + z^2 - 2(xy + yz + xz)}$$

We have $p_{ij}^2 = (p_i - p_j)^2$, $i, j = 0, 1, 2$ and $p_0 = 0$. For cyclic permutations of $i, j, k = 0, 1, 2$ the quantities $x_{i\pm}, y_{i\pm}, z_{0i}$ are

$$\begin{aligned} z_{0i} = \frac{1}{2\alpha p_{jk}^2} \{ & p_{jk}^2 \left[p_{jk}^2 - p_{ki}^2 - p_{ij}^2 + 2m_i^2 - m_j^2 - m_k^2 \right] \\ & - \left(p_{ki}^2 - p_{ij}^2 \right) \left(m_j^2 - m_k^2 \right) + \left(p_{ki}^2 - m_j^+ m_k^2 \right), \} \end{aligned} \tag{5.35}$$

$$x_{i\pm} = \frac{1}{2p_{jk}^2} \left[p_{jk}^2 - m_j^2 + m_k^2 + \alpha_i \right], \tag{5.36}$$

$$y_{i\pm} = z_{0i} - x_{i\pm}, \tag{5.37}$$

$$\alpha = \kappa(p_1^2, p_{21}^2, p_2^2) \tag{5.38}$$

$$\alpha_i = \kappa(p_{jk}^2, m_j^2, p_2^2)(1 + \frac{i\varepsilon}{p_{jk}^2}), \tag{5.39}$$

here $\mathrm{Li}_2(z)$ is the dilogarithm function, which is given by

$$\mathrm{Li}_2(z) = -\int_0^z \frac{\ln(1-t)}{t}\,\mathrm{d}t = -\int_0^1 \frac{\ln(1-zt)}{t}\,\mathrm{d}t, \tag{5.40}$$

where z is generally complex. Due to the branch cut of the logarithm on the negative axis the dilogarithm gets a cut on the positive real axis, i.e. for $z \in [1, \infty)$ the dilogarithm is multivalued. The $i\varepsilon$-prescription selects the correct part of the branch. The general solution in Eq. (5.34) applies for generally complex masses m_i and general momenta p_{ij}^2, and the η functions will compensate for branch crossings of the dilogarithm and logarithms [63].

We evaluate the three-point scalar integral directly using Eq. (5.34) for $C_0(m_\chi^2, m_\chi^2, q^2, M^2, m_\ell^2, M^2)$ and $C_0(m_\chi^2, m_\chi^2, q^2, m_\ell^2, M^2, m_\ell^2)$. We apply the mass hierarchy $M^2 > m_\chi^2 >> m_\ell^2$, which makes both three-point integrals in Eqs. (5.21) and (5.22) independent of m_ℓ^2.

5.2.2 Cross Section

We can now state the unpolarized cross section for pair production of this dark matter candidate in the photon channel. We consider the initial state to be a quark and anti-quark pair with a center of mass energy $\sqrt{s} = \sqrt{q^2} > 4m_\chi$. The differential cross-section is then

$$\frac{\mathrm{d}\sigma}{\mathrm{d}\Omega} = \frac{1}{4q^2}\sqrt{1 - \frac{4m_\chi^2}{q^2}}\frac{1}{(4\pi)^2}|\bar{\mathcal{M}}(q\bar{q} \to \chi\chi)|^2 \tag{5.41}$$

where $|\bar{\mathcal{M}}(q\bar{q} \to \chi\chi)|^2$ is the unpolarized amplitude given by

$$|\bar{\mathcal{M}}(q\bar{q} \to \chi\chi)|^2 = e^2 Q_q^2 \left(1 - \frac{4m_\chi^2}{q^2}\right) \left(\cos^2\theta + 1\right) \frac{g_{\text{NP}}^4}{(16\pi^2)^2} |F_{1A}(q^2)|^2, \quad (5.42)$$

where θ is the azimuthal angle Q_q is the charge of the quark q in units of the electron charge $e = g \sin\theta_W$. We have inserted for the fine-structure constant $e^2/4\pi$. For up type quarks up-type quark then $Q_u = +2/3$ and $Q_d = -1/3$ for down-type quarks. The total cross section is found by integrating over θ from 0 to π

$$\sigma = \frac{3\pi}{2} \frac{\alpha^2 Q_q g_{\text{NP}}^4}{(32\pi^2)^2} \frac{1}{q^2} \left(1 - \frac{4m_\chi^2}{q^2}\right)^{3/2} |F_{1A}(q^2)|^2, \quad (5.43)$$

We emphasize that for quarks colliding at a hadron collider, such as the LHC, this cross section needs to be integrated of the parton distribution functions (PDFs)for each quark flavor. Partons are quarks and gluons in a hadron, they carry a fractional part of the hadrons full momentum, the PDFs are flavour dependent probability distributions for a quarks fractional amount of the full momentum.

5.3 Results

In Fig. 5.2 we see a plot of the cross section as a function of the center of mass energy for the process $q\bar{q} \to \chi\chi$ in the photon channel. The cross section has a resonance at $\sqrt{s} = 2M$, where the scalar mass $M = 1500$ for this figure.

In Fig. 5.3 we see the cross section where the DM and scalar are close in mass. Here $M = 500$ GeV is with 11% of the DM-mass $m_\chi = 450$. This is where M is in the co-annihilation region. Here, the WIMP miracle described in Sec. 3.2.2, can not occur with self-annihilating DM. And co-annihilating processes $\eta\chi \to SM \times SM$ must also be taken into account. The η-resonance is barely visible in the Fig. 5.3, however, in Fig. 5.4 is plotted in a mass range closer to 1 TeV to highlight the resonance.

In Fig. 5.6 and in Fig. 5.5 we see the cross section as function of the ratio of the DM and scalar mass m_χ^2/M^2 with a fixed $M = 1500$. In Fig. 5.5 the center of mass energy is on the η-resonance. In Fig. 5.6 the center of mass energy is far from the resonance. We see that the cross section increases monotonically with increasing m_χ, however, at resonance the cross section appears to diverge as $m_\chi \to M/4$. When m_χ exceeds this limit $q^2 < 4m_\chi^2$ since $q^2 = M^2 = (8 \text{ TeV})$ in Fig. (5.6), i.e. the center of mass energy is not sufficient for production of $\chi\chi$.

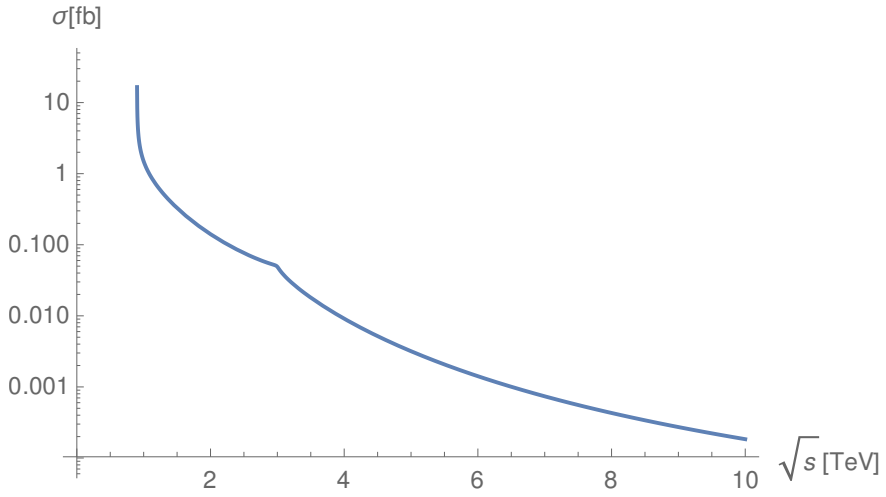

Figure 5.2: The cross section for $q\bar{q} \to \chi\chi$ in the photon channel. The chosen values are for the coupling $g_{NP} = 0.9$, the scalar mass is $M = 1500$ GeV and the DM mass is $m_\chi = 450$ GeV. There is a distinct resonance at $\sqrt{s} = 3000$ GeV, which is the η mass M resonance.

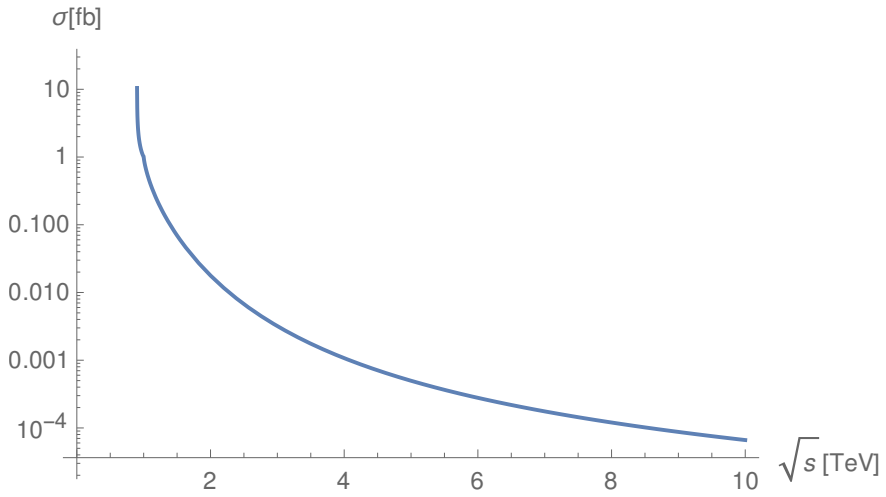

Figure 5.3: The cross section for $q\bar{q} \to \chi\chi$ in the photon channel. The chosen values are for the coupling $g_{NP} = 0.9$, the scalar mass is $M = 500$ GeV and the DM mass is $m_\chi = 450$ GeV. The η-resonance at 1 TeV is barely visible.

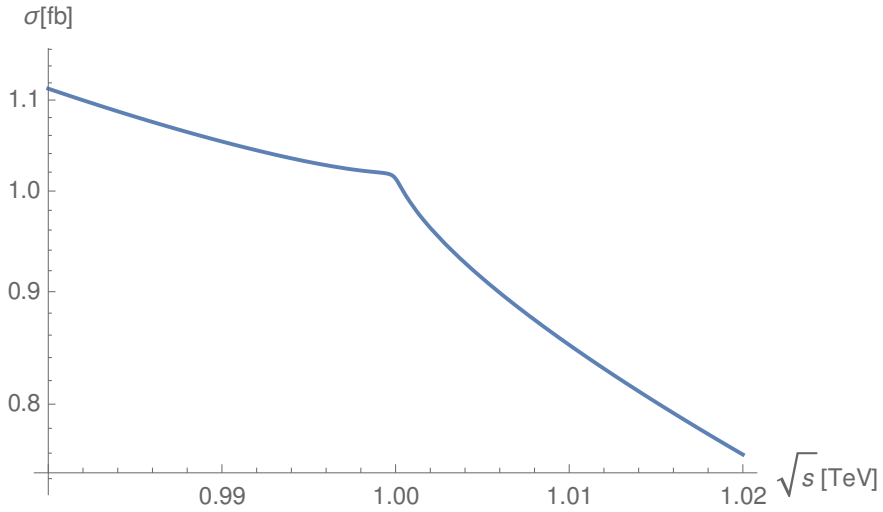

Figure 5.4: The cross section for $q\bar{q} \to \chi\chi$ in the photon channel. The chosen values are for the coupling $g_{NP} = 0.9$, the scalar mass is $M = 500$ GeV and the DM mass is $m_\chi = 450$ GeV. The graph is zoomed in around the η-resonance at 1 TeV.

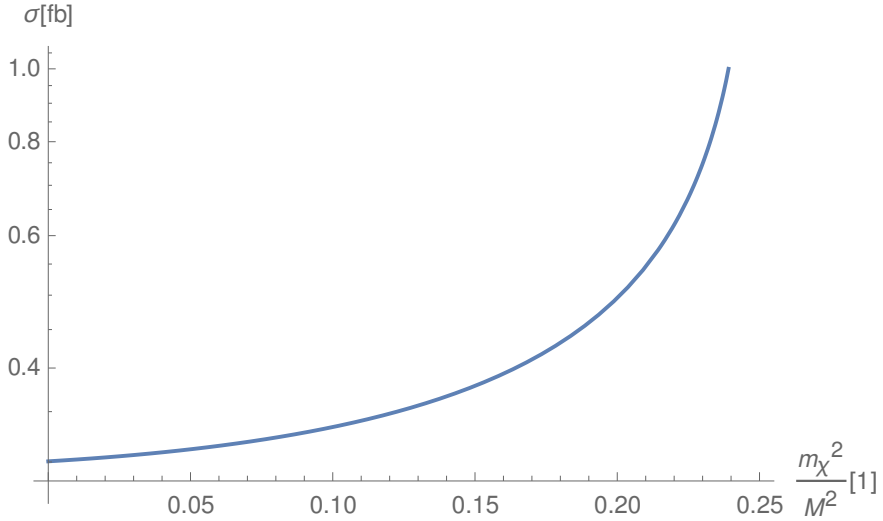

Figure 5.5: The cross section for $q\bar{q} \to \chi\chi$ in the photon channel as a function of the DM and scalar mass ratio m_χ^2/M^2 at a center of mass energy at resonance, $\sqrt{s} = 1500$. The chosen values are for the coupling $g_{NP} = 0.9$, the scalar mass is fixed at $M = 1500$ GeV.

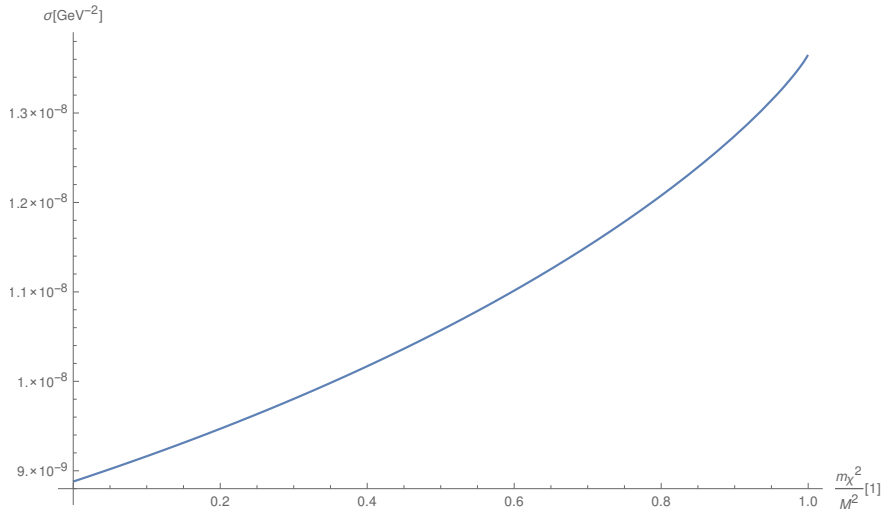

Figure 5.6: The cross section for $q\bar{q} \to \chi\chi$ in the photon channel as a function of the DM and scalar mass ratio m_χ^2/M^2 at a center of mass energy at resonance, $\sqrt{s} = 8000$. The chosen values are for the coupling $g_{NP} = 0.9$, the scalar mass is fixed at $M = 1500$ GeV.

5.3.1 Discussion

We have plotted results for some selected parameters for pair production of leptophilic DM in a collision between $q_u\bar{q}_u$ of same flavor in Figs. 5.2-5.5. We use the effective vertex given in terms of the form factors in Eq. (4.26), with the form factors found in Eqs. (5.21) and (5.22).

Neglecting the lepton masses results in a generation independent vertex, i.e. the SM leptons in the loop are either e, μ or τ for the cross sections in Figs. 5.2-5.5. Furthermore we can generalize the results to include the Z-channel, as the form factors are equal up to a constant for the one-loop processes $\gamma^* \to \chi\chi$ and $Z^* \to \chi\chi$ when all lepton masses are neglected.

The cross section at the η-resonance with the parameters in Fig. 5.2 is of order $\mathcal{O}(0.1fb)$, however, this does not directly translate into expected number of events at the LHC for a given luminosity. In order to get complete cross for $pp \to \chi\chi$ integration over the PDFs must be performed as well as summation over the quarks and anti-quark in the proton. For LHC applications the total center of mass energy is $\sqrt{s} = 14$ TeV in its second run, however only a fractional amount of each proton momentum is carried by the quarks that take part in the collision. Furthermore, the χ-pair will escape detection rendering measuring these events impossible.

In order to get a result that can be detected at the LHC further analysis is needed. One possibility is to study a higher order process where the final state is a jet in addition to a χ-pair. The jet comes from initial state radiation of a gluon from one of the incident quarks in the collision. If the jet carries high transverse

momentum the missing transverse momentum will be the χ-pair recoiling on the jet.

Chapter 6

Summary and Concluding Remarks

We begun in Chapter 1 by introducing the theoretical ingredients necessary for understanding the SM. We also introduced the Weyl spinor formalism, which is widely used to represent a Majorana fermion since it contains the degrees of freedom carried by a complex two-component object. We then turned to the questions left open by the SM. After giving a summary of the history of DM, we went through the evidence for its existence from cosmological observations and studies.

A class of particles consistent with the requirements for DM is the WIMPs. We have studied a model consisting of a WIMP interacting with SM charged leptons and neutrinos and two decaying scalar particles.

We studied the process $\gamma^* Z^* \to \chi\chi$ at next-to leading order. First we applied dimensional regularization and introduced Feynman parameters to find the general form of the effective vertex rule in this amplitude. We found that the effective vertex is UV-finite and that the cancellation occurs between the amplitudes corresponding to two different sets of Feynman diagrams. From the resulting form of the vertex we found that the Majorana particles had an pseudo-scalar and vector coupling to the neutral electroweak gauge bosons γ and Z. Furthermore, the vertex form factors for the effective coupling to the Z were found to be equal to the effective γ-coupling — up to a constant factor $\tan\theta_W$ — when the $\eta, \eta^\dagger$-masses are equal and the SM lepton masses were neglected in the loop.

In order to find a closed form expression for the vertex we used the Passarino-Veltmann method. This gave the form factors expressed in terms of scalar integrals. By applying the closed form solutions of the scalar integrals the effective vertex was retrieved in closed form.

Lastly, we investigated the cross section for free quarks annihilating into the pair $\chi\chi$.

6.1 Future Prospects

For the sampled value of the coupling $g_{\mathrm{NP}} = 0.9$ we get a cross section for free quarks to $\chi\chi$ of the order $\mathcal{O}(0.1$ fb) at the η-resonance for $M = 1500$ GeV and $m_\chi = 450$ GeV. For the integrated luminosity of the LHC, a cross-section of this order gives a non-negligible number of events, and this makes it tempting to speculate whether the cross section for $pp \to \chi\chi$ is of the same order of magnitude. The logical next step in order to examine this is to conduct a full study of the visible cross section using a mono-jet analysis. This can be done using Monte Carlo sampling from parton distribution functions of the initial state quarks, numerically generating events with initial state radiation showering, and performing a jet analysis for a sample of events.

Appendices

Appendix A

Quantum Electrodynamics

The Dirac Lagrangian

$$\mathcal{L} = \bar{\psi}\left(i\partial\!\!\!/ - m\right)\psi, \tag{A.1}$$

is invariant under the transformation $\psi \to e^{iQ\theta}\psi$. Where Q defines a charge, and θ is a real constant referred to as the *gauge parameter*. We call this sort of symmetry a global U(1) gauge-symmetry — all unitary 1×1-matrices i.e. phase shifts of the Dirac spinor.

We shall another complication by letting the gauge parameter be an arbitrary real function of space time $\theta \to \theta(x)$. By applying a local gauge transformation of the spinors in the free Dirac Lagrangian the differential operator in Eq. (A.1) picks up and extra term:

$$\begin{aligned}
\mathcal{L} &= \bar{\psi}(i\partial\!\!\!/ - m)\psi && \text{(A.2)}\\
&\to \bar{\psi}e^{-iQ\theta}\partial\!\!\!/\left(e^{iQ\theta}\psi\right) && \text{(A.3)}\\
&= \bar{\psi}\left(i\partial\!\!\!/ - m + iQ(\partial\!\!\!/\theta)\right)\psi \neq \mathcal{L}. && \text{(A.4)}
\end{aligned}$$

This Lagrangian is not invariant with respect to local U(1) gauge-transformations. We can still construct a Lagrangian which is invariant under these transformations, however we then have to introduce the *covariant derivative*

$$D_\mu \equiv \partial_\mu + ieQA_\mu(x). \tag{A.5}$$

Where we postulate the *connection* or *gauge field* $A_\mu(x)$. We perform the minimal substitution $\partial_\mu \to D_\mu$ in the Lagrangian of Eq. A.1, and if we desire the resulting Lagrangian to be invariant under local $U(1)$-transformations we can derive the desired transformation property for the gauge field. Let A'_μ denote the $U(1)$ transformed gauge field, we then have

$$\begin{aligned}
\mathcal{L} = \bar{\psi}\left(iD\!\!\!/ - m\right)\psi &= \bar{\psi}\left(i\partial_\mu - ieQA_\mu - m\right)\psi && \text{(A.6)}\\
&\overset{U(1)}{\to} \bar{\psi}\left(i\partial\!\!\!/ - ieQA'_\mu - m + iQ(\partial\!\!\!/\theta)\right)\psi. && \text{(A.7)}
\end{aligned}$$

It is clear that this expression for the Lagrangian is invariant only if the gauge fields transforms such that

$$\begin{aligned} Q\partial_\mu\theta + eQA'_\mu &= eQA_\mu \\ \Rightarrow A'_\mu &= A_\mu - \frac{1}{e}\partial_\mu\theta. \end{aligned} \tag{A.8}$$

And that is precisely the $U(1)$ transformation property we demand of an associated $U(1)$ gauge field.

We want to write down the most general Lagrangian which does not violate the local U(1)-symmetry, Lorentz-invariance and parity (C,P and T). As these are symmetries which are not broken by QED. There is another $U(1)$ gauge invariant quantity that can be formed using the gauge fields, and that is the field strength tensor. The field strength is defined from the commutator of the covariant derivative. For a $U(1)$ symmetry it is given by

$$\begin{aligned} ieF_{\mu\nu} &\equiv [D_\mu, D_\nu] \\ &= \partial_\mu A_\nu - \partial_\nu A_\mu. \end{aligned}$$

By applying the transformation property for the gauge field A_μ from Eq. (A.8) it is straight forward to show that

$$\begin{aligned} F_{\mu\nu} &\overset{U(1)}{\to} \partial_\mu\left(A_\nu - \frac{Q}{e}\partial_\nu\theta\right) - \partial_\nu\left(A_\mu - \frac{Q}{e}\partial_\mu\theta\right) \\ &= (\partial_\mu A_\nu - \partial_\nu A_\mu) = F_{\mu\nu}. \end{aligned}$$

Contracting the space time indices yields a Lorentz invariant quantity, and we can write down the full QED Lagrangian as

$$\mathcal{L}_{\text{QED}} = \bar{\psi}\left(i\not{D} - m\right)\psi - \frac{1}{4}F^{\mu\nu}F_{\mu\nu} \tag{A.9}$$

$$= \bar{\psi}\left(i\not{\partial} - m\right)\psi - e\bar{\psi}\not{A}\psi - \frac{1}{4}F^{\mu\nu}F_{\mu\nu}. \tag{A.10}$$

Varying the action with respect to the fields will produce the Dirac equation, and Maxwell's equation with source terms. The factor of 1/4 yields the correct normalization for Maxwell's equation with source terms. The two trivial Maxwell's equations is the Jacobi identity applied to the covariant derivative.

Varying the action $S = \int \mathrm{d}^4x\mathcal{L}_{\text{QED}}$ with respect to $\bar{\psi}$ gives the equation of motion for a spin-1/2 Dirac -field with charge eQ interacting with an electromagnetic field A^μ

$$0 = \left(i\not{D} - m\right)\psi = (i\gamma^\mu(\partial_\mu + ieQA_\mu) - m)\,\psi \tag{A.11}$$

And varying with respect to the electromagnetic potential A_μ will give Maxwell's equations on covariant form

$$\partial_\mu F^{\mu\nu} = eQj^\nu \qquad \text{(Gauss' law and Ampres law)}$$

where $j^\mu \equiv \bar{\psi}\gamma^\mu\psi$. We get Gauss' law for the magnetic fields and Farady's law of induction by applying the Jacobi identity

$$[D_\mu, [D_\nu, D_\lambda]] + [D_\lambda, [D_\mu, D_\nu]] + [D_\nu, [D_\lambda, D_\mu]] = 0$$

Where a lot of the terms cancel and we are left with

$$\partial_\mu F_{\nu\sigma} + \partial_\sigma F^{\mu\nu} + \partial_\nu F^{\sigma\mu} = 0,$$

compactly stated as

$$\varepsilon^{\mu\nu\rho\sigma}\partial_\nu F_{\rho\sigma} = 0 \qquad \text{(Faraday's law of induction and Gauss' law for magnetic fields)}$$

Appendix B

One Loop Momentum Integrals

Any one-loop integral can be decomposed as sum of integrals taking the form

$$L^{\mu_1 \cdots \mu_m} \int \frac{\mathrm{d}^d p}{(2\pi)^d} \frac{p^{\mu_1} \dots p^{\mu_m}}{\prod_{i=0}^{n} D_i}. \tag{B.1}$$

Where $D_i = (p - q_i)^2 - m_i^2 + i\varepsilon$ are the propagator denominators, and q_i are external momenta (or sums of external momenta). Here we perform the integral in arbitrary $d-$dimensions in stead of four. Initially, of course, the loop momentum is a four-vector in Minkowski space, i.e. a non-trivial metric. We can, however, analytically continue the integrand and simply rotate the time component in the complex plane. That is, we make the substitution

$$\begin{aligned} p^0 &= i p_E^0, \; p^i = p_E^i \\ p^2 &= -p_E^2 \end{aligned}$$

This gives the integration measure $\mathrm{d}^d p = i \mathrm{d}^d p_E$. Shifting to spherical cordinates in d-dimensions gives $\mathrm{d}^d p_E = \mathrm{d}\Omega_d \mathrm{d}|p_E| \; p_E^{d-1}$.Keeping only the highest powers of the loop momentum variable p_E gives the asymptotic behavior for the integrand, thus for high loop momenta the loop integral goes as

$$\sim \int_0^\infty \mathrm{d}p \; p^{d-1+m-2n} \tag{B.2}$$

Which is divergent for

$$d + m - 2n \geq 0. \tag{B.3}$$

One way to regularize these types of integrals is to cut off the integral in $d = 4$ dimensions. Then loop momentum is integrated to Λ, assuming that Λ is much larger than all external momenta in the problem. In the end of the calculation the limit $\Lambda \to \infty$ is taken. However, we use the method of dimensional regularization

where we perform all momenutm integration in $d-$ dimensions, and take the limit $d \to 4$ from below towards the end of the calculation.

In order to get an integrand which is even in the integration variable we apply Feynman's trick

$$\prod_{i=1}^{n} \frac{1}{A_i} = \int_0^1 \mathrm{d}x_1 \cdots \int_0^1 \mathrm{d}x_n \; \delta(\sum_{i=1}^{n} x_i - 1) \frac{(n-1)!}{[x_1 A_1 + \cdots + x_n A_n]^n}. \tag{B.4}$$

This will give a denominator which is even in a shifted loop variable ℓ. Due to this symmetry of the denominator, all terms proportional to an odd power of ℓ^μ in the numerator will vanish. This symmetry also allows to replace e.g.

$$\ell^\mu \ell^\nu \to \frac{1}{d} g^{\mu\nu} \ell^2, \tag{B.5}$$

and more complex expressions for higher powers of ℓ. We can thus get the integral in the form of

$$I_{mn}(\Delta; d) = \int \frac{\mathrm{d}^d \ell}{(2\pi)^d} \frac{(\ell^2)^n}{(\ell^2 - \Delta)^m}. \tag{B.6}$$

Wick rotating ℓ by the $i\ell_E^0 = \ell^0$ gives

$$I_{mn}(\Delta; d) = i\,(-1)^{n-m} \int \frac{\mathrm{d}\Omega_d}{(2\pi)^d} \int \mathrm{d}\ell_E \frac{\ell_E^{2n+d-1}}{(\ell_E^2 + \Delta)^m}$$

The angular integral in d-dimensions is the area of the d-dimnesional sphere divided by $(2\pi)^d$

$$\int \frac{\mathrm{d}\Omega_d}{(2\pi)^d} = \frac{1}{(4\pi)^{d/2}} \frac{2}{\Gamma(d/2)} \tag{B.7}$$

The radial integral can be evaluated using the Euler-Beta function

$$\int \mathrm{d}\ell_E \frac{\ell_E^{2n+d-1}}{(\ell_E^2 + \Delta)^m} = \frac{1}{2} \Delta^{n-m+d/2} B(n + d/2, m - n - d/2), \tag{B.8}$$

where the Euler-Beta function is $B(x,y) = \int_0^\infty \mathrm{d}t\, t^{x-1}/(1+t)^{x+y} = \Gamma(x)\Gamma(y)/\Gamma(x+y)$. Then we have the result

$$I_{mn}(\Delta; d) = i(-1)^{n+m} \frac{\Gamma\left(n + \frac{d}{2}\right) \Gamma\left(m - n - \frac{d}{2}\right)}{\Gamma\left(\frac{d}{2}\right) \Gamma(m)} \frac{\Delta^{n-m+d/2}}{(4\pi)^{d/2}} \tag{B.9}$$

Appendix C

The Vertex as a Feynman Parameter Integral

Here we calculate the effective vertex where an Z/γ^* creates a dark matter pair.

C.1 Fermion Diagrams

In the text we define $\gamma_0^\mu(p_1, p_2)$. By applying the trick in Eq. (B.4) we can write $\Gamma_0^\mu(p_1, p_2)$ as the integral

$$\begin{aligned} i\Gamma_0^\mu(p_1,p_2) = &- g_{\rm NP}^2 \int_{[0,1]^3} \mathrm{d}^3x\ \delta(x+y+z-1)\times \\ &2\int \frac{\mathrm{d}^d k}{(2\pi)^d} \frac{\left[(v_f - a_f)\not{k}\gamma^\mu \not{k}' + (v_f + a_f)m_f^2\gamma^\mu\right] P_R}{\left[(k-yq-zp_1)^2 - \Delta\right]^3}. \end{aligned} \tag{C.1}$$

Where $\Delta = 2yz(p_2^2 - p_1^2) + zM^2 + (1-z)m_\ell^2 - z(1-z)p_1^2 - xyq^2$, we also have momentum conservation implying $q = p_1 + p_2$. We see that the denominator is even in the variable $\ell = k - yq - zp_1$, this will be our shifted momentum. We also have the on shell criteria $p_1^2 = p_2^2 = m_\chi^2$ for the external, physical particles. Thus, since p_1 and p_2 are the momenta of two physical particles with identical mass we find that Δ is invariant under $p_1 \leftrightarrow p_2$. For reference we state the expression for Δ

$$\Delta = zM^2 + (1-z)m_f^2 - z(1-z)m_\chi^2 - xyq^2 - i\varepsilon. \tag{C.2}$$

We look at the numerator of Eq. (C.1) and perform the shift in loop momentum variable $\ell = k - yq - zp_1$ we neglect all terms linear in ℓ as they vanish due to symmetry. The numerator is then

$$(v_f - a_f)\left[\not{k}\gamma(\not{k} - \not{q}) + (v_f + a_f)m_f^2\gamma^\mu\right] P_R \tag{C.3}$$

$$= \left[(v_f - a_f)\left(\not{\ell}\gamma^\mu\not{\ell} + N_0^\mu(p_1,p_2)\right) + (v_f + a_f)m_f^2\gamma^\mu\right] P_R + \mathcal{O}(\ell). \tag{C.4}$$

Where $N_0^\mu(p_1,p_2) = (y\not{q} + z\not{p}_1)\gamma^\mu\left((y-1)\not{q} + \not{p}_1\right)$.

We can now quite easily find the sum of the two fermion diagrams. When both $i\Gamma^\mu(p_1,p_2)$ and $i\Gamma^\mu(p_2,p_1)$ are in the same form as in Eq. (C.1), the only terms that are distinguishable are those belonging to $N_0^\mu(p_1,p_2)$ and $N_0^\mu(p_2,p_2)$. Using the property $C^{-1}\gamma^\mu C = -(\gamma^\mu)^T$ we get

$$\begin{aligned} i\Gamma^\mu(q) &= i\Gamma_0^\mu(p_1,p_2)P_R + Ci\Gamma_0^\mu(p_2,p_1)^T P_L C^{-1} \\ &= -g_{\mathrm{NP}}^2 \int_{[0,1]^3} \mathrm{d}^3x\ \delta(x+y+z-1)\times \\ &\quad 2\int \frac{\mathrm{d}^d\ell}{(2\pi)^d}\frac{1}{\left[\ell^2-\Delta\right]^3}\left\{(v_f-a_f)\not{\ell}\gamma^\mu\not{\ell}(P_R-P_L)+\right. \\ &\qquad\qquad + (v_f+a_f)\, m_f^2\gamma^\mu(P_R-P_L) \\ &\quad \left. + (v_f-a_f)\left[N_0^\mu(p_1,p_2)P_R + CN_0^\mu(p_2,p_1)^T P_L C^{-1}\right]\right\}. \end{aligned} \tag{C.5}$$

We can write $N_0^\mu(p_1,p_2)P_R$ and $CN^\mu(p_2,p_1)^T P_L C^{-1}$ of the form

$$N_0^\mu(p_1,p_2)P_R = -\left[(1-x)\not{p}_1 + y\not{p}_2\right]\gamma^\mu\left[x\not{p}_1 + (1-y)\not{p}_2\right]P_R \tag{C.6}$$

$$CN^\mu(p_2,p_1)^T P_L C^{-1} = \left[x\not{p}_2 + (1-y)\not{p}_1\right]\gamma^\mu\left[(1-x)\not{p}_2 + y\not{p}_1\right]P_L. \tag{C.7}$$

It is now convenient to view these as functions of x and y. We therefore define $f^\mu(x,y) = N_0^\mu(p_1,p_2)$, we then have $CN^\mu(p_2,p_1)^T P_L C^{-1} = -f^\mu(y,x)P_L$. We then add them and get

$$\begin{aligned} &N_0^\mu(p_1,p_2)P_R + CN_0^\mu(p_2,p_1)^T P_L C^{-1} \\ &= \frac{1}{2}\left[N_0^\mu(p_1,p_2) + C[N_0^\mu(p_2,p_1)]^T C^{-1}\right] \\ &\quad + \frac{1}{2}\left[N_0^\mu(p_1,p_2) - C[N_0^\mu(p_2,p_1)]^T C^{-1}\right]\gamma^5 \\ &= \frac{1}{2}[f^\mu(x,y) - f^\mu(y,x)] + \frac{1}{2}[f^\mu(x,y) + f^\mu(y,x)]\gamma^5. \end{aligned} \tag{C.8}$$

That is, in one term proportional to γ^5 which is symmetric with respect to $x \leftrightarrow y$ and one term, proportional to the identity which is antisymmetric with repspect to the permutation $x \leftrightarrow y$. We see that the denominator in Eq. (C.5) is even under the permutation $x \leftrightarrow y$, and therefore the term which is antisymmetric with respect to this change will vanish when integrating over the Feynman parameters x, y and z. We are thus left with the term

$$\begin{aligned} N^\mu\gamma^5 &\equiv \frac{1}{2}\left[N_0^\mu(p_1,p_2) - C[N_0^\mu(p_2,p_1)]^T C^{-1}\right]\gamma^5 \\ &= -\frac{1}{2}\left[(1-x)\not{p}_1 + y\not{p}_2\right]\gamma^\mu\left[x\not{p}_1 + (1-y)\not{p}_2\right]\gamma^5 + (x \leftrightarrow y) \end{aligned} \tag{C.9}$$

In order to simplify N^μ further we may use the Dirac equation for the external momenta p_1 and p_2. The momenta p_1 and p_2 must meet $\bar{u}(p_1)$ or $v(p_2)$, respectively. There is the γ^5 matrix to the left in Eq. (C.9) and the remainder of the work of simplifying N^μ is to ensure that we move all the $\not{p}_1$ to the left, and all $\not{p}_2\gamma^5$ to the right. Then we can make the replacements $\not{p}_1 \to m_\chi$ and $\not{p}_2\gamma^5 \to m_\chi$. After the dust settles we are left with[1]

$$N^\mu\gamma^5 = -\left[z(1-z)+4xy\right] m_\chi q^\mu\gamma^5 - \left(z^2 m_\chi^2 - xyq^2\right)\gamma^\mu\gamma^5. \tag{C.10}$$

Solving the Momentum Integral

We can exploit the symmetry of the integrand in Eq. (C.5) to take $\not{\ell}\gamma^\mu\not{\ell} \to \left(\frac{2}{d}-1\right)\ell^2\gamma^\mu$. We then get

$$2\int \frac{\mathrm{d}^d\ell}{(2\pi)^d}\frac{\not{\ell}\gamma^\mu\not{\ell}\gamma^5}{\left[\ell^2-\Delta\right]^3} = \gamma^\mu\gamma^5\left(\frac{2}{d}-1\right)2\int\frac{\mathrm{d}^d\ell}{(2\pi)^d}\frac{\ell^2}{\left[\ell^2-\Delta\right]^3} \tag{C.11}$$

$$= \left(1-\frac{d}{2}\right)2I_{3,1}(\Delta;d)\gamma^\mu\gamma^5 \tag{C.12}$$

$$\tag{C.13}$$

Applying the formula in Eq. (B.9) we get

$$2I_{3,1}(\Delta;d) = 2\int\frac{\mathrm{d}^d\ell}{(2\pi)^d}\frac{\ell^2}{\left[\ell^2-\Delta\right]^3} \tag{C.14}$$

$$= \frac{i}{16\pi^2}\frac{d}{2}\Gamma\left(2-\frac{d}{2}\right)\left(\frac{4\pi}{\Delta}\right)^{2-\frac{d}{2}} \tag{C.15}$$

$$= \frac{i}{16\pi^2}\frac{d}{2}\left(\frac{1}{2-\frac{d}{2}} - \gamma_E + \ln\left(\frac{4\pi}{\Delta}\right) + \mathcal{O}\left(2-\frac{d}{2}\right)\right) \tag{C.16}$$

We expand the Γ-function around $2-d/2$ as in e.g. [11], here $\gamma_E = 0.5772\ldots$ is the Euler-Mascheroni constant. We see that $I_{3,1}(\Delta;d)$ is a divergent quantity in the $d\to 4$ limit. We also have the integral

$$2I_{3,0}(\Delta;d) = 2\int\frac{\mathrm{d}^d\ell}{(2\pi)^d}\frac{1}{\left[\ell^2-\Delta\right]^3} \tag{C.17}$$

$$= -\frac{i}{(4\pi)^{d/2}}\,\Gamma\left(3-\frac{d}{2}\right)\frac{1}{(\Delta)^{3-\frac{2}{d}}} \tag{C.18}$$

$$\overset{d\to 4}{\to} -\frac{i}{16\pi^2}\frac{1}{\Delta} \tag{C.19}$$

[1] We should have called the term N^μ by a different symbol after applying the Dirac equation, as Eq. (C.10) only holds true when sandwiched between $\bar{u}(p_1)$ and $v(p_2)$. We will nevertheless call the resulting expression N^μ.

Which is finite in the $d \to 4$ limit. We state the expression for Γ^μ in terms of $2\epsilon = 4 - d$ and take the limit $\epsilon \to 0$ wherever possible

$$\begin{aligned} i\Gamma^\mu(q) = -\frac{ig_{\rm NP}^2}{16\pi^2}\int_{[0,1]^3} \mathrm{d}^3x\ \delta(x+y+z-1)\ \times \\ \left\{(v_f - a_f)\,(\epsilon-1)\,\Gamma\,(\epsilon)\left(\frac{4\pi}{\Delta}\right)^{\epsilon}\gamma^\mu\gamma^5 \right. \\ \left. -\left[(v_f+a_f)\,m_f^2\gamma^\mu\gamma^5 + (v_f - a_f)N^\mu\gamma^5\right]\frac{1}{\Delta}\right\} \end{aligned} \tag{C.20}$$

For the fermion diagrams.

C.1.1 Scalar Diagrams

We introduce the Feynman parameters by the trick in Eq. (B.4). Then we get

$$i\Lambda_0^\mu(p_1,p_2) = -g_{\rm NP}^2 k_f \int_0^1 \mathrm{d}x \int_0^1 \mathrm{d}y \int_0^1 \mathrm{d}z\delta(x+y+z-1)\times \tag{C.21}$$

$$\times\, 2\int \frac{\mathrm{d}^d\ell}{(2\pi)^d}\frac{(2k+q)^\mu\,(\not{k}+\not{p}_1)P_R}{\left[(k+yq+zp_1)^2-\tilde{\Delta}\right]^3} \tag{C.22}$$

Where $\tilde{\Delta} = zm_f^2 + (1-z)M^2 - z(1-z)m_\chi^2 - xyq^2 - i\varepsilon$ after the external DM particles are put on shell. We make the shift in loop momentum variable $\ell = k + yq + zp_1$ to get the numerator of the form

$$2\not{\ell}\ell^\mu P_R + M_0^\mu(p_1,p_2)P_R, \tag{C.23}$$

where $M_0^\mu(p_1,p_2) = [(2x-1)p_1^\mu - (2y-1)p_2^\mu](x\not{p}_1 - y\not{p}_2)$. When adding the two diagrams in Fig. 4.4 we get

$$\begin{aligned} ig\Lambda^\mu &= i\Lambda_0^\mu(p_1,p_2)P_R + Ci\Lambda_0^\mu(p_2,p_1)^T P_L C^{-1} \\ &= -k_f g_{\rm NP}^2 \int_{[0,1]^3}\mathrm{d}^3x\ \delta(x+y+z-1)\ 2\int\frac{\mathrm{d}^d\ell}{(2\pi)^d}\frac{2\not{\ell}\ell^\mu\gamma^5 + M^\mu\gamma^5}{\left[\ell^2-\tilde{\Delta}\right]^3}. \end{aligned} \tag{C.24}$$

Where

$$\begin{aligned} M^\mu\gamma 5 &= M_0^\mu(p_1,p_2)P_R + CM_0^\mu(p_2,p_1)^T P_L C^{-1} \\ &= (x-y)^2 m_\chi q^\mu\gamma^5. \end{aligned} \tag{C.25}$$

Due to the symmetry in ℓ we can substitute $\not{\ell}\ell^\mu \to \frac{1}{d}\ell^2\gamma^\mu$. We then get

$$2\int\frac{\mathrm{d}^d\ell}{(2\pi)^d}\frac{2\not{\ell}\ell^\mu\gamma^5}{\left[\ell^2-\tilde{\Delta}\right]^3} = \frac{4}{d}\int\frac{\mathrm{d}^d\ell}{(2\pi)^d}\frac{\ell^2}{\left[\ell^2-\tilde{\Delta}\right]^3}\gamma^\mu\gamma^5 \tag{C.26}$$

$$= \frac{i}{16\pi^2}\Gamma\left(2-\frac{d}{2}\right)\left(\frac{4\pi}{\tilde{\Delta}}\right)^{2-2/d}\gamma^\mu\gamma^5, \tag{C.27}$$

which is divergent in the limit $d \to 4$. We state $i\Lambda^\mu$ in terms of $2\epsilon = 4 - d$ and take the limit $\epsilon \to 0$ wherever possible

$$\begin{aligned} i\Lambda^\mu = -\frac{ik_f g_{\rm NP}^2}{16\pi^2} \int_{[0,1]^3} \mathrm{d}^3x \; \delta(x+y+z-1)\times \\ \left\{ \Gamma\left(\epsilon\right) \left(\frac{4\pi}{\tilde{\Delta}}\right)^{\epsilon} \gamma^\mu\gamma^5 - \frac{M^\mu\gamma^5}{\tilde{\Delta}} \right\} \end{aligned} \tag{C.28}$$

C.2 The Effective Vertex

We can now compactly write the vertex in terms of the Feynman parameter integral

$$\begin{aligned} i\Xi_B^\mu(q) &= i\Gamma^\mu + i\Lambda^\mu \\ &= -\frac{ig_{\rm NP}^2}{16\pi^2} \int_{[0,1]^3} \mathrm{d}^3x \; \delta(x+y+z-1) \\ &\times \left\{ \Gamma(\epsilon) \left[(v_f - a_f)(\epsilon - 1) \left(\frac{4\pi}{\Delta}\right)^{\epsilon} + k_f \left(\frac{4\pi}{\tilde{\Delta}}\right)^{\epsilon} \right] \gamma^\mu\gamma^5 \right. \\ &- \left((v_f + a_f) m_\ell^2 \gamma^\mu\gamma^5 + (v_f - a_f) N^\mu\gamma^5 \right) \frac{1}{\Delta} \\ &\left. - \frac{k_f M^\mu\gamma^5}{\tilde{\Delta}} \right\}. \end{aligned} \tag{C.29}$$

Where we insert the relevant coupling factors for k_f, v_f and a_f for to get the photon- and Z-channel amplitudes.

C.2.1 DM Pair From a Photon

We consider the case when the vector particle B_μ is a photon. The particles which partake in the loop in Fig. 4.2 are then only charged lepton ℓ and the charged scalar η. We then insert $k_f = -\sin\theta_W, a_f = 0$ and $v_f = -\sin\theta_W$ in Eq. (C.29), in order to get the effective vertex factor given in terms of Feynman parameter

integrals. From the third line in Eq. (C.29) we then get when expanding in ϵ

$$\begin{aligned}
&\sin\theta_W\Gamma(\epsilon)\left[\left(\frac{4\pi}{\Delta}\right)^{\epsilon}(\epsilon-1)+\left(\frac{4\pi}{\tilde{\Delta}}\right)^{\epsilon}\right]\\
=&-\sin\theta_W\left(\frac{1}{\epsilon}-\gamma_E+\frac{1}{2}(\gamma_E^2+\frac{\pi^2}{6})\epsilon+\mathcal{O}(\epsilon^2)\right)\times\\
&\left[(\epsilon-1)\left(1+\epsilon\ln\frac{4\pi}{\Delta}\right)+1+\epsilon\ln\frac{4\pi}{\tilde{\Delta}}+\mathcal{O}(\epsilon^2)\right]\\
=&-\sin\theta_W\left(\frac{1}{\epsilon}-\gamma_E+\frac{1}{2}(\gamma_E^2+\frac{\pi^2}{6})\epsilon+\mathcal{O}(\epsilon^2)\right)\times\\
&\left[\epsilon+\epsilon\ln\frac{\Delta}{\tilde{\Delta}}+\mathcal{O}(\epsilon^2)\right]\\
=&-\sin\theta_W\left(1+\ln\frac{\Delta}{\tilde{\Delta}}\right),\ \text{as}\ \epsilon\to 0.
\end{aligned}\tag{C.30}$$

We can write this in terms of formfactors F_1 and F_2

$$i\Xi_A^\mu=\frac{ig_{NP}^2\sin\theta_W}{16\pi^2}\left[F_1(q)\gamma^5\gamma^\mu+F_2(q)\frac{q^\mu}{m_\chi}\gamma^5\right]\tag{C.31}$$

as the effective coupling factor for $\gamma^*\to\chi\chi$. Here the form factors are

$$F_1(q)=\int_{[0,1]^3}\mathrm{d}^3x\ \delta(x+y+z-1)\left[1+\ln\frac{\tilde{\Delta}}{\Delta}+\frac{(z^2m_\chi^2-xyq^2)-m_\ell^2}{\Delta}\right]\tag{C.32}$$

$$F_2(q)=\int_{[0,1]^3}\mathrm{d}^3x\ \delta(x+y+z-1)\left[\frac{z(1-z)+4xy}{\Delta}-\frac{(x-y)^2}{\tilde{\Delta}}\right]m_\chi^2.\tag{C.33}$$

C.2.2 DM Pair From a Z-boson

We now consider the case when a Z-boson carrying invariant center of mass energy q^2 creates two DM particles. We get the same types of diagrams as in Fig. 4.2, however, the particle in the loop are both charged SM leptons ℓ, and neutrinos ν_ℓ in addition to the scalars η and η_0. There are then in total 8 diagrams, 4 diagrams for the charged lepton ℓ and scalar η and 4 for the neutrino ν_ℓ and the charge neutral scalar η_0.
The contribution for $f=\ell$ is the vertex factor arising in the amplitude from the 4 diagrams with the charged lepton and scalar particles. The coupling factors a_ℓ and v_ℓ and k_ℓ are displayed in table 3.1, and we have $k_\ell=v_f-a_f=\frac{\sin^2\theta_W-1/2}{\cos\theta_W}$ such that the divergences cancel, we also get a term proportional to $v_f+a_f=\frac{\sin^2\theta_W}{\cos\theta_W}$.

For the four diagrams where $f=\nu_\ell$ the cancellation occurs in the same manner

as for $f = \ell$, as $v_{\nu_\ell} - a_{\nu_\ell} = k_{\nu_\ell} = 1/(2\cos\theta_W)$. Furthermore $v_{\nu_\ell} + a_{\nu_\ell} = 0$ so we get no term proportional to m_{ν_ℓ}.

The necessary algebra to find the Z-channel vertex factor for charged leptons- and neutrino- loop particles is analogous to the γ^* vertex. If we ignore the lepton masses m_ℓ and m_{ν_ℓ} we get the same form of the vertex as in Eq. (C.31), only with an overall factor of $\tan\theta_W$ after adding the amplitudes for all 8 diagrams. We state the vertex for completeness

$$i\Xi_Z = \frac{ig_{NP}^2 \sin\theta_W \tan\theta_W}{16\pi^2}\left[F_1(q)\gamma^5\gamma^\mu + F_2(q)\frac{q^\mu}{m_\chi}\gamma^5\right] \tag{C.34}$$

Where the form factors are given in Eqs. (C.32) and (C.33) neglecting m_ℓ^2.

Appendix D

Passarino Veltmann Integrals

D.1 Three-point rank-two tensor integral

We will here go through the details of how to calculate the three-point rank-two tensor integral from Eq. (5.10). Firstly, the decomposition into Passarino-Veltmann coefficients

$$C^{\mu\nu} = g^{\mu\nu}\ C_{00} + p_1^\mu p_1^\nu\ C_{11} + p_2^\mu p_2^\nu\ C_{22} + p_1^\mu p_2^\nu\ C_{12} + p_2^\mu p_1^\nu\ C_{21}.$$

We note that $C_{12} = C_{21}$ due to total symmetry in space-time indices. We can then set up another set of equations

$$p_1^\nu C^\mu{}_\nu = p_1^\mu\ C_{00} + p_1^\mu\ p_1^2\ C_{11} + p_1 \cdot p_2\ p_2^\mu\ C_{22} + (p_1^\mu\ p_1 \cdot p_2 + p_2^\mu p_1^2)\ C_{12} \tag{D.1}$$

$$p_2^\nu C^\mu{}_\nu = p_2^\mu\ C_{00} + p_1^\mu\ p_1 \cdot p_2\ C_{11} + p_2^2\ p_2^\mu\ C_{22} + (p_1^\mu\ p_1 \cdot p_2 + p_2^\mu p_1^2)\ C_{12} \tag{D.2}$$

$$C^\mu{}_\mu = dC_{00} + p_1^2\ C_{11} + p_2^2\ C_{22} + 2p_1 \cdot p_2\ C_{12} \tag{D.3}$$

We can also reduce these to a set of equations as Eq. (5.16), we can express $p_i^\nu C^\mu{}_\nu$ in terms of scalar integrals

$$\begin{aligned}
p_1^\nu C^\mu{}_\nu &= \frac{(2\pi\mu)^{4-d}}{i\pi^2} \int \mathrm{d}^d k\ \frac{k^\mu p_1 \cdot k}{D_0 D_1 D_2} \\
&= \frac{(2\pi\mu)^{4-d}}{i\pi^2} \int \mathrm{d}^d k\ \frac{1}{2}\left[\frac{k^\mu\,(D_1 - D_0 + m_1 - m_0 - p_1^2)}{D_0 D_1 D_2}\right] \\
&= \frac{(2\pi\mu)^{4-d}}{i\pi^2} \int \mathrm{d}^d k\ \frac{1}{2}\left[\frac{k^\mu}{D_0 D_2} - \frac{k^\mu\,(1)}{D_1 D_2} + \left(m_1 - m_0 - p_1^2\right)\frac{k^\mu}{D_0 D_1 D_2}\right] \\
&= \frac{1}{2} B^\mu(p_2^2, m_0^2, m_2^2) - \frac{1}{2} B^\mu((p_2 - p_1)^2, m_1, m_2) \\
&\quad + \frac{1}{2}(m_1 - m_0 - p_1^2) C^\mu(p_1^2, p_2^2, (p_2 - p_1)^2, m_1^2, m_0^2, m_2^2).
\end{aligned}$$

And analogously we have

$$p_2^\nu C^\mu{}_\nu = \frac{1}{2}B^\mu(p_1^2, m_0^2, m_1^2) - \frac{1}{2}B^\mu((p_2-p_1)^2, m_1, m_2) + \frac{1}{2}(m_2 - m_0 - p_2^2)C^\mu(p_1^2, p_2^2, (p_2-p_1)^2, m_1^2, m_0^2, m_2^2),$$

also for the trace

$$\begin{aligned} C^\mu{}_\mu &= \frac{(2\pi\mu)^{4-d}}{i\pi^2}\int \mathrm{d}^d k\ \frac{k^2}{D_0 D_1 D_2} \\ &= B_0((p_2-p_1)^2, m_0, m_1) + m_0^2 C_0(p_1^2, p_2^2, (p_2-p_1)^2, m_1^2, m_0^2, m_2^2). \end{aligned}$$

We have now to find the decomposition of the respecitve one-tensor integrals B^μ and C^μ. Once this is done set it in as left hand side in Eqs. (D.1) and (D.2), and we assume that p_1 and p_2 are linearly independent in order to find two new equations from each of the expressions for $p_i^\nu C^\mu{}_\nu$. In the end we end up with a set of equations analogous to the set in Eq. (5.16).

D.2 General Solution for the Scalar Two- and Three-Point Integrals

We here provide the general solutions for the scalar two-and three-point scalar integrals. A lot of the intermediary steps for the solution of the three-point scalar integral is found in [68].

D.2.1 Two-Point Scalar Integral

The two-point scalar integral is divergent as $d \to 4$ this corresponds to a UV-divergence. We will solve the integral in Eq. (**??**) by using Feynman parametrization. We then have

$$\begin{aligned} \frac{i}{16\pi^2}B_0(p^2, m_0^2, m_1^2) &= \mu^{4-d}\int \frac{\mathrm{d}^d k}{(2\pi)^d}\ \frac{1}{[k^2 - m_0^2]\,[(k+p)^2 - m_1^2]} \\ &= \mu^{4-d}\int \frac{\mathrm{d}^d k}{(2\pi)^d}\int_0^1 \mathrm{d}x\ \frac{1}{\left[(k+px)^2 - \Delta\right]^2} \\ &\overset{k\to k-xp}{=} \mu^{4-d}\int \mathrm{d}x\ \frac{i}{(4\pi)^{d/2}}\Gamma(2-d/2)\frac{1}{\Delta^{2-d/2}} \end{aligned}$$

Where $\Delta = -x(1-x)p_1^2 + m_0^2(1-x) + m_1^2 x - i\varepsilon$. We will take the expansion

$$\frac{\Gamma(2-d/2)}{4\pi^{d/2}}\left(\frac{\mu^2}{\Delta}\right)^{2-d/2} = \frac{1}{16\pi^2}\left(\frac{2}{\epsilon} - \ln\frac{\Delta}{\mu^2} - \gamma_E + \ln 4\pi\right) + \mathcal{O}(\epsilon)$$

We see that the mass dimension μ keeps the argument of the log dimensionless. We define $\delta_\epsilon = \frac{2}{\epsilon} - \gamma_E + \ln 4\pi$ and state the intermediate result[1]

$$B_0(p^2, m_0^2, m_1^2) = \delta_\epsilon - \int_0^1 \mathrm{d}x \ \ln\left[-x(1-x)\frac{p^2}{\mu^2} + \frac{m_0^2}{\mu^2}(1-x) + \frac{m_1^2}{\mu^2}x - \frac{i\varepsilon}{\mu^2}\right] + \mathcal{O}(\epsilon) \tag{D.4}$$

For nonzero masses and p^2 the general solution is

$$B_0(p^2, m_1^2, m_2^2) = \delta_\epsilon - \ln\left(\frac{p^2}{\mu^2}\right) - \sum_{i=1}^{2}\int_0^1 \mathrm{d}x \ln(x_i - x)$$

Where

$$\int_0^1 \mathrm{d}x \ln(t-x) = (1-t)\ln(t-1) + t\ln t - 1$$

Where $x_{1,2}$ are the roots of the equation

$$x^2 - x\left(1 - \frac{m_1^2}{p^2} + \frac{m_0^2}{p^2})\right) + \frac{m_0^2}{p^2} - \frac{i\varepsilon}{p^2} = 0.$$

They are found to be

$$x_1 = \frac{1}{2p^2}\left(p^2 - m_0^2 + m_1^2 + \sqrt{(p^2 - m_1^2 + m_0^2)^2 - 4p^2(m_0^2 - i\varepsilon)}\right) \tag{D.5}$$

$$x_2 = \frac{1}{2p^2}\left(p^2 - m_0^2 + m_1^2 - \sqrt{(p^2 - m_1^2 + m_0^2)^2 - 4p^2(m_0^2 - i\varepsilon)}\right) \tag{D.6}$$

$$= \frac{m_0^2 - i\varepsilon}{p^2}\frac{1}{x_1} \tag{D.7}$$

Applying Eq. (D.7) we can rewrite

$$\sum_{i=1}^{2}\int_0^1 \mathrm{d}x \ln(x_i - x) = \sum_{i=1}^{2}\left[\int_0^1 \mathrm{d}x \ln\left(1 - \frac{x}{x_i}\right) + \ln x_i\right]$$
$$= \ln\frac{p^2}{m_0^2 - i\varepsilon} + \sum_{i=1}^{2}(1-x_i)\ln\left(\frac{x_i - 1}{x_i}\right).$$

And we arrive at

$$B_0(p^2, m_0^2, m_1^2) = \delta_\epsilon + \ln\frac{\mu^2}{m_0^2 - i\varepsilon} + 2 - \sum_{i=1}^{2}(1-x_i)\ln\left(\frac{x_i - 1}{x_i}\right)$$

[1] We make the important distinction between ϵ which is used to regularize the UV-divergence, and the $i\varepsilon$ which is the propagator pole shift, and it also gives the desired branch of the logs.

References

[1] G. Aad *et al.*, "Observation of a new particle in the search for the Standard Model Higgs boson with the ATLAS detector at the LHC," *Phys. Lett.*, vol. B716, pp. 1–29, 2012. DOI: 10.1016/j.physletb.2012.08.020.

[2] S. Chatrchyan *et al.*, "Observation of a new boson at a mass of 125 GeV with the CMS experiment at the LHC," *Phys. Lett.*, vol. B716, pp. 30–61, 2012. DOI: 10.1016/j.physletb.2012.08.021.

[3] E. Noether, "Invariant variation problems," *Transport Theory and Statistical Physics*, vol. 1, pp. 186–207, jan 1971. DOI: 10.1080/00411457108231446.

[4] S.-Y. Xu *et al.*, "Discovery of a Weyl Fermion semimetal and topological Fermi arcs," *Science*, 2015. DOI: 10.1126/science.aaa9297.

[5] A. Garfagnini, "Neutrinoless Double Beta Decay Experiments," in *12th Conference on Flavor Physics and CP Violation (FPCP 2014) Marseille, France, May 26-30, 2014*, 2014.

[6] A. Zee, *Quantum Field Theory in a Nutshell*. Nutshell handbook, Princeton, NJ: Princeton Univ. Press, 2010.

[7] E. Majorana, "A symmetric theory of electrons and positrons," *Il Nuovo Cimento*, vol. **14**, pp. 171 – 184, 1937.

[8] P. B. Pal, "Dirac, Majorana and Weyl fermions," *Am. J. Phys.*, vol. 79, pp. 485–498, 2011. DOI: 10.1119/1.3549729.

[9] H. Haber and G. Kane, "The search for supersymmetry: Probing physics beyond the standard model," *Physics Reports*, vol. 117, no. 2, pp. 75 – 263, 1985. DOI: 10.1016/0370-1573(85)90051-1.

[10] D. Binosi, J. Collins, C. Kaufhold, and L. Theussl, "JaxoDraw: A Graphical user interface for drawing Feynman diagrams. Version 2.0 release notes," *Comput. Phys. Commun.*, vol. 180, pp. 1709–1715, 2009. DOI: 10.1016/j.cpc.2009.02.020.

[11] M. E. Peskin and D. V. Schroeder, *An Introduction to Quantum Field Theory; 1995 ed.* Boulder, CO: Westview, 1995. Includes exercises.

[12] J. Bjorken and S. Drell, *Relativistic quantum mechanics*. International series in pure and applied physics, McGraw-Hill, 1964.

[13] R. Aaij *et al.*, "Observation of $J/\psi p$ Resonances Consistent with Pentaquark States in $\Lambda_b^0 \to J/\psi K^- p$ Decays," *Phys. Rev. Lett.*, vol. 115, p. 072001, 2015. DOI: 10.1103/PhysRevLett.115.072001.

[14] Wikimedia Commons, "Standard Model of Elementary Particles." Licensed under the Creative Commons Attribution 3.0 Unported license.

[15] D. J. Griffiths, *Introduction to elementary particles; 2nd rev. version*. Physics textbook, New York, NY: Wiley, 2008.

[16] N. Cabibbo, "Unitary symmetry and leptonic decays," *Phys. Rev. Lett.*, vol. 10, pp. 531–533, Jun 1963. DOI: 10.1103/PhysRevLett.10.531.

[17] M. Kobayashi and T. Maskawa, "Cp-violation in the renormalizable theory of weak interaction," *Progress of Theoretical Physics*, vol. 49, no. 2, pp. 652–657, 1973. DOI: 10.1143/PTP.49.652.

[18] J. Charles, A. Höcker, H. Lacker, S. Laplace, F. R. Le Diberder, J. Malclés, J. Ocariz, M. Pivk, and L. Roos, "Cp violation and the ckm matrix: assessing the impact of the asymmetric b factories," *The European Physical Journal C - Particles and Fields*, vol. 41, no. 1, pp. 1–131, 2005. DOI: 10.1140/epjc/s2005-02169-1.

[19] Y. Fukuda *et al.*, "Evidence for oscillation of atmospheric neutrinos," *Phys. Rev. Lett.*, vol. 81, pp. 1562–1567, 1998. DOI: 10.1103/PhysRevLett.81.1562.

[20] Z. Maki, M. Nakagawa, and S. Sakata, "Remarks on the unified model of elementary particles," *Progress of Theoretical Physics*, vol. 28, no. 5, pp. 870–880, 1962. DOI: 10.1143/PTP.28.870.

[21] B. Pontecorvo, "Inverse beta processes and nonconservation of lepton charge," *Sov. Phys. JETP*, vol. 7, pp. 172–173, 1958. [Zh. Eksp. Teor. Fiz.34,247(1957)].

[22] H. Kurashige, "Highlight of results from {ATLAS} at {LHC}," *Physics Procedia*, vol. 80, pp. 14 – 18, 2015. 26th International Conference on Nuclear Tracks in Solids (ICNTS26) Kobe, Japan 15th 19th September 2014.

[23] S. P. Martin, "A Supersymmetry primer," 1997. DOI: 10.1142/9789812839657_0001.

[24] G. Aad *et al.*, "Measurement of three-jet production cross-sections in *pp*pp collisions at 7 tev centre-of-mass energy using the atlas detector," *The European Physical Journal C*, vol. 75, no. 5, pp. 1–33, 2015. DOI: 10.1140/epjc/s10052-015-3363-3.

[25] V. Khachatryan *et al.*, "Measurement of the inclusive 3-jet production differential cross section in protonproton collisions at 7 TeV and determination of the strong coupling constant in the TeV range," *Eur. Phys. J.*, vol. C75, no. 5, p. 186, 2015. DOI: 10.1140/epjc/s10052-015-3376-y.

[26] D. Hanneke, S. Fogwell, and G. Gabrielse, "New measurement of the electron magnetic moment and the fine structure constant," *Phys. Rev. Lett.*, vol. 100, p. 120801, Mar 2008. DOI: 10.1103/PhysRevLett.100.120801.

[27] D. Hanneke, S. Fogwell Hoogerheide, and G. Gabrielse, "Cavity control of a single-electron quantum cyclotron: Measuring the electron magnetic moment," *Phys. Rev. A*, vol. 83, p. 052122, May 2011. DOI: 10.1103/PhysRevA.83.052122.

[28] T. Aoyama, M. Hayakawa, T. Kinoshita, and M. Nio, "Tenth-order qed contribution to the electron $g-2$ and an improved value of the fine structure constant," *Phys. Rev. Lett.*, vol. 109, p. 111807, Sep 2012. DOI: 10.1103/PhysRevLett.109.111807.

[29] A. G. Riess *et al.*, "Observational evidence from supernovae for an accelerating universe and a cosmological constant," *Astron. J.*, vol. 116, pp. 1009–1038, 1998. DOI: 10.1086/300499.

[30] S. Perlmutter, M. S. Turner, and M. J. White, "Constraining dark energy with SNe Ia and large scale structure," *Phys. Rev. Lett.*, vol. 83, pp. 670–673, 1999. DOI: 10.1103/PhysRevLett.83.670.

[31] F. Zwicky, "Republication of: The redshift of extragalactic nebulae," *General Relativity and Gravitation*, vol. 41, no. 1, pp. 207–224, 2009. DOI: 10.1007/s10714-008-0707-4.

[32] T. S. van Albada, J. N. Bahcall, K. Begeman, and R. Sancisi, "Distribution of dark matter in the spiral galaxy NGC 3198," *Astronomy and Astrophysics*, vol. 295, pp. 305–313, aug 1985. DOI: 10.1086/163375.

[33] K. Garrett and G. Duda, "Dark Matter: A Primer," *Adv. Astron.*, vol. 2011, p. 968283, 2011. DOI: 10.1155/2011/968283.

[34] V. C. Rubin and W. K. Ford, Jr., "Rotation of the Andromeda Nebula from a Spectroscopic Survey of Emission Regions," *Astrophys. J.*, vol. 159, p. 379, feb 1970. DOI: 10.1086/150317.

[35] D. Clowe, M. Bradac, A. H. Gonzalez, M. Markevitch, S. W. Randall, C. Jones, and D. Zaritsky, "A direct empirical proof of the existence of dark matter," *Astrophys. J.*, vol. 648, pp. L109–L113, 2006. DOI: 10.1086/508162.

[36] P. Fischer, G. Bernstein, G. Rhee, and J. A. Tyson, "The mass distribution of the cluster 0957+561 from gravitational lensing," *Astron. J.*, vol. 113, p. 521, 1997. DOI: 10.1086/118272.

[37] A. A. Penzias and R. W. Wilson, "A Measurement of Excess Antenna Temperature at 4080 M c/s.," *The Astrophysical Journal*, vol. 142, pp. 419–421, July 1965. DOI: 10.1086/148307.

[38] P. A. R. Ade *et al.*, "Planck 2015 results. XIII. Cosmological parameters," 2015.

[39] G. Hinshaw, D. Larson, E. Komatsu, D. N. Spergel, C. L. Bennett, J. Dunkley, M. R. Nolta, M. Halpern, R. S. Hill, N. Odegard, L. Page, K. M. Smith, J. L. Weiland, B. Gold, N. Jarosik, A. Kogut, M. Limon, S. S. Meyer, G. S. Tucker, E. Wollack, and E. L. Wright, "Nine-year wilkinson microwave anisotropy probe (wmap) observations: Cosmological parameter results," *The Astrophysical Journal Supplement Series*, vol. 208, no. 2, p. 19, 2013. DOI: 10.1088/0067-0049/208/2/19.

[40] N. Suzuki *et al.*, "The hubble space telescope cluster supernova survey. v. improving the dark-energy constraints above z ¿ 1 and building an early-type-hosted supernova sample," *The Astrophysical Journal*, vol. 746, no. 1, p. 85, 2012.

[41] E. Hawkins *et al.*, "The 2dF Galaxy Redshift Survey: Correlation functions, peculiar velocities and the matter density of the universe," *Mon. Not. Roy. Astron. Soc.*, vol. 346, p. 78, 2003. DOI: 10.1046/j.1365-2966.2003.07063.x.

[42] K. Abazajian *et al.*, "The Third Data Release of the Sloan Digital Sky Survey," *Astron. J.*, vol. 129, pp. 1755–1759, 2005. DOI: 10.1086/427544.

[43] V. Springel *et al.*, "Simulating the joint evolution of quasars, galaxies and their large-scale distribution," *Nature*, vol. 435, pp. 629–636, 2005. DOI: 10.1038/nature03597.

[44] G. Servant and T. M. P. Tait, "Is the lightest Kaluza-Klein particle a viable dark matter candidate?," *Nucl. Phys.*, vol. B650, pp. 391–419, 2003. DOI: 10.1016/S0550-3213(02)01012-X.

[45] Q. Yang, "Axions and Dark Matter," 2015.

[46] yvind Grn and S. Hervik, *Einsteins General Theory of Relativity: With Modern Applications in Cosmology*. Nutshell handbook, Berlin: Springer, 2007. DOI: 10.1007/978-0-387-69200-5.

[47] E. W. Kolb and M. S. Turner, *The Early Universe*. Addison-Wesley, 1990. Frontiers in Physics, 69.

[48] G. Jungman, M. Kamionkowski, and K. Griest, "Supersymmetric dark matter," *Physics Reports*, vol. 267, no. 56, pp. 195 – 373, 1996. DOI: 10.1016/0370-1573(95)00058-5.

[49] J. Lewin and P. Smith, "Review of mathematics, numerical factors, and corrections for dark matter experiments based on elastic nuclear recoil," *Astroparticle Physics*, vol. 6, no. 1, pp. 87 – 112, 1996. DOI: 10.1016/S0927-6505(96)00047-3.

[50] R. J. Gaitskell, "Direct detection of dark matter," *Ann. Rev. Nucl. Part. Sci.*, vol. 54, pp. 315–359, 2004. DOI: 10.1146/annurev.nucl.54.070103.181244.

[51] R. Bernabei *et al.*, "The DAMA/LIBRA apparatus," *Nucl. Instrum. Meth.*, vol. A592, pp. 297–315, 2008. DOI: 10.1016/j.nima.2008.04.082.

[52] J. Naganoma, "The xenon dark matter search experiment," *Journal of Instrumentation*, vol. 11, no. 02, p. C02048, 2016. DOI: 10.1088/1748-0221/11/02/C02048.

[53] J. E. Y. Dobson, "Searching for Dark Matter with the LUX experiment," in *Proceedings, 20th International Conference on Particles and Nuclei (PANIC 14)*, pp. 373–377, 2014. DOI: 10.3204/DESY-PROC-2014-04/95.

[54] E. Aprile *et al.*, "Physics reach of the XENON1T dark matter experiment," *JCAP*, vol. 1604, no. 04, p. 027, 2016. DOI: 10.1088/1475-7516/2016/04/027.

[55] M. Ackermann *et al.*, "Searching for Dark Matter Annihilation from Milky Way Dwarf Spheroidal Galaxies with Six Years of Fermi Large Area Telescope Data," *Phys. Rev. Lett.*, vol. 115, no. 23, p. 231301, 2015.

[56] A. Karelin, "The high energy electrons with the PAMELA calorimeter," in *Proceedings, 33rd International Cosmic Ray Conference (ICRC2013): Rio de Janeiro, Brazil, July 2-9, 2013*, p. 0302, 2013.

[57] W. B. Atwood *et al.*, "The large area telescope on the fermi gamma-ray space telescope mission," *The Astrophysical Journal*, vol. 697, no. 2, p. 1071, 2009. DOI: 10.1088/0004-637X/697/2/1071.

[58] M. Aaboud *et al.*, "Search for new phenomena in final states with an energetic jet and large missing transverse momentum in pp collisions at $\sqrt{s} = 13$ TeV using the ATLAS detector," 2016.

[59] S. Coleman and J. Mandula, "All possible symmetries of the s matrix," *Phys. Rev.*, vol. 159, pp. 1251–1256, Jul 1967. DOI: 10.1103/PhysRev.159.1251.

[60] R. Haag, J. T. Lopuszaski, and M. Sohnius, "All possible generators of supersymmetries of the s-matrix," *Nuclear Physics B*, vol. 88, no. 2, pp. 257 – 274, 1975. DOI: 10.1016/0550-3213(75)90279-5.

[61] S. Ferrara, L. Girardello, and F. Palumbo, "General mass formula in broken supersymmetry," *Phys. Rev. D*, vol. 20, pp. 403–408, Jul 1979. DOI: 10.1103/PhysRevD.20.403.

[62] G. Passarino and M. Veltman, "One-loop corrections for e^+e^- annihilation into $\mu^+\mu^-$ in the weinberg model," *Nuclear Physics B*, vol. 160, no. 1, pp. 151 – 207, 1979. DOI: 10.1016/0550-3213(79)90234-7.

[63] A. Denner, "Techniques for calculation of electroweak radiative corrections at the one loop level and results for W physics at LEP-200, arxiv:0709.1075," *Fortsch. Phys.*, vol. 41, pp. 307–420, 1993. DOI: 10.1002/prop.2190410402.

[64] V. Shtabovenko, R. Mertig, and F. Orellana, "New Developments in FeynCalc 9.0, arXiv:1601.01167," 2016.

[65] R. Mertig, M. Bohm, and A. Denner, "Feyn calc - computer-algebraic calculation of feynman amplitudes," *Computer Physics Communications*, vol. 64, no. 3, pp. 345 – 359, 1991. DOI: 10.1016/0010-4655(91)90130-D.

[66] A. Denner and S. Dittmaier, "Reduction schemes for one-loop tensor integrals, arXiv:hep-ph/0509141," *Nucl. Phys.*, vol. B734, pp. 62–115, 2006. DOI: 10.1016/j.nuclphysb.2005.11.007.

[67] R. K. Ellis and G. Zanderighi, "Scalar one-loop integrals for QCD, arXiv:0712.1851," *JHEP*, vol. 02, p. 002, 2008. DOI: 10.1088/1126-6708/2008/02/002.

[68] G. 't Hooft and M. Veltman, "Scalar one-loop integrals," *Nuclear Physics B*, vol. 153, pp. 365 – 401, 1979. DOI: 10.1016/0550-3213(79)90605-9.